ACTA PROTOZOOLOGICA

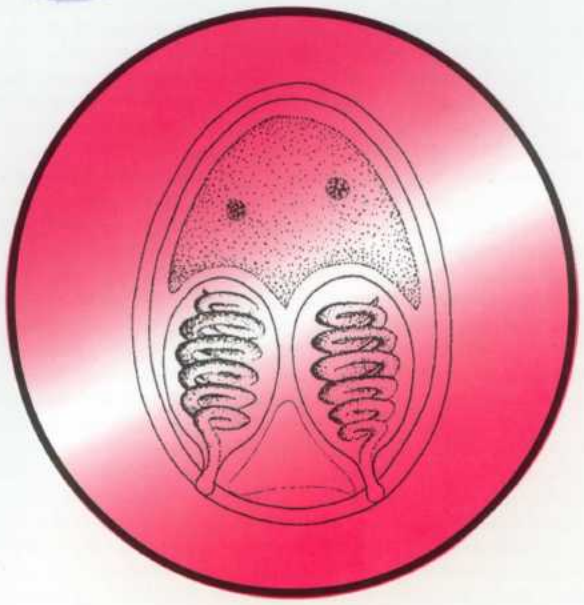

NENCKI INSTITUTE OF EXPERIMENTAL BIOLOGY
WARSAW, POLAND

2002

VOLUME 41 NUMBER 1
ISSN 0065-1583

Polish Academy of Sciences
Nencki Institute of Experimental Biology
and
Polish Society of Cell Biology

ACTA PROTOZOOLOGICA
International Journal on Protistology

ACTA PROTOZOOLOGICA appears quarterly.

The price (including Air Mail postage) of subscription to ACTA PROTOZOOLOGICA at 2002 is: US $ 200.- by institutions and US $ 120.- by individual subscribers. Limited numbers of back volumes at reduced rate are available. TERMS OF PAYMENT: check, money oder or payment to be made to the Nencki Institute of Experimental Biology account: 111-01053-401050001074 at Państwowy Bank Kredytowy XIII Oddz. Warszawa, Poland. For matters regarding ACTA PROTOZOOLOGICA, contact Editor, Nencki Institute of Experimental Biology, ul. Pasteura 3, 02-093 Warszawa, Poland; Fax: (4822) 822 53 42; E-mail: jurek@ameba.nencki.gov.pl For more information see Web page **http://www.nencki.gov.pl/ap.htm**).

Front cover: Molnár K., Ranzani-Paiva M. J., Eiras J. C. and Rodrigues E. L. (1998) *Myxobolus macroplasmodialis* sp. n. (Myxozoa: Myxosporea), a parasite of the abdominal cavity of the characid teleost, *Salminus maxillosus*, in Brazil. *Acta Protozool.* **37:** 241-245

This publication is supported by the State Committee for Scientific Research

Desktop processing: Justyna Osmulska, Data Processing Laboratory of the Nencki Institute
Printed at the MARBIS, ul. Poniatowskiego 1, 05-070 Sulejówek, Poland

Acta Protozool. (2002) 41: 1 - 9

ACTA
PROTOZOOLOGICA

Phylogenetic Positions of *Aspidisca steini* and *Euplotes vannus* within the Order Euplotida (Hypotrichia: Ciliophora) Inferred from Complete Small Subunit Ribosomal RNA Gene Sequences

Zigui CHEN and Weibo SONG

Laboratory of Protozoology, KLM, College of Fisheries, Ocean University of Qingdao, Qingdao, P. R. China

Summary. The small subunit rRNA (SSrRNA) genes were sequenced for the hypotrichous ciliates, *Aspidisca steini* and *Euplotes vannus*. These two genera form a monophyletic clade and branch first in the euplotid clade at a long level with strong bootstrap support in both distance matrix and maximum parsimony tree construction methods. The phylogenetic trees further suggest the postulated relationships among families within the order Euplotida that (1) the order Euplotida, represented by *Uronychia*, *Diophrys*, *Euplotidium*, *Euplotes* and *Aspidisca*, forms a paraphyletic group; (2) the families Euplotidae and Aspidiscidae, likely as a monophyletic clade, share a common ancestor; (3) two other "related" genera, *Uronychia* and *Diophrys*, which were usually placed in the family Uronychiidae, branch later and share closer relationship each other than they are to other euplotids. On the contrary, *Euplotidium arenarium*, placed in the family Gastrocirrhidae, might be more closely related to *Uronychia-Diophrys* than to the *Aspidisca-Euplotes* group.

Key words: *Aspidisca steini, Euplotes vannus*, monophyletic, paraphyletic, phylogenetic positions, SSrRNA.

INTRODUCTION

Members of the hypotrichous genera, *Euplotes*, *Aspidisca*, *Diophrys* and *Uronychia*, are among the best known and most readily recognized ciliates with cirri on the functional ventral surface-"hypotrichs" within the order Euplotida Small and Lynn, 1985. They are united by many morphological, morphogenetic, ultrastructural and life history characters, e.g. patterns of ciliature, structure of oral apparatus, number and arrangement of frontal, ventral as well as caudal cirri (Fleury and Fryd-Versavel 1981, Foissner 1982, Fleury *et al.* 1986, Song and Packroff 1993, Berger 2001).

Morphological attributes, features of the life cycle and physiological properties are used to deduce relationships among the families within the order Euplotida (Borror 1972, Curds and Wu 1983, Borror and Hill 1995, Song 1995). However, the euplotid phylogeny still remains confusing considering their evolutionary process and systematic positions of many well-known groups. This is due to the high diversity of the morphology, the difficulty in recognizing which similarities are due to convergent evolution, and the loss of intermediate forms during the long period of time euplotids have existed.

Sequence information from homologous macromolecules shared by all members of a group can be used to

Address for correspondence: Weibo Song, Laboratory of Protozoology, College of Fisheries, Ocean University of Qingdao, Qingdao, 266003, P. R. China; Fax: +86 532 203 2283; E-mail: wsong@ouqd.edu.cn

measure the extent of genetic relationships between organisms (Zuckerlandl and Pauling 1965). In the last few years, molecular characters and ribosomal RNA in particular have been used to reevaluate ciliate phylogeny (Elwood *et al.* 1985, Sogin and Elwood 1986, Lynn and Sogin 1988, Greenwood *et al.* 1991, Schlegel *et al.* 1991, Shin *et al.* 2000). These studies revealed many different results from traditional morphological and ontogenetic characters. Within the ciliates, molecular data indicate that the heterotrich ciliates represent a very basic branch of the tree, and prostome and haptorid ciliates branch off later (Schlegel and Eisler 1996, Lynn and Small 1997).

Including descriptions of the ultrastructure of both morphostatic and morphogenetic states and analyses of gene sequences, particularly the small (SSrRNA) and large subunit ribosomal RNA (LSrRNA) genes, Lynn and Small (1997) presented a revised classification of the phylum Ciliophora Doflein, 1901 which includes 10 classes, 17 subclasses and 57 orders. Together with other three subclasses (Protocruziidia, Choreotrichia and Oligotrichia), the Hypotrichia Stein, 1859 (including the order Kiitrichia and Euplotida) and Stichotrichia Small and Lynn, 1985 (including the order Plagiotomida, Stichotrichida, Urostylida and Sporadotrichida) have been placed in the class Spirotrichea Bütschli, 1889. However, this revision for hypotrichs and stichotrichs (*sensu* Lynn and Small 1997) was mainly based on few published analyses of SSrRNA gene sequences (Elwood *et al.* 1985, Schlegel *et al.* 1991, Sogin *et al.* 1986). With the supplement of more molecular data, particularly the SSrRNA and LSrRNA genes of hypotrichous and stichotrichous ciliates, the more detailed description of their phylogenetic relationships might be proposed.

As part of a comprehensive analysis of ciliate phylogeny, we have studied recently the SSrRNA gene sequences from two "critical" marine hypotrichous ciliates, *Aspidisca steini* and *Euplotes vannus*, in order to provide more information of their phylogenetic positions. Together with sequences of other hypotrichs and stichotrichs, our molecular evolution studies further explore the phylogenetic relationships within this "highly evolved" group. Meantime, the relationships among families within the order Euplotida based on molecular data are preparatory postulated in our work.

MATERIALS AND METHODS

Ciliate collection and culture. *Aspidisca steini* (Buddenbrock, 1920) Kahl, 1932 and *Euplotes vannus* (Müller, 1786) Diesing, 1850 were collected from the coast of Qingdao, China (salinity about 32-34 ‰). Clonal cultures were established and maintained in autoclaved marine water at room temperature with rice grains to enrich natural bacteria as food for the ciliates.

Identification of species. Live specimens were observed with phase contrast and differential interference microscopes at various magnifications. Protargol silver impregnation technique (Wilbert 1975) was applied to reveal the infraciliature. The silverline system was impregnated with Chatton-Lwoff method introduced by Corliss (1953). Specimens were compared to previous papers (Curds 1975, Wu and Curds 1979, Song and Packroff 1996/97, Song and Wilbert 1997). Authorship of species is according to Berger (2001). Systematic and terminology at the ordinal level and above are mainly based on Lynn and Small (1997).

Extraction of genomic DNA. Cells were rinsed three times with sterile artificial marine water after being starved overnight and then pelleted by centrifugation. 0.5 ml lysis buffer (10mM Tris-HCl, pH 8.3; 50mM KCl; 2.5mM $MgCl_2$; 0.6% Tween 20; 0.6% Nonidet P40; 60μg/ml Proteinase K) was added to extract DNA at 56 °C for 2 h. After incubation, DNA was extracted with an equal volume of phenol:chloroform-isoamyl alcohol (25:24:1) and precipitated with 70% alcohol. DNA was stored at -20 °C (Kusch and Heckmann 1996, Chen *et al.* 2000, Chen and Song 2001).

PCR amplification. Amplifications by PCR were carried out in a total volume of 100 μl containing 10 mM Tris-HCl, pH 8.3; 50 mM KCl; 0.1% Triton X-100; 3 mM $MgCl_2$; 0.2 mM dNTP; 0.5 mM of each oligonucleotide primer (16s-like F: 5'-AACCTGGTTGATCCT GCCAGT-3'; 16s-like R: 5'-TGATCCTTCTGCAGGTTCACC TAC-3'); 50 ng of genomic DNA and 5U Taq Pfu DNA polymerase (Sangon Bio. Co., Canada). The reaction mixtures were denatured at 94 °C for 5 min before the polymerase added, followed by the first 5 cycles consisting of denaturation for 1 min at 94 °C, primer annealing for 2 min at 56 °C, and extension for 2 min at 72 °C. In the subsequent 35 cycles, the annealing temperatures were rise to 62 °C. The circulation was followed by a final extension step for 5 min at 72 °C (Elwood *et al.* 1985, Medlin *et al.* 1988, Chen and Song 2001).

Cloning and Sequencing of SSrRNA gene. The amplified products were extracted with UNIQ-5 DNA Cleaning Kit (Sangon Bio. Co., Canada) and inserted into a pUCm-T vector. The plasmid mini-prep spin column kit (Sangon Bio. Co., Canada) was used to harvest and purify plasmid DNA. DNA sequencing for *Aspidisca steini* and *Euplotes vannus* was accomplished using the ABI Prism 377 Automated DNA Sequencer (Applied Biosystems Inc.) with three forward and three modified reverse 16S sequencing primers (Elwood *et al.* 1985, Medlin *et al.* 1988) as well as the RV-M and M13-20 primers. All sequences were confirmed from both strands.

Sequence availability. The nucleotide sequences in this paper are available from the GenBank/EMBL databases under the following accession numbers: *Diophrys appendiculata* AY004773 (Chen and Song 2001), *Euplotidium arenarium* Y19166 (Petroni *et al.* 2000), *Euplotes aediculatus* X03949 (Sogin *et al.* 1986), *Holosticha multistylata* AJ277876 (Shin *et al.* 2000), *Onychodromus quadricornutus* X53485 (Schlegel *et al.* 1991), *Oxytricha granulifera* X53486 (Schlegel *et al.* 1991), *Sterkiella nova* (= *Oxytricha nova*) X03948 (Elwood *et al.* 1985), *Stylonychia pustulata* X03947 (Elwood *et al.* 1985), *Uronychia transfuga* AF260120 (Chen and Song 2001). *Protocruzia* sp1 X65153 (Hammerschmidt *et al.* 1996), *Protocruzia* sp2 AF194409 (Shin *et al.* 2000) and *Blepharisma americanum* M97909 (Greenwood *et al.* 1991) were used as the outgroup species.

Phylogenetic analyses. The sequences were aligned with other SSrRNA gene sequences using a computer assisted procedure, Clustal W, ver. 1.80 (Thompson *et al.* 1994), and refined by considering the conservation of both primary and secondary structures (Elwood *et al.* 1985). PHYLIP package, ver. 3.57c (Felsenstein 1995) was used to calculate the sequence similarity and evolutionary distances between pairs of nucleotide sequences using the Kimura (1980) two-parameter model. Distance-matrix trees were then constructed using the Fitch and Margoliash (1967) least-squares [LS] method and the neighbor-joining [NJ] method (Saitou and Nei 1987). For the maximum-parsimony [MP] analysis, sequence data were reduced from 1790 sites to 648 phylogenetically informative sites. The DNAPARS program in PHYLIP was used to find the most parsimonious tree (Kluge and Farris 1969). Both parsimony and distance data were bootstrap resampled 1,000 times (Felsenstein 1985).

RESULTS

Sequences and Comparisons

The complete SSrRNA gene sequences were determined for *Aspidisca steini* (1746 nucleotides, GenBank/EMBL accession number AF305625) and *Euplotes vannus* (1890 nucleotides, GenBank/EMBL accession number AY004772) (Fig. 1). The GC content (44.96% *A. steini*; 43.81% *E. vannus*) is in the similar range as in other ciliates (Elwood *et al.* 1985, Sogin *et al.* 1986, Schlegel *et al.* 1991, Chen and Song 2001).

Structural similarity and evolutionary distance values were calculated pairwise as described (Jukes and Cantor 1969, Elwood *et al.* 1985) between the sequences aligned in Fig. 1 and those of other hypotrichs as well as *Blepharisma americanum* (Table 1). The sequence of *E. vannus* differed in 132 nucleotides from the sequence of *E. aediculatus* (structural similarity 90.93%). 225 sites are different between *A. steini* and *E. vannus* (structural similarity 82.95%), and 229 sites differ between *A. steini* and *E. aediculatus* (structural similarity 82.86%).

Distance Matrix Analysis

Both least-squares [LS] and neighbor-joining [NJ] analyses provide strong bootstrap support for the monophyly of the class Spirotrichea *sensu* Lynn and Small 1997 (100% [LS], 100% [NJ], Fig. 2), as well as the stichotrichs (e.g. *Sterkiella nova*, *Stylonychia pustulata*, *Onychodromus quadricornutus*, *Holosticha multistylata* and *Oxytricha granulifera*) (100% [LS], 98% [NJ], Fig. 2). The subclass Protocruziidia, represented by *Protocruzia*, forms a sister clade to other spirotrichs (100% [LS], 100% [NJ], Fig. 2). However, the sister group relationship between hypotrichs (e.g. *Uronychia transfuga*, *Diophrys appendiculata*, *Euplotidium arenarium*, *Aspidisca steini*, *Euplotes aediculatus* and *E. vannus*) and stichotrichs is not bootstrap supported.

As shown in Fig. 2, *Euplotes* and *Aspidisca* branch first from the hypotrichous clade at a very long level and form a monophyletic clade as a sister group to all other hypotrichous / stichotrichous taxa with strong bootstrap support (100% [LS], 100% [NJ]). *Euplotidium*, *Diophrys* and *Uronychia* represent other branching lineage though some bootstrap values are not very high. The stichotrichs might diverge later from hypotrichous line. Hence, the subclass Hypotrichia, as well as the order Euplotida, is supported as a paraphyletic clade. However, the separations between some genera within the euplotids are very deep and difficult to be resolved, e.g. the large distance between *E. aediculatus* and *U. transfuga* or *Aspidisca steini* and *Diophrys appendiculata* (Table 1).

Maximum Parsimony Analysis

The major aspects of the topology of the maximum parsimony trees (Fig. 3) are similar to those of the distance matrix trees (Fig. 2).

DISCUSSION

Phylogenetic Positions of *Euplotes* and *Aspidisca*

Since the density of species in a clade can stabilize that clade's position in the topology (Smith 1994), we hence sequenced another *Euplotes* species, *E. vannus*, to assess its systematic position within the subclass Hypotrichia. Together with the new SSrRNA gene sequence for *Aspidisca steini*, the molecular data provide a strong and unambiguous result: the order Euplotida (*Uronychia*, *Diophrys*, *Euplotidium*, *Euplotes* and *Aspidisca et al.*) should be placed as the earliest diverging taxon after the hypotrichs separated from the main line (Figs 2, 3). Further, the long branching of *Euplotes* and *Aspidisca* in our trees might be the consequence of unusually high genetic substitution rates or "fast evolutionary clock speeds" in Euplotida (Sogin *et al.* 1986). To our knowledge, both of them are likely more evolved than other sister groups within the subclass Hypotrichia.

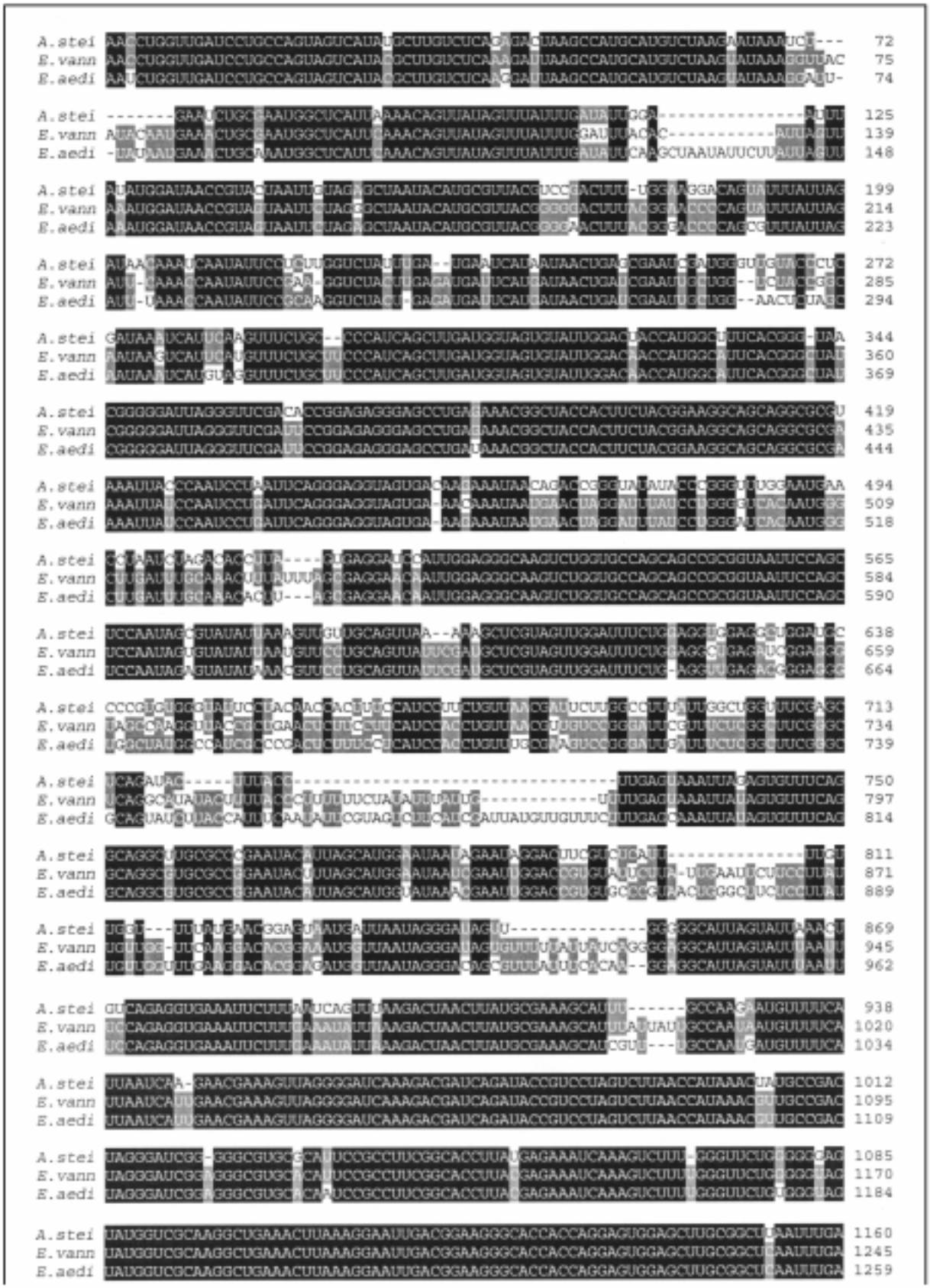
A.stei
E.vann
E.aedi

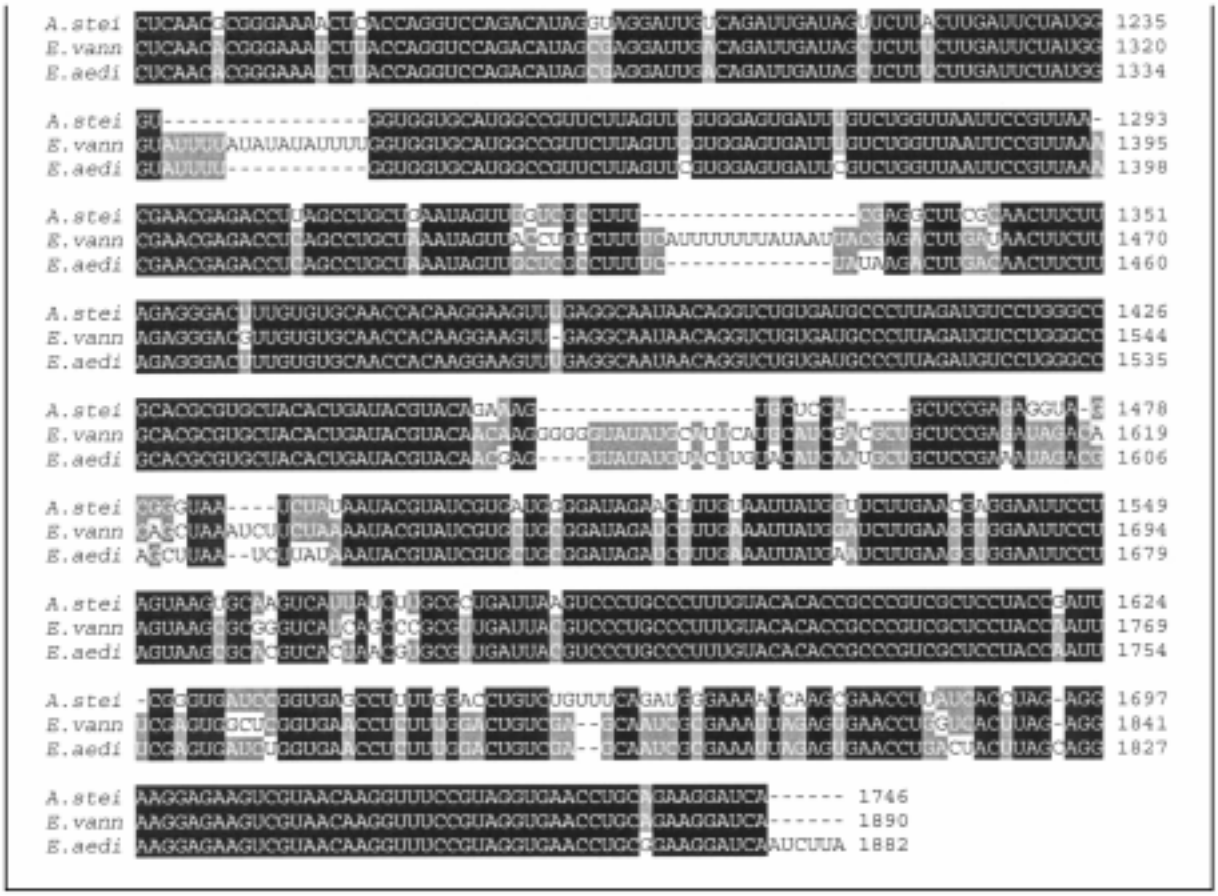

Fig. 1. Small subunit rRNA gene sequences of the euplotid ciliates *Aspidisca steini* (*A. stei*) and *Euplotes vannus* (*E. vann*) aligned with the sequences from *Euplotes aediculatus* (*E. aedi*) (Sogin *et al.* 1986). Numbers at the end of lines indicate the number of nucleotides. The differences in sequence length were compensated for by introducing alignment gaps (-) in the sequences. Matched sites are marked with black color, while unmatched are gray

Postulated evolutionary order for the families within the order Euplotida

Borror and Hill (1995) divided the order Euplotida into five families: Gastrocirrhidae, Certesiidae, Uronychiidae, Aspidiscidae and Euplotidae on the basis of morphology, stomatogenesis, ultrastructure, cyst structure, and behavior. Including some morphological and ontogenetic characters involved in early differentiation of members of the order Euplotida (e.g. short and stubby dorsal cilia, relatively stable number of five developmental streaks in the fronto-ventral cirri field, lower ratio of cell length and width), they postulated phylogenetic relationships among these families. Our current work supports their hypothesis basically: (1) Euplotidae and Aspidiscidae diverge first from the euplotid line and share a common ancestor as a monophyletic clade (Figs 2, 3); and (2) *Uronychia* and *Diophrys*, placed in the family Uronychiidae by Borror and Hill 1995, branch later and share closer relationship each other (with structural similarity 0.9119) than they are to other euplotids (Table 1).

However, our molecular data indicate that *Euplotidium arenarium*, a member of the family Gastrocirrhidae by Borror and Hill (1995), is more closely related to *Uronychia-Diophrys* than to *Aspidisca-Euplotes* group (Figs 2, 3). Considering the unique pattern of ciliature, specialized macronuclei, absence of the caudal cirri and the single left marginal cirrus, *Euplotidium* shows evidently closer relation to *Euplotes* than to other euplotids (Song 1995). Since there is only

Table 1. 16s-like SSrRNA structural similarity (upper half) and evolutionary distance (lower half) data determined by the Elwood *et al.* (1985) and Jukes and Cantor (1969) formulas for conversion of structural similarity for available hypotrichous ciliates. Sources of data for the aligned SSrRNA gene sequences are listed in Materials and Methods

	S. nov	*S. pus*	*O. qua*	*O. gra*	*H. mul*	*U. tra*	*D. app*	*E. are*	*A. ste*	*E. aed*	*E. van*
S. nov	-	0.9853	0.9774	0.9642	0.9563	0.9275	0.9121	0.9191	0.8905	0.8278	0.8304
S. pus	0.0148	-	0.9752	0.9608	0.9473	0.9196	0.9109	0.9157	0.8888	0.8262	0.8282
O. qua	0.0241	0.0270	-	0.9603	0.9462	0.9241	0.9155	0.9169	0.8894	0.8240	0.8304
O. gra	0.0353	0.0418	0.0406	-	0.9679	0.9257	0.9120	0.9213	0.8916	0.8246	0.8310
H. mul	0.0436	0.0527	0.0533	0.0316	-	0.9172	0.8973	0.9173	0.8706	0.8148	0.8162
U. tra	0.0777	0.0796	0.0827	0.0780	0.0851	-	0.9119	0.9098	0.8898	0.8167	0.8302
D. app	0.0924	0.0956	0.0872	0.0941	0.1065	0.0910	-	0.9085	0.8900	0.8254	0.8258
E. are	0.0776	0.0789	0.0808	0.0762	0.0801	0.0880	0.0958	-	0.8959	0.8258	0.8372
A. ste	0.1221	0.1255	0.1262	0.1232	0.1344	0.1240	0.1208	0.1088	-	0.8286	0.8295
E. aed	0.1779	0.1837	0.1816	0.1833	0.1830	0.1903	0.1833	0.1653	0.1667	-	0.9093
E. van	0.1746	0.1811	0.1732	0.1728	0.1757	0.1742	0.1738	0.1569	0.1552	0.0781	-

Abbreviation: *S. nov - Sterkiella nova*; *S. pus - Stylonychia pustulata*; *O. qua - Onychodromus quadricornutus*; *O. gra - Oxytricha granulifera*; *H. mul - Holosticha multistylata*; *U. tra - Uronychia transfuga*; *D. app - Diophrys appendiculata*; *E. are - Euplotidium arenarium*; *A. ste - Aspidisca steini*; *E. aed - Euplotes aediculatus*; *E. van - Euplotes vannus*

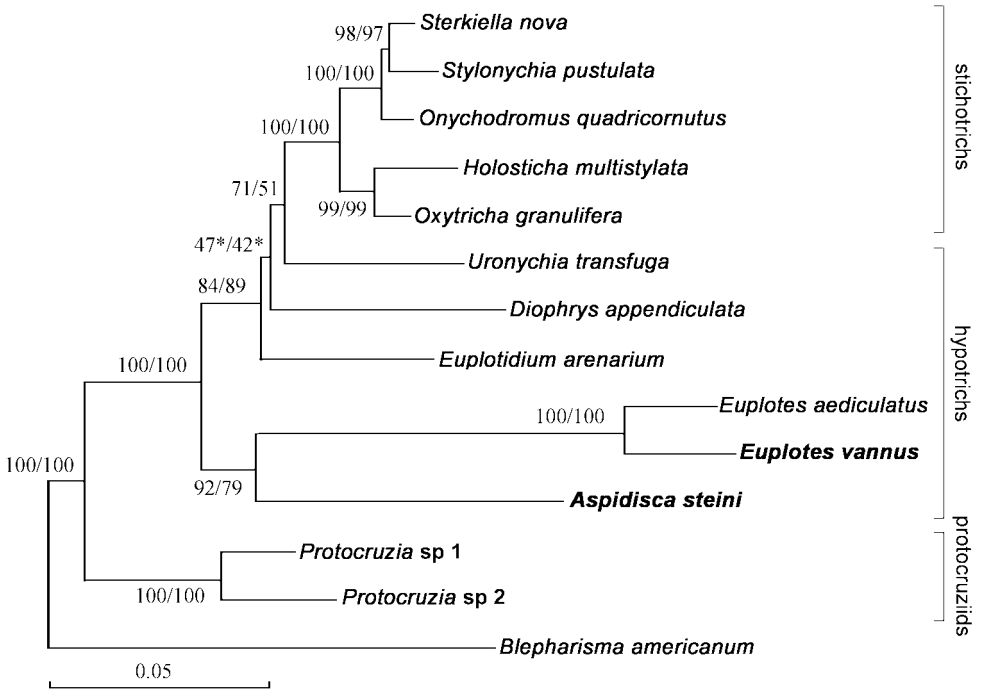

Fig. 2. A distance tree of the hypotrichous ciliates inferred from complete 16s-like small subunit ribosomal RNA gene sequences showing the systematic position of *Aspidisca steini* and *Euplotes vannus* and phylogenetic relationships among the available hypotrichs. Evolutionary distances were calculated by the Kimura (1980) two-parameter correction model and constructed by the Fitch and Margoliash (1967) least-squares [LS] method. The numbers at the nodes represented the bootstrap percentages of 1,000 for the LS method followed by the bootstrap values for the Saitou and Nei (1987) neighbor-joining [NJ] method. Asterisks indicate bootstrap values less than 50%. Evolutionary distance is represented by the branch length to separate the species in the figure. The scale bar corresponds to 5 substitutions per 100 nucleotide positions. The new sequences are represented in boldface

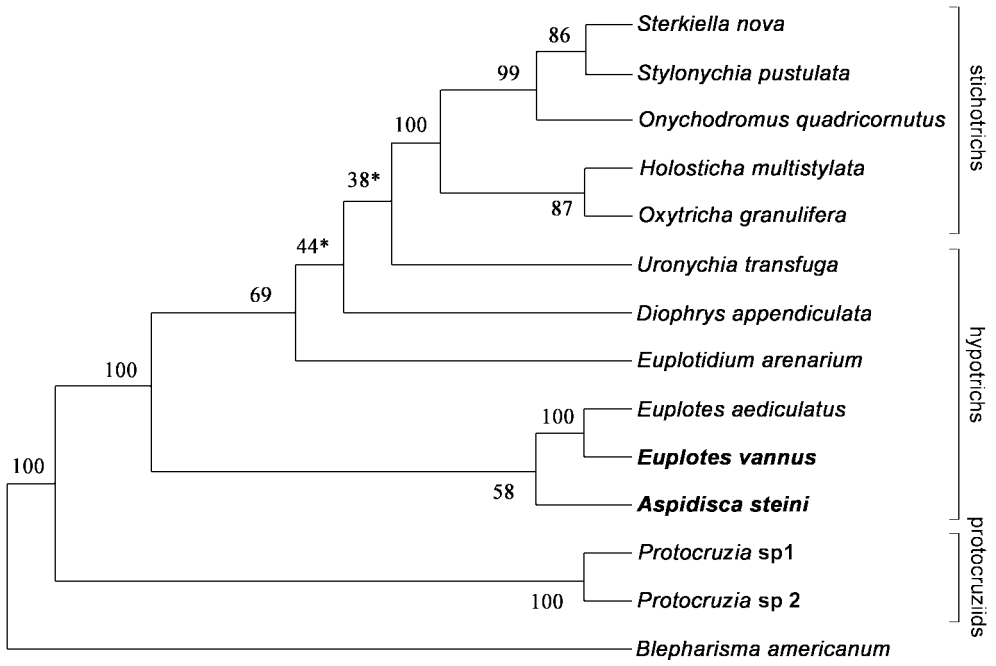

Fig. 3. A maximum-parsimony tree of the hypotrichous ciliates constructed from complete 16s-like small subunit ribosomal RNA sequences indicating the systematic position of *Aspidisca steini* and *Euplotes vannus* and phylogenetic relationships among the available hypotrichs. The numbers at the forks exhibit the percentage of times the group occurred out of the 1,000 trees. No significance is placed on branch lengths connecting the species. The new sequences are represented in boldface

one published analysis of SSrRNA sequence of *Euplotidium* within the family Gastrocirrhidae, it may be premature to define its exact phylogenetic position among Euplotida before more molecular data for euplotids, such as *Gastrocirrhus*, *Cytharoides*, *Certesia*, are available.

Postulated relationships between the subclass Hypotrichia and Stichotrichia

Historically, protozoologist classified *Euplotes* and its presumed relatives with other "highly developed" ciliates in hypotrichs. Based mostly upon ultrastructural characteristics of the dikinetid, Small and Lynn (1985) aligned the order Euplotida in the "primitive" subclass Nassophorea. However, Sogin *et al.* (1986) considered *Euplotes* more closely allied to oxytrichids than to *Paramecium* and *Tetrahymena* based on the SSrRNA gene sequences. Martin (1982) even suggested that *Euplotes*-like ciliates arose from *Oxytricha*-like hypotrichs by increase in size of the buccal cavity and reduction in number of cirri. Later, Lynn and Sogin (1988) described that hypotrichs, stichotrichs, and choreotrichs might be of the same evolutionary branch. According to the molecular data, Lynn (1996) placed oligotrichs, hypotrichs and stichotrichs in the class Spirotrichea that contains five subclasses: Protocruziidia, Hypotrichia, Choreotrichia, Stichotrichia and Oligotrichia (Lynn and Small 1997). Both distance-matrix and maximum-parsimony analyses in our work (Figs 2, 3) support: (1) the monophyly of the class Spirotrichea; (2) the monophyly of the subclass Protocruziidia and Stichotrichia; and (3) the paraphyly of the subclass Hypotrichia, as well as the order Euplotida. Since (1) there is no sister group relationship between hypotrichs and stichotrichs from our trees, (2) *Diophrys* and *Uronychia*, placed in the family Uronychiidae, likely do not branch with the hypotrichs, but with the stichotrichs, and (3) stichotrichs might diverged later from hypotrichous line within the class Spirotrichea, our results suggest that the subclass Stichotrichia and Hypotrichia might be incorporated together.

Acknowledgements. This work was supported by "The Natural Science Foundation of China" (project number: 39970098), the "Cheung Kong Scholarship Programme" and a research grant by the Educational Ministry of China. We are grateful to Dr. D. H. Lynn, University of Guelph, Canada, Dr. A.-D. G. Wright, Animal

Production, CSIRO, Private Bag, Australia and Dr. A. Liang, Laboratory of Biological Engineering, Shanxi University, P. R. China for some constructive suggestions. Our thanks are also due to Miss H. Shang, graduate student of the Laboratory of Protozoology, College of Fisheries, Ocean University of Qingdao, for some assistance in PCR reaction and data treatment.

REFERENCES

Berger H. (2001) Catalogue of Ciliate Names 1. Hypotrichs. Verlag Helmut Berger, Salzburg

Borror A. C. (1972) Revision of the order Hypotrichida (Ciliophora, Protozoa). *J. Protozool*. **19:** 1-23

Borror A. C., Hill B. F. (1995) The order Euplotida (Ciliophora): taxonomy, with division of Euplotes into several genera. *J. Euk. Microbiol.* **42:** 457-466

Chen Z., Song W. (2001) Phylogenetic positions of *Uronychia transfuga* and *Diophrys appendiculata* (Euplotida, Hypotrichia, Ciliophora) within hypotrichous ciliates inferred from the small subunit ribosomal RNA gene sequences. *Europ. J. Protistol.* (in press)

Chen Z., Song W., Warren A. (2000) Studies on six *Euplotes* spp. (Ciliophora: Hypotrichida) using RAPD fingerprinting, including a comparison with morphometric analyses. *Acta. Protozool.* **39:** 209-216

Corliss J. O. (1953) Silver impregnation of ciliated protozoa by the Chatton-Lwoff technique. *Stain. Technol.* **28:** 97-100

Curds C. R. (1975) A guide to the species of the genus *Euplotes* (Hypotrichida, Ciliatea). *Bull. Br. Mus. nat. Hist. (Zool.)* **28:** 1-61

Curds C. R., Wu I. C. H. (1983) A review of the Euplotidae (Hypotrichida, Ciliophora). *Bull. Br. Mus. Nat. Hist. (Zool.)* **44:** 191-247

Elwood H. J., Olsen G. J., Sogin M. L. (1985) The small-subunit ribosomal RNA gene sequences from the hypotrichous ciliates *Oxytricha nova* and *Stylonychia pustulata*. *Mol. Biol. Evol.* **2:** 399-410

Felsenstein J. (1985) Confidence limits on phylogenies: An approach using the bootstrap. *Evolution* **39:** 783-791

Felsenstein J. (1995) "PHYLIP: Phylogeny Inference Package," Version 3.57c. Department of Genetics, University of Washington, Seattle, WA

Fleury A., Fryd-Versavel G. (1981) Données nouvelles sur quelques processus morphogénétiques cgez les hypotriches, notamment dans le genera *Euplotes*: leur contribution a l'approche evolutionniste du probleme de la regulation de l'activité morphogénétique chez les cilie. *J. Protozool.* **28:** 283-291

Fleury A., Iftode F., Deroux G., Fryd-Versavel G. (1986) Unity and diversity in the Hypotricha (Protozoa, Ciliata): III. Elements of comparative ultrastructure of various members of the suborder Pseudohypotrichina and general remarks. *Protistologica*. **22:** 65-88

Fitch W. M., Margoliash E. (1967) Construction of phylogenetic tree. *Science* **155:** 279-284

Foissner W. (1982) Ökologie und Taxonomie der Hypotrichida (Protozoa: Ciliophora) einiger Österreichischer Boden. *Arch. Protistenk.* **126:** 19-143

Greenwood S. J., Schlegel M., Sogin M. L., Lynn D. H. (1991) Phylogenetic relationships of *Blepharisma americanum* and *Colpoda inflata* within the phylum Ciliophora inferred from complete small subunit rRNA gene sequence. *J. Protozool.* **38:** 1-6

Hammerschmidt B., Schlegel M., Lynn D. H., Leipe D. D., Sogin M. L., Raikov I. B. (1996) Insights into the evolution of nuclear dualism in the ciliates revealed by phylogenetic analysis of rRNA sequences. *J. Eukaryot. Microbiol*. **43:** 225-230

Jukes T. H., Cantor C. R. (1969) Evolution of protein molecules. In: Mammalian Protein Metabolism, (Ed. H. N. Munro). Academic Press, New York, 21-132

Kimura M. **(**1980) A simple method of estimating evolutionary rates of base substitutions through comparative studies of nucleotide sequences. *J. Mol. Evol.* **16:** 111-120

Kluge A. G., Farris J. S. (1969) Quantitative phyletics and the evolution of anurans. *Syst. Zool.* **18:** 1-32

Kusch J., Heckmann K. (1996) Population structure of *Euplotes* ciliates revealed by RAPD fingerprinting. *Ecoscience* **3:** 378-384

Lynn D. H. (1996) Systematics of ciliates. In: Ciliates: Cells as Organisms, (Eds K. Hausmann and P. C. Bradbury). Gustav Fischer, Stuttgart, 51-72

Lynn D. H., Small E. B. (1997) A revised classification of the phylum Ciliophora Doflein, 1901. *Rev. Soc. Mex. Hist. Nat.* **47**: 65-78

Lynn D. H., Sogin M. L. (1988) Assessment of phylogenetic relationships among ciliated protists using partial ribosomal RNA sequences derived from reverse transcripts. *BioSystems.* **21:** 249-254

Petroni G., Spring S., Schleifer K. H., Verni F., Rosati G. (2000) Defensive extrusive ectosymbionts of *Euplotidium* (Ciliophora) that contain microtubule-like structures are bacteria related to Verrucomicrobia. *Proc. Natl. Acad. Sci. U.S.A.* **97:** 1813-1817

Martin J. (1982) Évolution des patrons morphogénétique et phylogenese dans le sous-ordre des Sporadotrichina (Ciliophora, Hypotrichida). *Protistologica.* **18:** 431-447

Medlin L., Elwood H. J., Stickel S., Sogin M. L. (1988) The characterization of enzymatically amplified eukaryotic 16S-like rRNA-coding regions. *Gene* **71:** 491-499

Saitou N., Nei M. (1987) The neighbor-joining method: A new method for reconstructing phylogenetic trees. *Mol. Biol. Evol.* **4:** 406-425

Schlegel M., Eisler K.(1996) Evolution of ciliates. In: Ciliates: Cells as Organisms, (Eds K. Hausmann and P. C. Bradbury). Gustav Fischer, Stuttgart, 73-94

Schlegel M., Elwood H. J., Sogin M. L. (1991) Molecular evolution in hypotrichous ciliates: sequence of the small subunit RNA genes from *Onychodromus quadricornutus* and *Oxytricha granulifera* (Oxytrichidae, Hypotrichida, Ciliophora). *J. Mol. Evol.* **32:** 64-69

Shin M. K., Hwang U. W., Kim W., Wright A.-D. G., Krawczyk C., Lynn D. H. (2000) Phylogenetic position of the ciliates *Phacodinium* (order Phacodiniida) and *Protocruzia* (subclass Protocruziidia) and systematics of the spirotrich ciliates examined by small subunit ribosomal RNA gene sequences. *Europ. J. Protistol.* **36:** 293-302

Small E. B., Lynn D. H. (1985) Phylum Ciliophora. In: An Illustrated Guide to the Protozoa, (Eds J. J. Lee, S. H. Hutner and E. C. Bovee). Society of Protozoologists Special Publication, Lawrence, KA, 393-575

Smith A. B. (1994) Rooting molecular trees: problems and strategies. *Biol. J. Linn. Soc.* **51:** 279-292

Sogin M. L., Elwood H. J. (1986) Primary structure of the *Paramecium tetraurelia* small-subunit rRNA coding region: phylogenetic relationships within the Ciliophora. *J. Mol. Evol.* **23:** 53-60

Sogin M. L., Swanton M. T., Gunderson J H., Elwood H. J. (1986) Sequence of the small subunit ribosomal RNA gene from the hypotrichous ciliate *Euplotes aediculatus*. *J. Protozool.* **33:** 26-29

Song W. (1995) Preliminary studies on the phylogenetic relationship of genera within the family Euplotidae (Ciliophora, Hypotrichida). *Oceanol. Limnol. Sinica.* **26:** 527-534 (in Chinese)

Song W., Packroff G. **(**1993) Beitrag zur Morphogeneses des marinen Ciliaten *Diophrys scutum* (Dujardin, 1841) (Ciliophora, Hypotrichida). *Zool. Jb. Anat.* **123:** 85-95

Song W., Packroff G. (1996/97) Taxonomische Untersuchungen an marinen Ciliaten aus China mit Beschreibungen von Zwei neuen Arten, *Strombidium globosaneum* nov. spec. und *S. platum* nov. spec. (Protozoa, Ciliophora). *Arch. Protistenkd.* **147:** 331-360

Song W., Wilbert N. (1997) Morphological investigation on some free living ciliates (Protozoa, Ciliophora) from China Sea with description of a new hypotrichous genus, *Hemigastrostyla* nov. gen. *Arch. Protistenkd.* **148:** 413-444

Thompson J. D., Higgins D. G., Gibson T. J. **(**1994) CLUSTAL W: improving the sensitivity of progressive multiple sequence alignment through sequence weighting, positions-specific gap penalties and weight matrix choice. *Nucl. Acis. Rese.* **22:** 4673-4680

Wilbert N. (1975) Eine verbesserte Technik der Protärgolimpragnation für Ciliaten. *Mikrokosmos* **64:** 171-179

Wu I. C. H., Curds C. R. (1979) A guide to the species of the genus *Aspidisca*. *Bull. Br. Mus. nat. Hist.* (*Zool.*) **36:** 1-34

Zuckerlandl E., Pauling L. **(**1965) Molecules as documents of evolutionary history. *J. Theor. Biol.* **8:** 357-366

Received on 7th May, 2001; accepted on 2nd October, 2001

Acta Protozool. (2002) 41: 11 - 16

ACTA
PROTOZOOLOGICA

Pulsed Field Gel Electrophoresis of Three Microsporidian Parasites of Fish

Josep M. AMIGÓ[1], Maria Pilar GRACIA[1], Humbert SALVADÓ[1] and Christian P. VIVARÉS[2]

[1]Laboratori de Protozoologia, Departament de Biologia Animal, Universitat de Barcelona, Barcelona, Spain ; [2]Laboratoire de Biologie Comparee des Protistes, Université Blaise Pascal, Clermont-Ferrand, France

Summary. The technique of pulsed field gel electrophoresis has been used to differentiate the chromosomes of *Glugea stephani*, *Microgemma ovoidea*, and two isolates of *Spraguea lophii* from different regions of Spain (Atlantic Ocean at Galicia and Mediterranean Sea at Catalonia). Although the karyotype of *M. ovoidea* could not be completely resolved, the range of sizes of its chromosomes was obtained (282-2601Kb). *G. stephani* showed 15 bands ranging 340-2654Kb and an estimated total size of the haploid genome of about 16775Kb. Both isolates of *S. lophii* had a very similar karyotype with 10 bands for the Atlantic isolate (range 266-1076 Kb) and 11 bands for the Mediterranean isolate (range 271-1120Kb). Digital processing of the gels allowed detection of non-homologous chromosome co-migration and revealed that both *S.lophii* isolates had 15 different kinds of DNA fragments, which could be interpreted by a homozygotic hypothesis (15 chromosomes) or a heterozygotic hypothesis (14 chromosome pairs, 13 pairs with the same size for both homologous, and a pair formed by a chromosome of about 423-490 Kb and its homologous of 353-495Kb).

Key words: DNA, *Glugea stephani*, heterozygosis, *Microgemma ovoidea*, PFGE, *Spraguea lophii*.

INTRODUCTION

Few studies of the microsporidian genome have been undertaken. The ribosomal RNA sequences have been the most studied field, especially for use in molecular phylogenies (Vossbrinck *et al*. 1987, 1993; Vossbrinck and Woese 1989; Hartakeerl *et al*. 1993; Malone and McIvor 1993; Zhu *et al*. 1993a, b, c, d; 1994). However, one of the perspectives for the future is the potential of those sequences for in vitro hybridization diagnosis (Zhu *et al*. 1993a).

Addres for correspondence: Josep M. Amigó, Laboratori de Protozoologia, Departament de Biologia Animal, Universitat de Barcelona, 08028 Barcelona, Spain

Despite this relative availability of sequence data there is little information on the organization of the microsporidian genome. This is due to the fact that microsporidian cells divide by cryptomitosis and therefore the different chromosomes cannot be seen as they can be seen in higher eukaryots during cell division. However the technique of pulsed field gel electrophoresis (PFGE) has permitted the separation of very large DNA fragments, so that chromosomes can be counted and sized. These are called molecular karyotypes.

Various molecular karyotypes can be found in the literature: *Nosema furnacalis, Nosema pyrausta* (Munderloh *et al*. 1990), *Vavraia oncoperae*, *Vairimorpha sp.* and *Nosema costelytrae* (Malone and McIvor 1993), *Glugea atherinae* and *Spraguea lophii*

(Biderre *et al.* 1994), *Nosema locustae* studied by Street (1994) and *Nosema bombycis*, studied per Kawakami *et al.* (1994). Some other data are available in the literature on other aspects of the microsporidian genome such as the location of RNAr genes in the chromosomes of about 770Kb (Kawakami 1994). The ploidy of some species of *Vairimorpha* are also known, although the available data is based on observations made on different species of this genus (Canning 1988). Other techniques such as flow cytometry have been used to compare the relative DNA contents of different microsporidian spores (Amigó *et al.* 1994)

In this paper a study is presented on the molecular karyotypes of spores of the microsporidian parasites of fish, *Glugea stephani*, *M. ovoidea* and two isolates of *Spraguea lophii* (from fish of the Atlantic Ocean and the Mediterranean Sea).

MATERIALS AND METHODS

Organisms. *Microgemma ovoidea* (Thèlohan, 1895) Amigó *et al.* (1996) obtained from *Cepola macrophthalma* L. caught in the Catalan coasts (NW Mediterranean Sea); *Glugea stephani* (Hagenmüller, 1899) Woodcock (1904) from *Platichthys flesus* L. in the western coast of Denmark; *Spraguea lophii* (Doflein, 1898) Weissenberg (1976) from *Lophius piscatorius* L. in Galicia (NW Spain); and *S. lophii* from *Lophius budegassa* L. in the Catalan coasts (NW Mediterranean). Microsporidian cysts were taken from hosts and homogenized. Spore suspensions were purified from this homogenate by centrifugation in discontinuous Percoll gradients (Jouvenaz 1981) and finally washed by centrifugation in Ringer's medium.

Sample preparation. Samples for PFGE were prepared according to Biderre *et al.* (1994), thus, each sample was centrifuged until a pellet of spores was obtained and resuspended in 500 µl of PBS at 37°C. 500 µl of agarose 2,3% at 37°C were added to this suspension and blocks were prepared in 100 µl molds. Spore suspensions had previously been adjusted to obtain approximately 10^8 spores/agarose block. Once gelified, blocks were treated with a solution of hydrogen peroxide 3% for 20 min at 37°C to induce spore germination (Vavra and Maddox 1976). Under these conditions, and since the sporoplasm emerges from the spore coat via the polar tube, the microsporidian DNA is accessible with only membrane digestion: after induction of germination, the blocks were washed with PBS and finally kept at 50°C for 49 h in a lysis buffer EDTA (0.5M)/n-lauroyl sarcosine (1%)/Proteinase K (2mg/ml). After this digestion, the blocks were ready for analysis.

Electrophoresis. The electrophoresis was made with a gel of agarose 1% in TBE 0.5x (Tris buffer 0,05M, sodium borate 0.025M, EDTA 1mM; adjusted to pH 8,5) in a Hoeffer rotating gel with 3L of TBE 0,5x in a bath kept at 15°C, with a program of 48 h and pulses of 55-95 s. In order to estimate the size of DNA fragments, a preparation of *Saccharomyces cerevisiae* (Strain S28C) was analyzed in parallel. Once finished, the electrophoresis gels were stained with ethidium bromide 0.4 µg/ml for 24 h and photographs obtained with an ultraviolet transilluminator (254 nm) and Polaroid film.

Digital analysis of gels. Prints of the obtained gels were digitallized with a scanner and analyzed using Imat software for electrophoresis gels developed by the Image Analysis and Process Unit of Scientific-Technical Services, University of Barcelona. This analysis permitted automatic recognition of bands, which were lately confirmed manually, giving a very precise location of the band front. After recognition of standard sample location, the program determines the best regression line relating the logarithm of distance and size in Kb, while also making fine adjustments for the trapezoid geometry of the gel.

After this step the program gave the sizes of each DNA band in the gel. Additionally, a quantitative densiometric analysis was made on each band to detect the possible occurrence of multiple bands as a consequence of the presence of non-homologous chromosomes of similar sizes. For this analysis the profiles of intensity of the different samples were obtained by calculating the surface corresponding to each band. Once each peak area was obtained, these were divided by the corresponding size in Kb. An average of four clearly simple bands was made to obtain a common denominator for a quotient that would give the number of fragments for each band (Fig. 1, Table 2)

RESULTS

Of the four analyzed isolates, bands and sizes were resolved for three: both *Spraguea lophii* isolates and *Glugea stephani* (Table 1). *Microgemma ovoidea* could not be resolved, although the range of sizes of chromosomes was obtained. (Fig. 1)

Table 1. Bands/sizes for the isolates of *Glugea stephani* and *Spraguea lophii*

Band number	Size (Kb)		
	Glugea stephani	*Spraguea lophii* (Atlantic isolate)	*Spraguea lophii* (Mediterranean isolate)
1	2654	1076	1120
2	2402	887	915
3	1990	767	796
4	1807	679	607
5	1340	490	510
6	1237	440	453
7	1022	388	423
8	918	353	374
9	690	301	314
10	607	266	295
11	539	271	
12	432		
13	418		
14	379		
15	340		

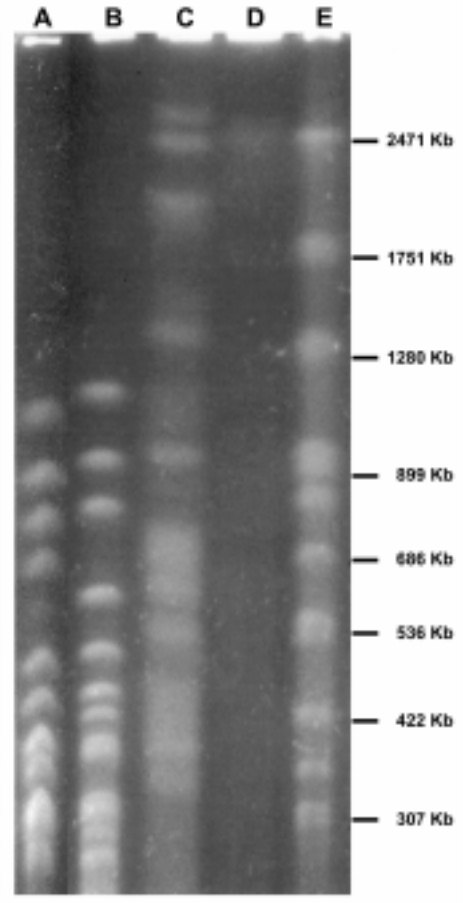

Fig. 1. PFGE of the different samples. A - *Spraguea lophii* (Atlantic); B - *Spraguea lophii* (Mediterranean Sea); C - *Glugea stephani*; D - *Microgemma ovoidea*; E - *Saccharomyces cerevisiae* S28C. Markers correspond to sizes of column E (Sample A had its position and contrast modified in this image to improve visibility)

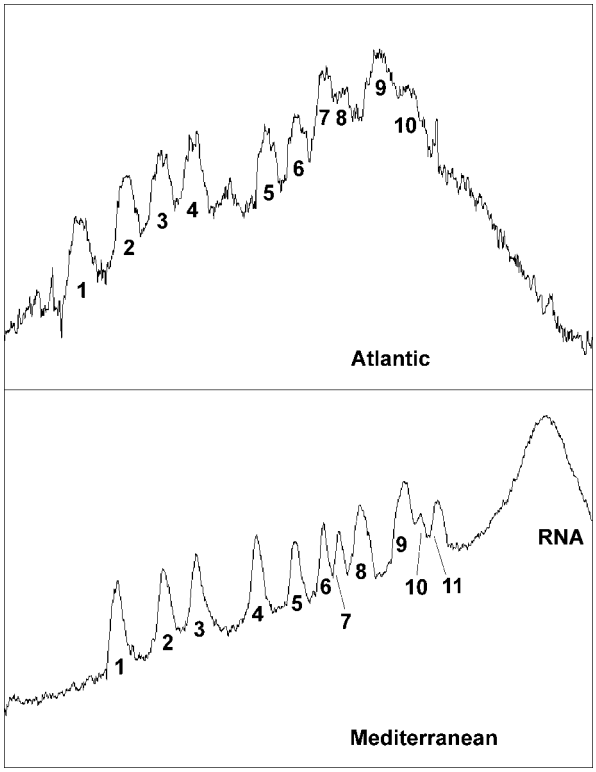

Fig. 2. Profiles of fluorescence intensity of the PFGE of both *Spraguea lophii* isolates

Glugea stephani showed a karyotype with poorly defined bands that could be resolved with a combination of digital analysis techniques and improved photo enhancements. This organism showed 15 bands distributed in a range of 340-2654Kb, giving a total size of the haploid endowment of approximately 16775Kb. Given the poor intensity of bands, no quantification was made for the detection of non-homologous chromosome co-migration.

Atlantic *S. lophii* showed a karyotype with clearly defined bands which was easily resolved with digital image processing (Figs 1, 2). This isolate showed 10 bands in a range of 266-1076 Kb. Naked eye observation of the gel suggested bands 7, 9 and 10 were multiple and the digital analysis based on intensity profiles suggested doublets for bands 7 and 10 and a quartet for band 9. This digital analysis also showed that band 8 had a relative endowment of 0.5 and band 5 a relative endowment of 1.5, which suggested that two homologous chromosomes had different sizes thus migrating to bands 5 and 8. This result suggests heterozygosis in this isolate. Multiple band analysis suggests that the total size of haploid endowment of the Atlantic isolate of *S. lophii* would be of 7272 Kb if the heterozygotic hypothesis is considered, or 7204 Kb if this heterozygotic hypothesis is not considered.

The Mediterranean isolate of *S. lophii* showed an exceptionally clear karyotype with 11 bands very clearly defined in the range of 271-1120 Kb (Figs 1, 2). Digital analysis of the gels showed the composition of multiple bands; thus bands 8 and 11 were doublets, and band 9 a triplet. Migration of homologous chromosomes was also detected with digital analysis of bands 7 and 10. With the homozygotic hypothesis this would then give a haploid

Table 2. Quantitative study of the bands of both *Spraguea lophii* isolates. The weighted number of bands (E) is the result of the division of the column surface/size (C) by the average surface/size of the simple bands (D)

	Spraguea lophii (Atlantic isolate)				Number of fragments	
Band number	(A) size	(B) Surface	(C) Surface/Size	(E) Weighted number of bands	Homozygosis hypothesis	Heterozygosis hypothesis
1	1076	821	0.763	0.92	1	1
2	887	701	0.790	0.95	1	1
3	767	598	0.780	0.94	1	1
4	679	620	0.913	1.10	1	1
5	490	555	1.133	1.37	1	1.5
6	440	394	0.895	1.08	1	1
7	388	691	1.781	2.15	2	2
8	353	183	0.518	0.63	1	0.5
9	301	976	3.243	3.91	4	4
10	266	490	1.842	2.22	2	2
(D) Average surface/size of simple bands (1, 2, 3, 4, 6)			0.828			
	Spraguea lophii (Mediterranean isolate)				Number of fragments	
Band number	(A) size	(B) Surface	(C) Surface/Size	(E) Weighted number of bands	Homozygosis hypothesis	Heterozygosis hypothesis
1	1120	1210	1.080	0.88	1	1
2	915	1012	1.106	0.90	1	1
3	796	1065	1.338	1.09	1	1
4	607	871	1.435	1.17	1	1
5	510	662	1.298	1.06	1	1
6	453	495	1.093	0.89	1	1
7	423	365	0.863	0.70	1	0.5
8	374	929	2.484	2.03	2	2
9	314	1048	3.338	2.72	3	3
10	295	528	1.790	1.46	1	1.5
11	271	672	2.480	2.02	2	2
(D) Average integral/size of simple bands (1, 2, 3, 4, 5, 6)			1.225			

endowment of 7351 Kb while the heterozygotic hypothesis would give a haploid size of 7287Kb for this isolate.

DISCUSSION

The protocol used for the preparation of samples has given optimal results for *S. lophii* isolates but poor results for *G. stephani* and quite bad results for *M. ovoidea*. This difference in the efficiency of the method might be due to the germination rate of each isolate being 4% in the case of *M. ovoidea*, 11% *G. stephani* and 40-50% in *S. lophii*. Furthermore it must also be considered that each isolate of *S. lophii* had been obtained from one cluster of cysts. This procedure not only reduces the heterogeneity of the genomic structure within the isolate but, given the clarity of gel results, suggests a clonal origin of each cluster of

Table 3. Comparison of known microsporidian molecular karyotypes

Species/isolate	Number of bands	Number of chromosomes	Range of sizes (Kb)	Estimate of genome size (Kb)	Reference
Nosema pyrausta	13	-	1390-440	10240	Munderloh *et al.* (1990)
Nosema furnacalis	13	-	1360-440	10240	Munderloh *et al.* (1990)
Nosema locustae	18	-	651-139	5364	Street (1994)
Nosema bombycis	18	-	1500-380	15330	Kawakami *et al.* (1994)
Nosema costelytrae	min 8	-	1810-290	7420	Malone and McIvor (1993)
Vairimorpha sp.	min 8	-	720-1790	9250	Malone and McIvor (1993)
Vavraia oncoperae from "grass grubs"	14	-	1930-130	8000	Malone and McIvor (1993)
Vavraia oncoperae from *Wiseana* sp.	16	-	1830-140	10240	Malone and McIvor (1993)
Glugea atherinae	16	-	2700-420	19510	Biderre *et al.* (1994)
Spraguea lophii from *L. piscatorius* (Atlantic)	12	-	980-230	6220	Biderre *et al.* (1994)
S. lophii from *L. piscatorius* (Atlantic)	10	15	1076-266	7272	Present work
S. lophii from *L. budegassa* (Mediter.)	11	15	1120-271	7287	Present work
Glugea stephani	15	-	2654-340	16775	Present work
Microgemma ovoidea	-	-	2601-282	-	Present work

cysts of *S. lophii*. In the case of *G. stephani* and *M. ovoidea*, clusters do not occur and this procedure of isolation cannot be followed, so the bands tend to be wider and loosely defined since homologous chromosomes of different individuals might show slight differences in size. In this sense, in *G. stephani* isolates there seems to be a dominant haplotype shown by the most clearly defined bands and other minority haplotypes shown as badly defined bands or shadows around the better defined ones.

Comparison of the karyotypes obtained in this study shows that there are clear differences in size of genome and range of chromosome size of *G. stephani* and *S. lophii*, which is not so surprising given the fact that both organisms belong to different genera with very different life and nuclear cycles. Comparison of data presented here with those of other authors shows that *G. stephani* has an endowment quite similar in size and range to *Glugea atherinae*. Furthermore, the results from *S. lophii* are very similar to those presented for the same organism by Biderre *et al.* (1994), despite the fact that the total estimated size is now a bit higher given the results of the digital analysis of gels. A comparison of the literature available on karyotypes is provided on Table 3. In this table, trends can be observed: *Glugea* and *Vavraia* (closely related genera) isolates show karyotypes with a wide range (from hundreds to about 2000 Kb); while isolates from genera with diplokaryotic spores, e.g. *Nosema*, *Vairimorpha* and *Spraguea*, tend to have small genomes of about 7000-9000 Kb. The exception here is *Nosema bombycis* with a 15000 Kb genome.

Special mention must be made on the variability found in the molecular karyotype of *S. lophii*, since despite an observed uniformity in the total size of endowment and number of bands in the isolate studied, the chromosome size seems to change. Such differences cannot be attributed to geographical origin since the number of analyzed samples is too low and, furthermore, our two isolates seem to differ as widely as the isolate of Atlantic origin analyzed by Biderre *et al.* (1994). The heterozygotic hypothesis of karyotype composition of *S. lophii* would then be supported by this variability.

Acknowledgements. The authors wish to thank Dr B. Pinya and Ms. D. Nadal from "Centre d'Investigació i Desenvolupament" (CSIC, Barcelona) for their help and availability to use their technical knowledge and equipment on PFGE, as well as for their advice on the course of this research. This research was supported by funds of the DGICYT (project PB-0807) as well as the Maritime Fisheries Department from the Generalitat de Catalunya.

REFERENCES

Amigó J. M., Gracia M. P., Comas J., Salvadó H., Vivarés C. P. (1994) Comparative study of microsporidian spores by flow cytometric analysis. *J. Euk. Microbiol.* **41:** 210-214

Amigó J. M., Salvadó H., Gracia M. P., Vivarés C. P. (1996) Ultrastructure and development of *Microsporidium ovoideum* (Thél. 1895) Sprague 1977, a microsporidian parasite if the red band fish (*Cepola macrophthalma* L.). Redescription of the organism and reassignment to the genus *Microgemma*, Ralphs & Matthews 1986. *Eur. J. Protistol.* **32:** 532-538

Biderre C., Pagés M., Metenier G., David D., Bata J., Prensier G., Vivarés C. P. (1994) On small genomes in eukaryotic organisms: molecular karyotypes of two microsporidian species (Protozoa) parasites of vertebrates. *C. R. Acad. Sci. Paris (Sciencies de la Vie)* **317:** 399-404

Canning E. U. (1988) Nuclear division and chromosome cycle in microsporidia. *Biosystems* **21:** 333-340

Hagenmüller M. (1899) Sur une nouvelle Myxosporidie, *Nosema Stephani*, parasite du *Flesus passer* Moreau. *C. R. Acad. Sci. Paris* **129:** 836-839

Hartakeerl R. A., Schuitema A. R., De Wachter R. (1993) Secondary structure of the small subunit ribosomal sequence of the microsporidium *Encephalitozoon cuniculi*. *Nul. Acids Res.* **21:** 1489

Jouvenaz D. P. (1981) Percoll: an effective medium for cleaning microsporidian spores. *J. Inverteb. Pathol.* **37:** 319

Kawakami Y., Inoue T., Ito K., Kitamizu K., Hanawa C., Ando T., Iwano H., Ishihara R. (1994) Identification of a chromosome harboring the small subunit ribosomal RNA gene of *Nosema bombycis*. *J. Invert. Pathol.* **64:** 147-148

Malone L. A. , McIvor C. A. (1993) Pulsed field gel electrophoresis of DNA from four microsporidian isolates. *J. Invert. Pathol.* **61:** 203-205

Munderloh U. G., Kurti T. J., Ross S .E. (1990) Electrophoretic characterization of chromosomal DNA from two microsporidia. *J. Invert. Pathol.* **56:** 243-248

Street D. A. (1994) Analysis of *Nosema locustae* (Microsporidia: Nosematidae) chromosomal DNA with pulsed-field gel electrophoresis. *J. Invert. Pathol.* **63:** 301-303.

Thèlohan P. (1895) Recherches sur les myxosporidies. *Bull. Sci. Fr. Belg*. **26:** 100-394

Vavra J., Maddox J. V. (1976) Methods in microsporidiology. In: Comparative Pathobiology. I. Biology of the Microsporidia. (Eds. L. A. Bulla and T. C Cheng) Plenum Press, New York 281-319

Vossbrinck C. R., Woese C. R. (1989) Eukaryotic ribosomes that lack a 5.85S RNA. *Nature* **320:** 287-288

Vossbrinck C. R:, Maddox J. V., Friedman S., Debrunner-Vossbrinck B. A., Woese B. (1987) Ribosomal RNA sequence suggests microsporidia are very ancient eukaryotes. *Nature* **326:** 411-414

Vossbrinck C. R., Baker M. D., Didier E. S., Debrunner-Vossbrinck B. A., Shadduck J. A. (1993) Ribosomal DNA sequences of *Encephalitozoon hellem* and *Enchaphalitozoon cuniculi*: species identification and phylogenetic contruction. *J. Euk. Microbiol.* **40:** 354-362

Woodcock H. M. (1904) On myxosporidia in flat fish. *Trans. Biol. Soc. Liverpool* **18:** 46-62

Zhu X., Tanowitz H. B., Wittner M., Cali A., Weiss L. M. (1993a) Ribosomal RNA sequences of *Enterocytozoon bieneusi* and its potential diagnostic role. *J. Infect. Dis*. **168:** 1570-1575

Zhu X., Tanowitz H. B., Wittner M., Cali A., Weiss L. M. (1993b) Nucleotide sequence of small ribosomal RNA of *Encephalitozoon cuniculi*. *Nucl. Acid Res.* **21:** 1315

Zhu X., Tanowitz H. B., Wittner M., Cali A., Weiss L. M. (1993c) Nucleotide sequence of the small ribosomal RNA of *Septata intestinalis*. *Nucl. Acid Res.* **21:** 4846

Zhu X., Tanowitz H. B., Wittner M., Cali A., Weiss L. M. (1993d) Nucleotide sequence of the small ribosomal RNA of *Ameson michaelis*. *Nucl. Acids Res*. **21:** 3895

Zhu X., Tanowitz H. B., Wittner M., Cali A., Weiss L. M. (1994) Ribosomal RNA sequences of *Enterocytozoon bieneusi*, *Septata intestinalis* and *Ameson michaelis*: Phylogenetic construction and structural correspondence. *J. Euk. Microbiol*. **41:** 204-209

Received on 19th March, 2001; accepted on 12th November, 2001

Acta Protozool. (2002) 41: 17 - 22

ACTA
PROTOZOOLOGICA

The Structure of the Nucleus of *Odonaticola polyhamatus* (Gregarinea: Actinocephalidae), a Parasite of *Mnais strigata* (Hagen) (Odonata: Calopterygidae)

Kasumi HOSHIDE[1] and John JANOVY, Jr.[2]

[1]Biological Institute, Faculty of Education, Yamaguchi University, Yamaguchi, Japan; [2]School of Biological Sciences, University of Nebraska Lincoln, Nebraska, USA

Summary. The nucleus of *Odonaticola polyhamatus* was isolated from the body and observed with light, scanning electron and transmission electron microscopy. The nucleus had a thick thread-like structure with which it was tied to the septum. This thread-like structure has not been reported or described previously. The gregarine nuclear surface was covered with a fine fibrous net. This is the first report of the surface structure of a gregarine nucleus as revealed by SEM. Inside the nuclear membrane was a thin honeycomb layer similar to that reported for some other gregarines. Several spherical nucleoli and numerous electron dense small structures were observed inside the nucleus.

Key words: gamont, Gregarinea, nucleolus, nucleus, *Odonaticola polyhamatus*.

INTRODUCTION

The nuclei of several species of gregarines have been observed by transmission electron microscopy (TEM), but none have been observed by scanning electron microscopy (SEM) (Beam *et al.* 1957, 1959; Desportes 1974). The nuclei of gregarines are sturdy and keep their shape when they are isolated from the body. We have taken an interest in the structure of gregarine nuclei and have tried to clarify some of the structural features that provide their sturdiness. The gregarines which parasitize Odonata are very large and their nuclei are correspondingly large and stout. Therefore, gregarines such as *Odonaticola polyhamatus* are excellent material to use in order to investigate the nuclear ultrastructure by SEM. The huge nucleus of *O. polyhamatus* always exists near the cell's septum, so we also studied the mechanism by which this intracellular location was maintained.

Odonaticola polyhamatus (K. Hoshide, 1977) was first described from the damselfly *Mnais strigata* Hagen, under the name *Hoplorhynchus polyhamatus* (Hoshide 1977). Amoji and Kori (1992) shifted the species from *Hoplorhynchus* Carus to *Odonaticola*

Address for correspondence: Kazumi Hoshide, Biological Institute, Faculty of Education, Yamaguchi University, Yamaguchi, 753-8513 Japan; FAX. +81-83-933-5347; E-mail: khoshide@inf.edu.yamaguchi-u.ac.jp

Sarkar and Haldar, 1981 but misspelled the specific epithet as *polyhematus*; the proper spelling is *polyhamatus* (= "many hooks").

MATERIALS AND METHODS

The species used in this study, *Odonaticola polyhamatus*, is a parasite of the damselfly *Mnais strigata* (Hagen). Host damselflies were collected at Inunaki Gorge in the suburbs of Yamaguchi City, Japan, in June, 1994. The intestines of the host were removed, placed in Ephrussi-Beadle Ringer's salt solution (NaCl 7.3g, KCl 3.5g, $CaCl_2$ 2.8g, in 1 l distilled water), and dissected, and the gamonts removed. Gamont nuclei were isolated from the deutomerite by disrupting individual cells with fine needles. Nuclei were then washed with a stream of Ringer's solution from a fine pipette. Specimens for transmission electron microscopy were prefixed in 5% glutaraldehyde in cacodylate buffer for 2 h and post fixed with 1% osmium tetroxide for 2 h. After fixation, the specimens were dehydrated through an ethanol series and embedded in Spurr's resin. Thin sections were made using an LKB ultramicrotome with a diamond knife and examined in a JEM-1200 EX TEM. Specimens for scanning electron microscopy were fixed and dehydrated using the same methods. Following dehydration with ethanol, they were placed in isoamylacetate and critical point dried using CO_2 as the transition liquid. The dried samples were then placed on an aluminum stub, sputter-coated with gold, and examined with a JEOL T-300 scanning electron microscope.

RESULTS

Odonaticola polyhamatus is a large, solitary, gregarine. The average length of the body is about 2600 μm and reaches a maximum size of 3300 μm. The nucleus is spherical or ellipsoidal, about 50-100 μm in diameter, and always located in the center of the deutomerite endoplasm just behind the septum. Ordinarily, observation of the nucleus of mature gamonts *in vivo* is hindered by the density of the endoplasm (Fig. 1). On rare occasions, the nucleus is located on one side and can be observed near the surface (Figs 2, 3). Following dissection of the deutomerite, the isolated nucleus was covered with debris of endoplasm. The isolated nucleus held its spherical or ellipsoidal shape after removal of this debris with a water-jet from a fine pipette (Figs 4, 5). The nucleus was fixed at the center of the septum by a thick, transparent, thread-like structure 70-80 μm long and 5 μm in diameter (Fig. 6). The surface of nucleus was different from that of most other animal cells. In some specimens the nucleus had an irregular rough surface (Fig. 7), and several grooves extended radially from the point where the thread was attached (Figs 7-9). Many spherical or ellipsoidal granules adhered to the anterior one-fifth surface area, and a thin fibrous net covered these granules (Figs 7, 8). The rest of the surface was covered with a homogeneous multi-layered fine fibrous net (Figs 7-11).

By light microscopy the nucleus was transparent except for the many brown nucleoli. Ten to twenty nucleoli were contained in each nucleus (Figs 3-5). By TEM the nucleoli were spherical and highly electron dense, although some nucleoli had a hollow that was less electron dense (Figs 12, 13). The nucleus was bounded by a double membrane and on the outside could be seen many fine electron dense threads. Between the inner and outer membranes there was a thin, space of low electron density. The inner membrane was lined with a relatively thick porous cortical layer (Figs 12, 13). Tangential sections revealed that this layer had a honeycomb pattern.

DISCUSSION

The nucleus of septate gregarines is always located in the deutomerite, but the location within this part of the cell varies depending on the species. In some species the nucleus is located in the anterior part of the deutomerite, in other species it is in the middle, and in some is found closest to the posterior end. The nucleus of *Odonaticola polyhamatus* is always located near the septum but until the present study, we didn't know why it was fixed in this position. The dense endoplasm made it impossible to see the thread-like structure that connected the nucleus so the center of the septum. With successful isolation of the nucleus, this thread-like structure was observed for the first time. This type of connection has not been observed in gregarines until now. It was not be determined in this study whether the thread-like structure functions only to hold the nucleus in place, or whether it plays other roles in the life of the gregarine.

This is also the first observation of an isolated gregarine nucleus using the scanning electron microscope. The whole body of many gregarines has been shown by SEM, but there has been no observation of an isolated nucleus (Heller and Wise1973, Hildebrand and Vinckier 1975, Walker *et al.* 1979). In most species it is technically difficult to make specimens of isolated nuclei using critical point drying because the nucleus is rather small and fragile compared to the whole body. The nucleus of *O. polyhamatus*, however, is large, and is connected to the septum. At the time of isolation, the nucleus remains

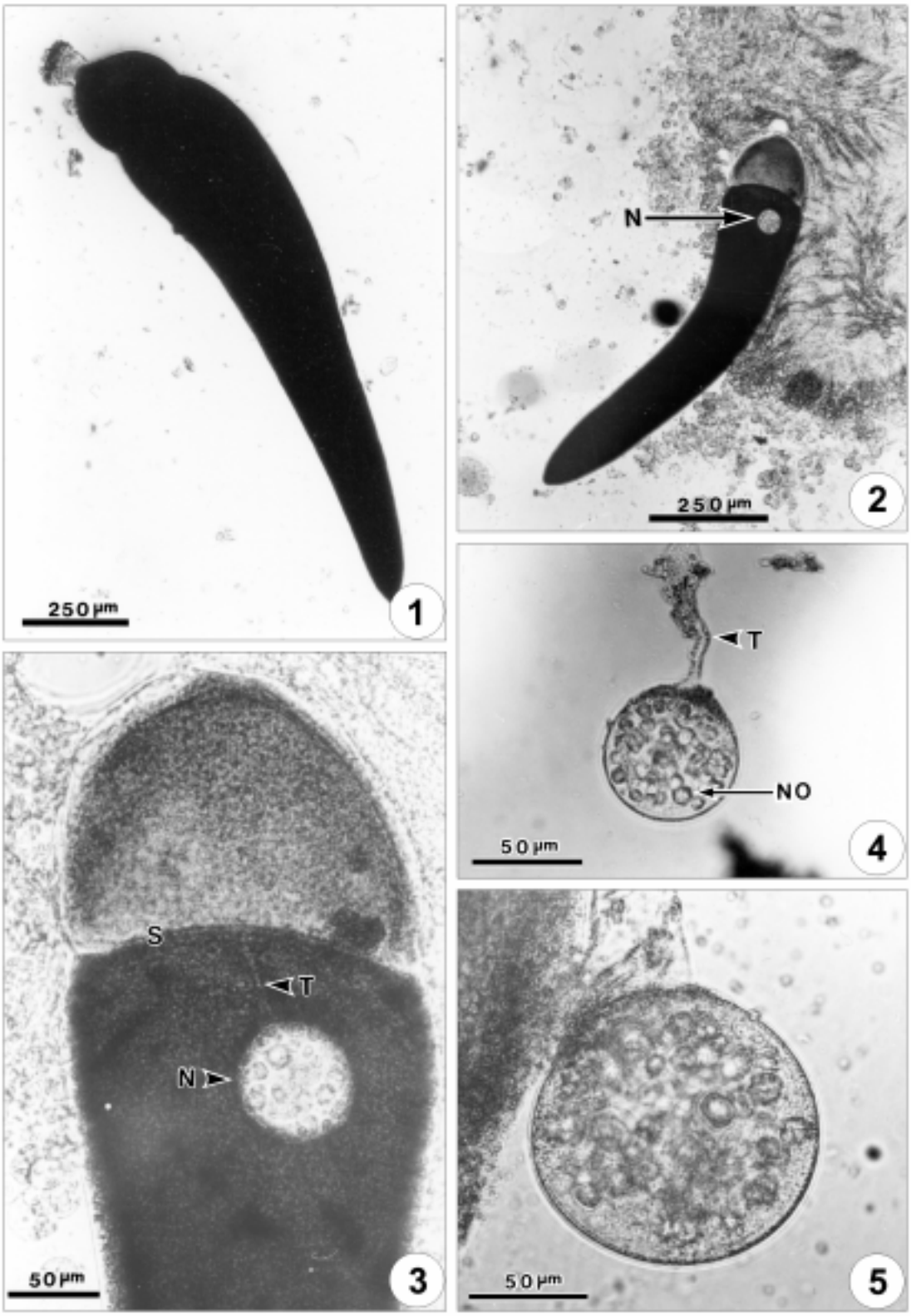

Fig. 1. Mature gamont of *Odonaticola polyhamatus*. Observation of the nucleus is hindered by the dense endoplasm. **Fig. 2.** Another gamont, the nucleus is observed from the surface. N-nucleus. **Fig. 3.** Nucleus in the mature gamont. T-thread-like structure. S-septum. **Fig. 4.** Isolated nucleus with the thread like-structure. Many nucleoli were observed inside the nucleus by light microscope. NO-nucleoli. **Fig. 5.** Another isolated nucleus by light microscope

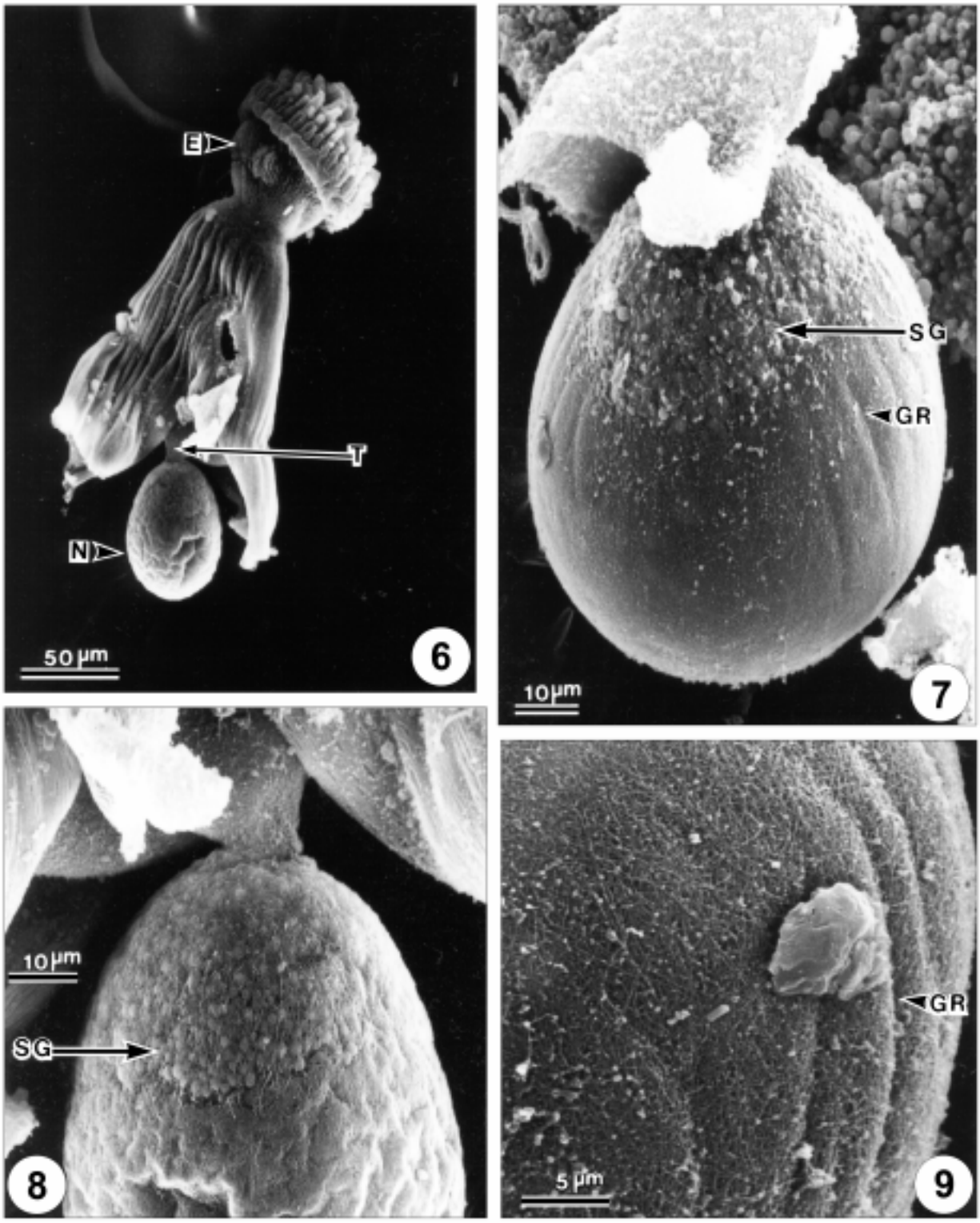

Fig. 6. Dissected gregarine with the nucleus by SEM. E-epimerite. **Fig. 7.** Isolated nucleus connected with a part of the septum. SG-spherical granule, GR-grooves. **Fig. 8.** Anterior part of another isolated nucleus with rough surface. **Fig. 9.** Surface of the nucleus with the fine fibrous net

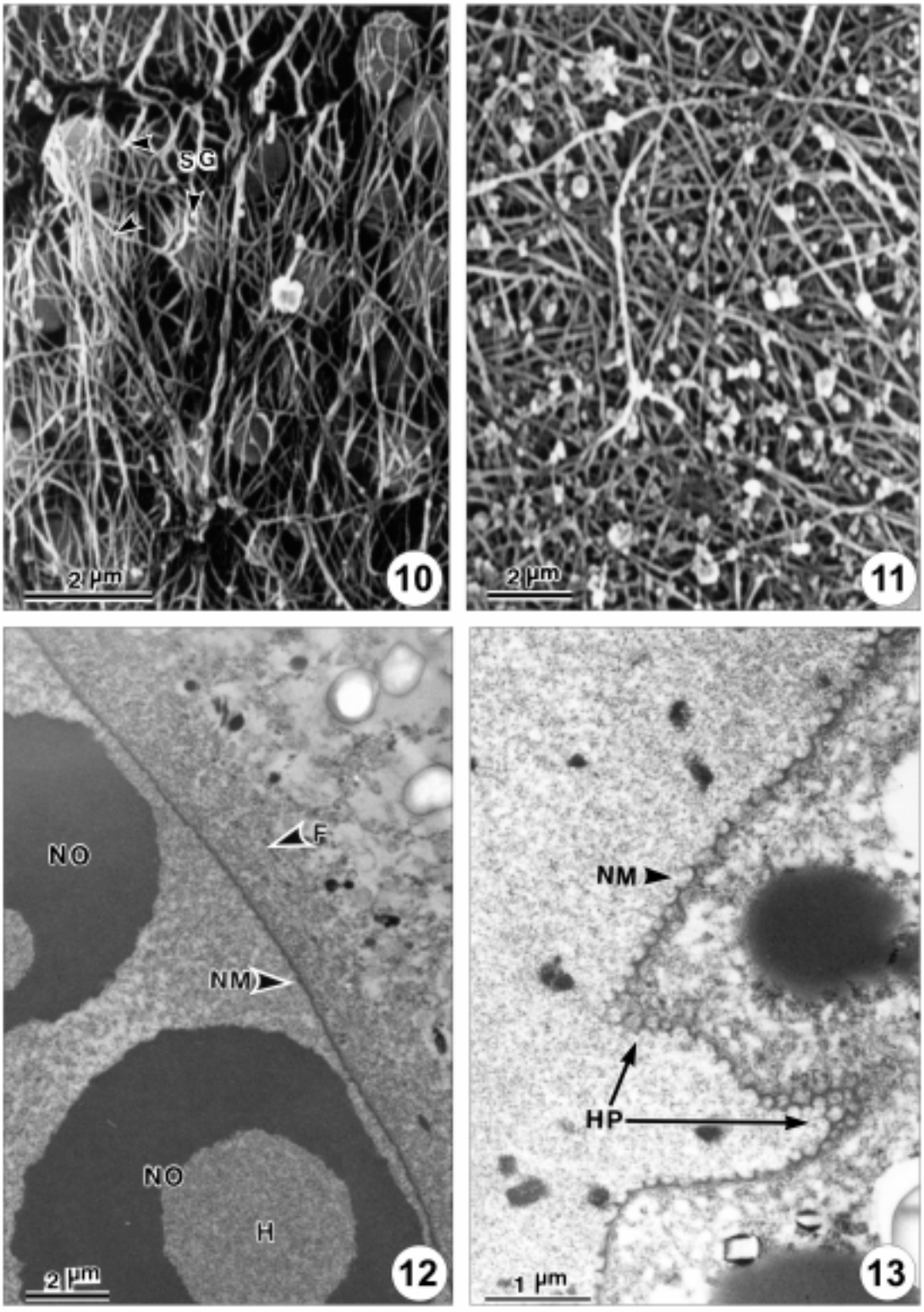

Fig. 10. Magnified fibrous net of the anterior part of nucleus, spherical granules were covered by the fibrous net. **Fig. 11.** Magnified fibrous net of nucleus. **Fig. 12.** Nuclear membrane and nucleolus; fibrous net can be seen outside the nuclear membrane. F-fine fibrous net, NM-nucleus membrane, NO-nucleoli, H-hollow. **Fig. 13.** Nuclear membrane and nucleolus. HP-honeycomb pattern

fastened to a large fragment of the body. Thus we were able to observe the nucleus during processing, and ensure that it was retained during critical point drying.

The nuclear surface of a number of other protozoans has been studied by freeze-fracture techniques. For example, *Trichomonas vaginalis, Tritrichomonas foetus*, and *Blastocystis hominis* have all been shown to have both nuclear pores (Honigberg *et al.* 1984, Yoshikawa *et al.* 1988). No pores were evident on the nucleus of *O. polyhamatus*, but the surface was covered with a fine fibrous network. Thus the *O. polyhamatus* nucleus has a completely different external appearance from the flagellates studied by Yoshikawa *et al.* (1988) and Honigberg *et al.* (1984). In a previous paper, the point was made that comparative ultrastructure could be a key to finding evolutionary relationships among protozoan groups (Hoshide and Todd 1996). Various gregarine species other than *O. polyhamatus* have also been shown to have a honeycomb layer on the nuclear surface (Beam *et al.* 1957, Théodoridès 1959, Hukui 1966, Desportes 1974) and a similar layer was reported earlier for *Amoeba proteus* by Harris and James (1952) and Pitelka (1963). Although the evolutionary significance of this layer is still unknown, the honeycomb and fibrous network are probably the reason why the *O. polyhamatus* nucleus is so stout. Highly electron dense nucleoli have been reported in some gregarines (Hukui 1966, Tronchin and Schrevel 1977) and the nucleoli of *O. polyhamatus* are similarly dense, although some had low density hollows.

In summary, these studies have revealed a new and unique structure in gregarines. The observations explain why nuclear position within the deutomerite is constant in *O. polyhamatus*, and suggest that nuclear position may have a structural basis in other gregarine species. If connections between the nucleus and septum occur in other species, then nuclear position becomes a potential taxonomic character in gregarines.

Acknowledgements. This study was supported in part by Grant-in-Aid 06640905 for Scientific Research from the Ministry of Education, Science and Culture of Japan.

REFERENCES

Amoji S. D., Kori S. S. (1992) Revision of the genus *Odonaticola* Sarkar et Haldar, 1981(Apicomplexa: Sporozoasida: Gregarinasina). *Acta Protozool*. **31:**169-171

Beam H. W., Tahmisian T. N., Devine R., Anderson W. (1957) Ultrastructure of the nuclear membrane of gregarine parasite in grasshoppers. *Exp. Cell Res.* **13:** 200-204

Beam H. W.,Tahmisian T. N., Devine R., Anderson W. (1959) Studies on the fine structure of a gregarine parasitic in the gut of the grasshopper, *Melanoplus differentialis. J. Protozool*. **6:** 136-146

Desportes I. (1974) Ultrastructure et evolution nucléarie des trophozoites d'une grégarine d'ephéméroptère; *Enterocystis fungoides* M. Codreanu. *J. Protozool.* **21:** 83-94

Harris P., James T. W. (1952) Electron microscope study of the nuclear membrane of *Amoeba proteus* in thin section. *Experientia* **8:** 384-385

Heller G., Weise R. W. (1973) A scanning electron microscope study of *Gregarina sp*. from *Udeopsylla nigra*. *J. Protozool*. **20:** 61-64

Hildebrand H. F., Vinckier D.(1975) Nouvelles observations sur la grégarine *Didymophyes gigantea* Stein. *J. Protozool*. **22:** 200-213

Honigberg B. M., Volkmann D., Entzeroth R., Scholtyseck E. (1984) A freeze-fracture electron microscope study of *Trichomonas vaginalis* Donne and *Tritrichomonas foetus* (Riedmuller). *J. Protozool*. **31:** 116-131

Hoshide K. (1977) Notes on the gregarines in Japan. 8. Three new species of Eugregarina from Odonata. *Bull. Fac. Educ. Yamaguchi Univ.* **27:** 93-125

Hoshide K., and Todd K. S. (1996) The fine structure of cell surface and hair-like projections of *Filipodium ozakii* Hukui 1939 gamonts. *Acta Protozool*. **35:** 309-315

Hukui T. (1966) The electron microscopical studies on *Stenophora sp.* from *Skleroprotopus ikedai* Takakuwa, 1940. *Bull. Fukuoka Univ. Educ*. **16:** 141-151

Pitelka D. R.(1963) Electron-Microscopic Structure of Protozoa. Pergamon Press, New York

Sarkar N. K., Haldar D. P. (1981) Observations on a new cephaline gregarine (Protozoa: Sporozoa), *Acanthospora bengalensis* n. sp. from an odonate insect. *Arch. Protistenk.* **124:** 378-384

Théodoridès J. (1959) Etude des eugrégarines au microscope électronique. Proc.15th Intern. Congr. Zool. London, 1958**:** 477-478

Tronchin G., Schrevel J. (1977) Chronologie des modifications ultrastructurales au cours de la croissance de *Gregarina blaberae*. *J. Protozool*. **24:** 67-82

Walker M. H., Mackenzie S. P., Bainbridge S. P., Orme C. (1979) A study of the structure and gliding movement of *Gregarina garnhami. J. Protozool*. **26:** 566-574

Yoshikawa H., Yamada M., Yoshida Y. (1988) Freeze-fracture study of *Blastocystis hominis*. *J. Protozool*. **35:** 522-528

Received on 11th December, 2000; accepted on 12th November, 2001

Acta Protozool. (2002) 41: 23 - 61

ACTA
PROTOZOOLOGICA

Faunistic Studies on Marine Ciliates from the Antarctic Benthic Area, Including Descriptions of One Epizoic Form, 6 New Species and, 2 New Genera (Protozoa: Ciliophora)

Weibo SONG[1] and Norbert WILBERT[2]

[1]Laboratory of Protozoology, Ocean University of Qingdao, Qingdao, China; [2]Institut für Zoophysiologie, Universität Bonn, Bonn, Germany

Summary. The morphology and taxonomy of 22 marine benthic ciliates including 2 new genera and 6 new species from the Antarctic area are described using live observations and silver impregnation techniques: *Metacystis* sp., *Litonotus antarcticus* sp. n., *Dysteria calkinsi* Kahl, 1931, *Chlamydonella* sp., *Orthodonella shenae* sp. n., *Aegyriana paroliva* gen. n., sp. n. *Pleuronema coronatum* Kent, 1881, *Cyclidium varibonneti* Song, 2000, *Metanophrys antarctica* sp. n., *Scyphidia* sp., *Zoothamnium* sp., *Condylostoma remanei* Spiegel in Kahl, 1932, *Heterostentor coeruleus* gen. n., sp. n., *Holosticha diademata* (Rees, 1884), *Metaurostylopsis rubra* sp. n., *Uronychia binucleata* Young, 1922, *Diophrys oligothrix* Borror, 1965, *Diophrys scutum* Dujardin, 1842, *Euplotes balteatus* (Dujardin, 1841), *Aspidisca polypoda* (Dujardin, 1841), *Aspidisca crenata* Fabre-Domerque, 1885 and *Aspidisca quadrilineata* Kahl, 1932. The diagnosis for the new genus *Heterostentor*: slightly to strongly contractile, free-living Heterotrichina with elongated body shape; no conspicuous buccal cavity or cytopharynx; oral apparatus *Stentor*-like, restricted apically around small truncated frontal plate; without peristomial kineties, paroral membrane highly degenerated or absent; somatic ciliature with suture on ventral side. According to the rule of the ICZN (1985), reestablishment for the "non-existing"genus *Aegyriana* gen. n. has been made, its diagnosis: dorsoventrally flattened Dysteriidae with tail-shaped podite, oral structure reduced to 3 fragment-like kineties, postoral kineties making no gap in median; one bald space present subcaudally, which is completely surrounded by kinetosomes and where the podite is positioned; cytopharyngeal rods dominant. Based on the data obtained, the following species are considered as junior synonyms: *Euplotes alatus* Kahl, 1932; *E. quinquecarinatus* Gelei, 1951; *E. magnicirratus* Carter, 1972 and *E. plicatum* Valbonesi *et al*., 1997 [possibly conspecific with *Eupotes balteatus* (Dujardin, 1841) Kahl 1932]; *Diophrys magnus* Raikov & Kovaleva, 1968 and *D. kasymovi* Agamaliev, 1971 (junior synonyms of *Diophrys scutum* Dujardin, 1842). One new combination is suggested: *Scyphidia marioni* (Van As *et al*., 1998) comb. n. (formerly *Mantoscyphidia marioni* Van As *et al*., 1998).

Key words: Antarctic benthic ciliates, morphology, new genus, new species, taxonomy.

INTRODUCTION

In recent decades, the ciliated protozoa in the Antarctic area have become of great interest to protozoologists working both in the taxonomic and ecological fields, simply because of the special faunistic structure and high degree of morphological as well as biological diversity (Dragesco 1963; Fenchel and Lee 1972; Thompson 1972; Thompson and Croom 1978; Corliss and Snyder 1986; Agatha *et al.* 1990, 1993; Valbonesi and Luporini 1990a, b, c; Wilbert *et al.* 1993; Petz 1994, 1995; Petz *et al.* 1995; Foissner 1996; Song and Wilbert 1999, 2000a).

However, these investigations concerned basically only the pelagic forms or those found in the sea ice; ciliates living in the periphyton communty remain largely

Address for correspondence: Norbert Wilbert, Institut für Zoophysiologie, Poppelsdorfer Schloss, 53115 Bonn, Germany; E-mail: Wilbert@uni-bonn.de

unknown though it is commonly accepted that in this biotope lives a different community, usually with greater species richness, as revealed in studies performed in other geographical habitats (Kahl 1931, 1935; Dietz 1964; Agamaliev 1968; Hartwig 1973; Deroux 1974, 1978; Song and Wilbert 1989; Foissner *et al.* 1991; Wilbert 1995).

In January-February, 2000, a comprehensive taxonomic survey of the periphytic ciliates was thus carried out, supported by a DFG (Deutsche Forschungsgemeinschaft) research project, in order to supply some basic data about these organisms.

MATERIALS AND METHODS

Organisms and preparation. Specimens were collected (January-February, 2000) from a rock pool and in the littoral of Potter Cove, King George Island (62° 14'S; 58° 40'W)

Specimens were either observed immediately with a pre-cooled microscope and photographed by a video camera or maintained for days in the laboratory. Wheat grains were added to the medium to provide bacterial food. Nitrate silver and protargol impregnations according to Song and Wilbert (1995) and Wilbert (1975) were applied to reveal the silverline system and the infraciliature.

Counts and measurements on stained specimens were performed at a magnification of x1250. Drawings were made with the help of a camera lucida. Terminology and systematics basically follow Kahl (1932), Lom (1961) and Corliss (1979).

Ecological features. The water temperature in the period of sampling was about 1°C, salinity about 33 ‰ (Wiencke *et al.* 1998).

Deposition of slides. Holotypes as permanent slides (using either protargol or silver nitrate impregnations) are deposited in the Oberösterreichisches Landesmuseum, A-4040 Linz, Austria, while paratypes and slides for little-known species are in the collection of the senior author in the Laboratory of Protozoology, College of Fisheries, Ocean University of Qingdao, China.

RESULTS

Order Prostomatida Schewiakoff, 1896
Genus *Metacystis* Cohn, 1866
***Metacystis* sp.** (Figs 2A-C, 18-19)

We observed this organism on a protargol-impregnated slide with only a few individuals, and the lorica was not found. Hence identification is difficult and we can give here only a description of the infraciliature.

Description. Body shape cylindrical with posterior 1/3 distinctly narrowed and broadly pointed caudal end; cells about 160 x 35 μm in size after protargol impregnation. Single macronucleus oval in shape, length x width *ca* 15 x 20 μm (Fig. 2A). Oral apparatus consisting of two circles of paired circumoral kineties (Fig. 2C, CK) and 4 and one-half circles of monokinetids. In the latter, the middle one positioned only on "dorsal side", thus only half circle (Fig. 2C, arrowhead). All structures of oral apparatus considerably more densely ciliated than somatic ones.

Somatic ciliature as shown in Figs 2A and B: uniform and arranged in tufts or bands, especially in the anterior portion of body, basal bodies never paired. Somatic kineties (SK) about 25-30 in number and loosely ciliated, longitudinal fibres associated with basal bodies (Fig. 2C).

Remarks. With respect to the infraciliature, our organism differs clearly from the related *Pelatractus grandis* Penard, 1922 in the structure of the buccal apparatus: the former has a circumoral structure consisting of closely packed fragment-like kineties (Dragesco *et al.* 1974). *Vasicola ciliata* Tatem, 1869 is possibly also a similar form, but its oral apparatus has a completely different appearance: two belts, each with densely spaced rows of monokinetids; in addition, its somatic kineties are composed of dikinetids (Dragesco *et al.* 1974).

Order Pleurostomatida Schewiakoff, 1896
Genus *Litonotus* Ehrenberg, 1830
***Litonotus antarcticus* sp. n.** (Figs 3A-I, 21-23; Table 1)

Diagnosis for the new species. Highly metabolic, small to medium-sized marine *Litonotus in vivo* about 70-150 μm with basically broad lanceolate body shape, 2 macronuclear nodules and 1 micronucleus; 4-5 left and 8-10 right somatic kineties (including perioral kineties), of which most right ones are considerably shortened anteriad; one contractile vacuole terminally positioned. Extrusomes rod-shaped, *in vivo* about 4-5 μm long, regularly arranged along the edge of cytostome.

Description. Cells *in vivo* mostly smaller than 120 μm (in "normal", non-extending state) though shape very variable, from broad oval to slender lanceolate when fully extended. Anteriorly typical of genus, highly contractile and curving backwards. Posterior end often broadly round or even truncated; in smaller specimens, yet not seldom with narrowed end, but never forming prominent tail (Figs 3A, C). Cells laterally compressed about 3:1.

Pellicle thin and flexible; left body convex and vaulted, about 4 longitudinal grooves often slightly spiral, in which kineties originate (Figs 3A, D). Cytoplasm colourless, with many greasily shining globules rendering main part

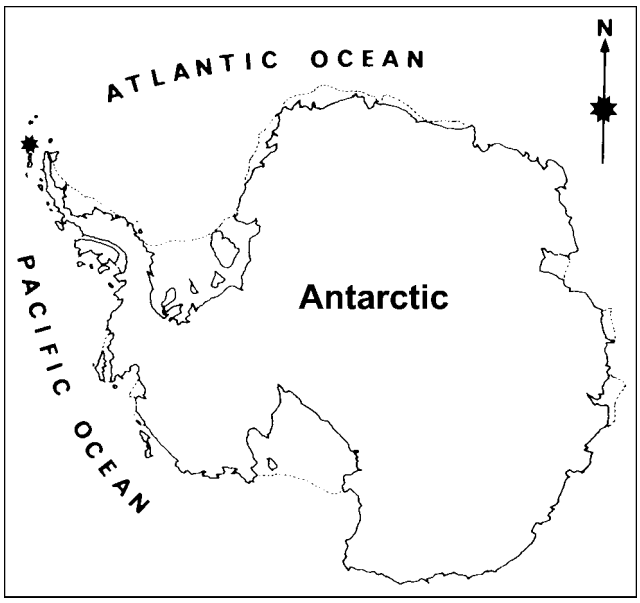

Fig. 1. Sampling site (asterisk)

of body rather opaque (especially at low magnification). Cells basically hyaline anteriorly and in area of mouth; food vacuoles containing brown or green inclusion (algae) or pinnate diatoms. 2 macronuclear nodules, in mid-body, ellipsoid, with several small spherical or single large nucleolus. Micronucleus between macronuclear nodules. Contractile vacuole small, terminally positioned. Extrusomes rod-shaped, straight and conspicuous *in vivo*, about 4-6 µm long; densely distributed in oral region and scattered in other parts of body (Fig. 3I).

Cilia *ca* 6-8 µm long, movement genus-typical, slowly gliding on substrate.

Oral slit about half of body length. Oral structure typical of genus (Foissner 1984): 3 perioral kineties, i.e. 2 on right and 1 on left of cytostome. Anterior portion of both row 1 and 2 (about length of oral slit) composed of densely positioned dikinetids, while basal body pairs in row 3 are widely spaced (Figs 3G, H). Characteristically, perioral kinety 2 terminating about half way along body (Fig. 3F, double-arrowheads). Nematodesmata long and highly developed, originating from perioral kinetids about 90% of cell length (Fig. 3I).

Somatic ciliature as shown in Figs 3F and G. With exception of number 2 (numbered form dorsal to ventral in Fig. 3F, the leftmost-but-one), all other somatic kineties on right side anteriorly shortened considerably (arrowheads in Fig. 3F). On left side, almost consistently with 4 kineties (including perioral kinety 3), of which only two kineties extending along whole length of cell, while the rightmost and the one between the P3 and dorsal brosse shortened anteriad (double-arrowheads in Fig. 3G). Dorsal brosse (DK) composed of about 20 basal body pairs, each with short bristle-like cilium, continuous posteriorly with row of densely spaced monokinetids (Fig. 3G).

Comparison. Up to now, over 15 small *Litonotus*-species from various habitats have been investigated using modern methods, of which at least 5 forms -based on general ciliature, body shape and size, position of contractile vacuole and the habitat- should be compared with the new species described here: *L. lamella, L. yeanae, L. obtus, L. lamella uninucleata* and *L. emmerichi* (Borror 1963, Fryd-Versavel *et al.* 1975, Wilbert and Kahan 1981, Dragesco and Dragesco-Kernéis 1986, Song 1991). Among them, *L. lamella uninucleata* is a very small species with only one macronucleus (Wilbert and Kahan 1981). The new

Table 1. Morphometric characterization of *Litonotus antarcticus* sp. n. All data are based on protargol-impregnated specimens. Measurements in µm. CV - coefficient of variation in %; Max - maximum; Mean - arithmetic mean; Min - minimum; SD - standard deviation; SE - standard error of mean

Character	Min	Max	Mean	SD	SE	CV	n
Body length	60	114	88.9	22.63	6.82	25.5	11
Body width	25	46	37.5	5.72	1.72	15.3	11
Number of somatic kineties on left side*	4	5	4.1	0.33	0.11	8.1	9
Number of somatic kineties on right side**	8	10	8.8	0.87	0.29	9.9	9
Number of macronuclei	1	2	1.87	0.35	0.09	18.8	13
Number of dikinetids in perioral kinety 3	13	15	-	-	-	-	-
Number of dikinetids in dorsal brosse	18	20	-	-	-	-	-

* perioral kinety 2 not counted; **including perioral kinety 1

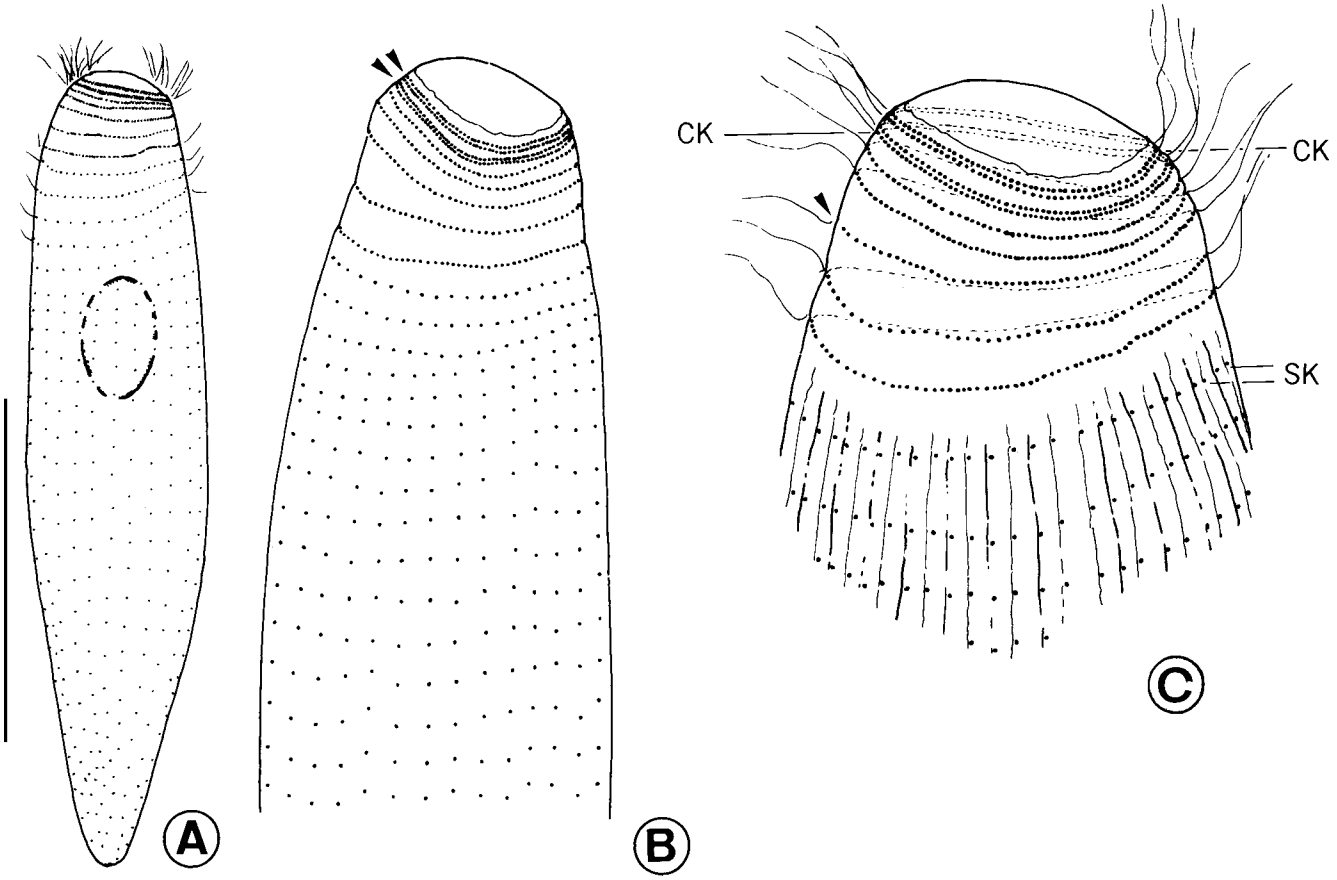

Figs 2A-C. *Metacystis* sp. from protargol impregnation. **A** - general view; **B** -anterior portion, arrowheads marking the double-rowed circumoral kinety; **C** - detail of anterior portion, to show the oral structure; arrowhead indicating the perioral kinety which surrounds only one side of the cell. CK - circumoral kineties, SK -"normal" somatic kineties. Scale bar - 50 μm

species can be separated from *L. yeanae, L. obtus* and *L. emmerichi* in combined characters of size, number of somatic kineties on right side and the distinctly different arrangement of ciliature of right side: in all other known forms the kineties never shortened anteriorly.

Compared with the form described by Fryd-Versavel *et al.* (1975), under the name of *L. lamella*, the present species can be recognized in body shape (never caudally-pointed in posterior end *vs*. having a narrowed tail) and a definitely different ciliature pattern on the right side, i.e. all kineties in *L. lamella* on right side extend the whole length of the cell (*vs*. being shortened anteriad).

Order Cyrtophorida Fauré-Fremiet in Corliss (1956)
Genus *Orthodonella* Bhatia, 1936
***Orthodonella shenae* sp. n.** (Figs 4A-G, 20)

Diagnosis for the new species. Large marine *Orthodonella* species *in vivo* about 120-180 x 40-70 μm in size with "moveable" and conspicuous snout-like projection, with which the cell glides on the substrate; *ca* 45 somatic kineties on ventral and 25 on dorsal side; dominant synhymenium consisting of about 80 paired kinetosomes, which is arranged in a typical pattern of the genus; pharyngeal basket composed of *ca* 13 rods; 2 contractile vacuoles on left cell side; one oval macronucleus.

Dedication. We dedicate this species to the protozoologist, Prof. Shen Yunfen, the Institute of Hydrobiology, Chinese Academy of Sciences, to express our respect for her contributions to ciliate studies.

Description. Cells generally acontractile; outline elongate elliptical, right margin convex, left straight, con-

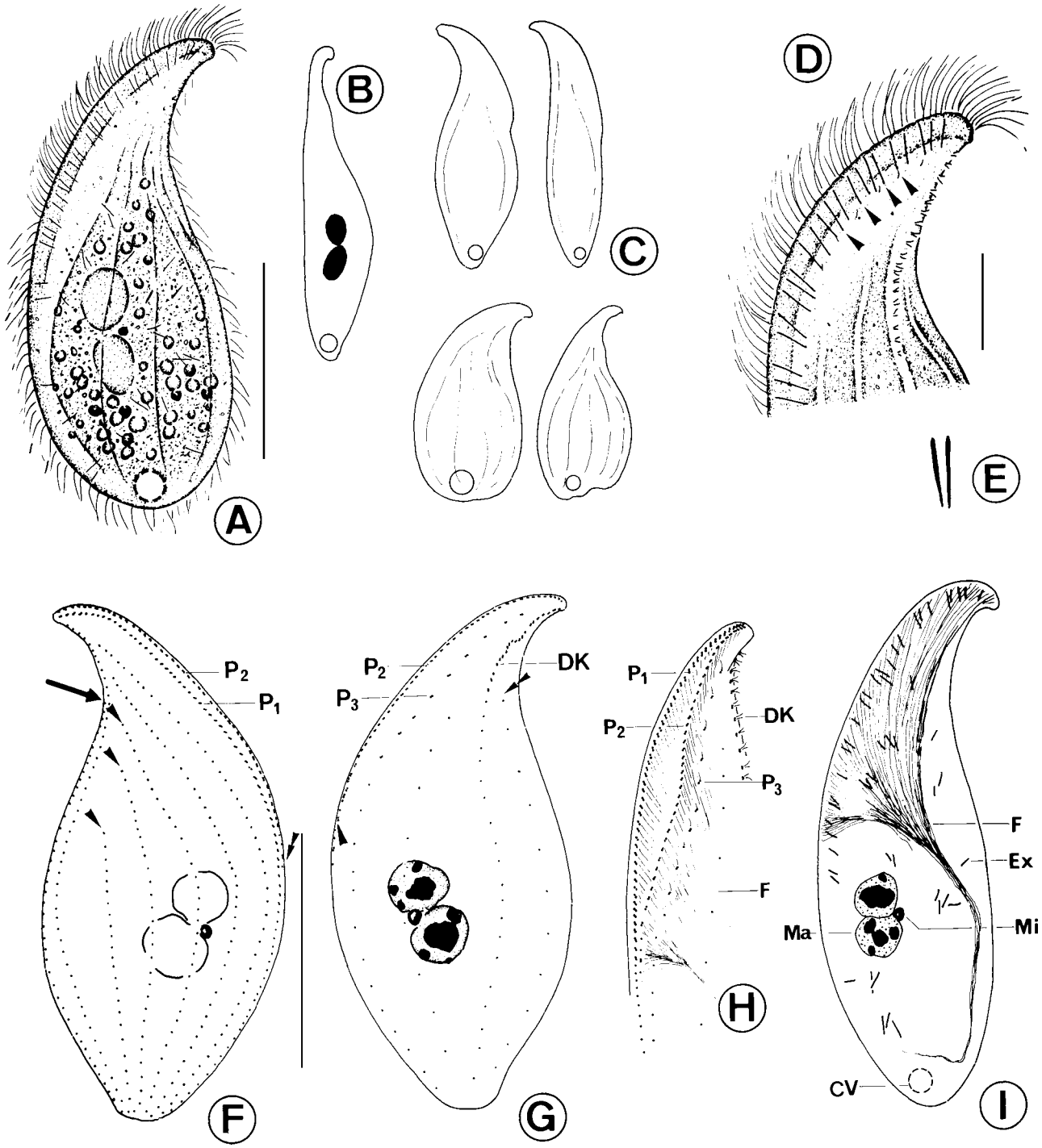

Figs 3A-I. *Litonotus antarcticus* sp. n. from life (A-E) and protargol impregnation (F-I). **A** - left view; **B** - lateral view; **C** - to show different body shapes; **D** - left view of anterior portion, arrows marking the extrusomes; **E** - extrusomes; **F** - right view of infraciliature, arrowheads indicating the shortened anterior end of some kineties, double-arrowheads referring the posterior end of perioral kinety 2; note that the leftmost kinety on the right side terminates sub-apically (arrow); **G** - left view of infraciliature; arrowhead indicates the posterior end of perioral kinety 2, while the double-arrowheads mark the anterior end of the rightmost kinety on the left side; **H** - left view, to show the detail of the anterior portion and the buccal apparatus; **I** - left view, to demonstrate the nematodesmata (cytopharyngeal fibres) and the distribution of the extrusomes. CV - contractile vacuole, DK - dorsal brosse, Ex - extrusomes, F - cytopharyngeal fibres, Ma - macronucleus, Mi - micronucleus, P_{1-3} - perioral kinety 1-3. Scale bars: A, F - 40 µm, E - 15 µm

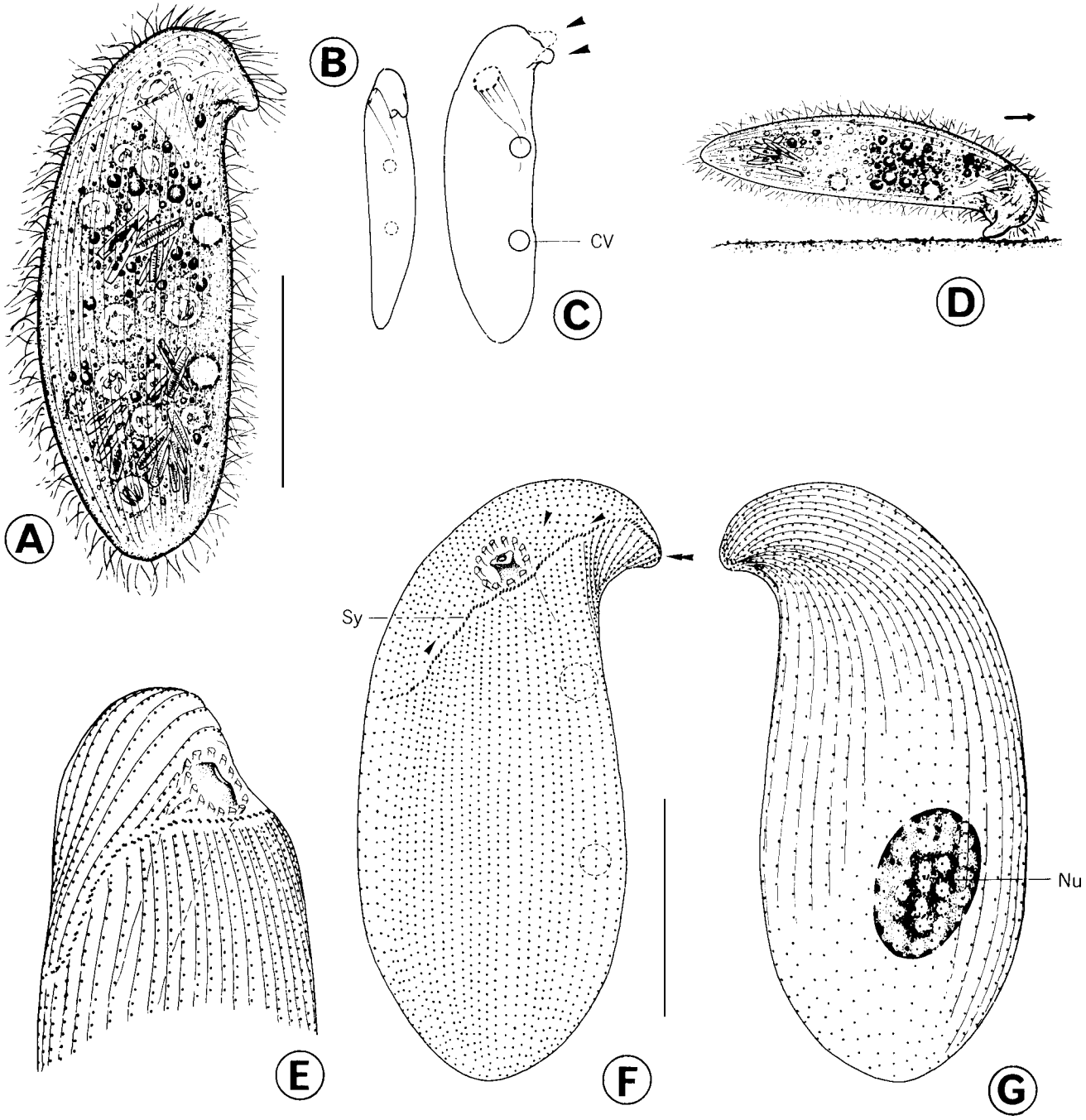

Figs 4A-G. *Orthodonella shenae* sp. n. from life (A-D) and after protargol impregnation (E-G). **A** - ventral view; **B** - lateral view; **C** - ventral view, arrowheads mark the movable snout-like projection; **D** - ventrolateral view, to show the cell gliding on the substrate, arrow indicates the direction of movement; **E** - right ventrolateral view; **F, G** - ventral and dorsal view of the same specimen, to show the general infraciliature; arrowheads indicate the "broken" kineties, double-arrowheads the snout. Nu - nucleoli, Sy - synhymenium. Scale bars: A - 80 μm, F - 50 μm

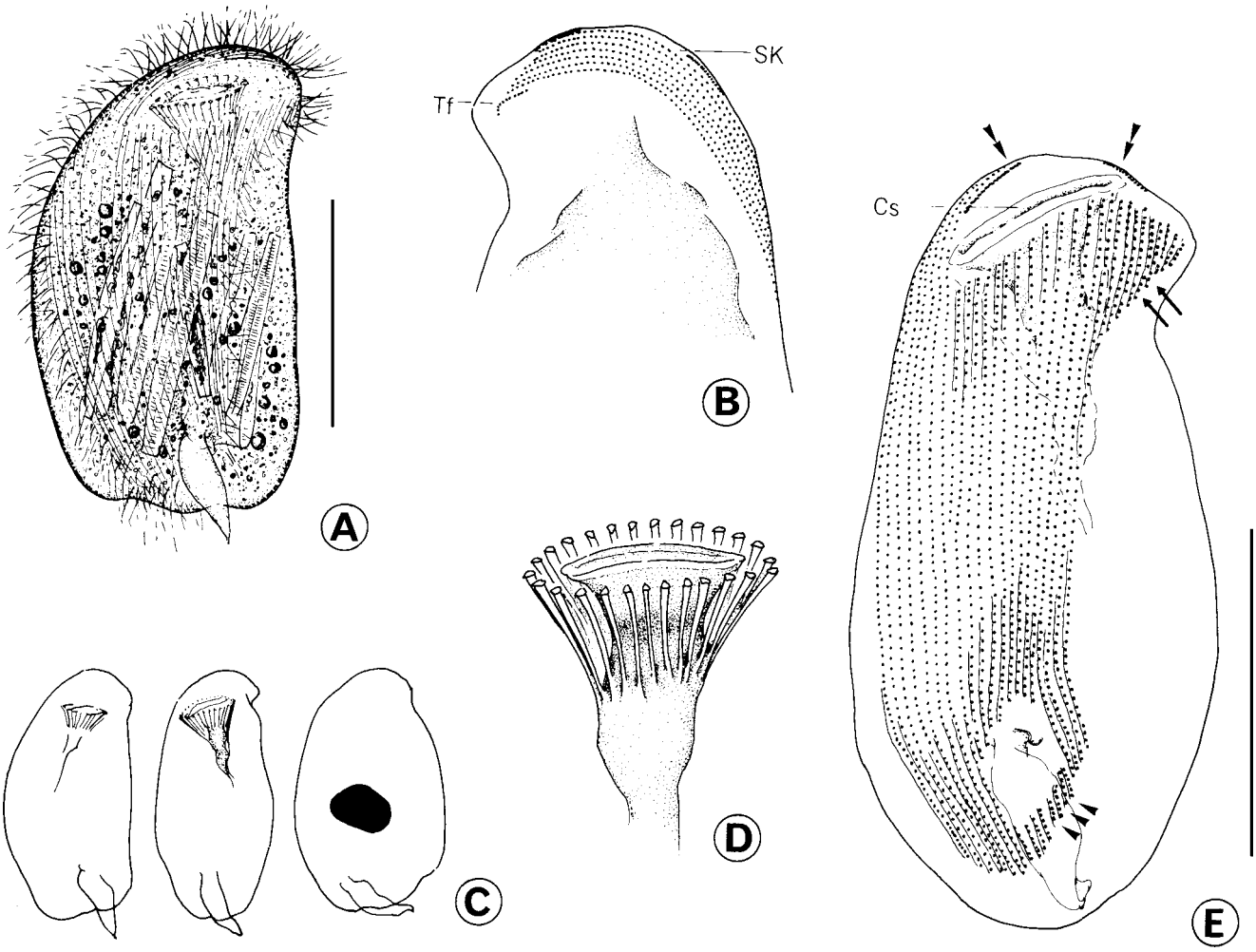

Figs 5A-E. *Aegyriana paroliva* gen. n., sp. n. from life (A, C) and after protargol impregnation (B, D, E). **A** - ventral view of a typical individual; **B** - dorsal view of anterior portion, to show the right somatic kineties, which shift to dorsal side; **C** - ventral views, to show different body shapes; **D** - detail of buccal "basket", to show the toothed cytopharyngeal rods; **E** - ventral view of infraciliature; arrows indicate the shortened left somatic kineties, double-arrowheads mark the perioral kineties, which are close to the curved right somatic kineties, while the arrowheads show the fragment-like kineties, which are posterior to the podite. Cs - cytostome, SK - right somatic kineties, Tf - terminal fragment of kinety. Scale bars - 30 μm

spicuous snout-like projection extending far to left when viewed ventrally, both anterior and posterior end broadly pointed or tapering (Fig. 4A). Dorsoventrally about 3:1 flattened. Cytoplasm colourless, often with many large, shiny granules (3-5 μm across). Food vacuoles usually with pinnate diatoms and flagellates. Two contractile vacuoles positioned along left body margin, one in anterior 1/3 and another in posterior 1/3 of body length. Nematodesmata (pharyngeal rods) conspicuous, forming funnel-shaped basket, extending posterior-left (Figs 4A, C). Single macronucleus slightly behind midbody, ellipsoidal , containing many small spherical chromatin bodies and one large centrally positioned nucleolus (Fig. 4G, Nu). Micronucleus not discernible.

Movement very distinctive: when gliding, characteristically ventral side up, often with its snout swinging up-and-down and "attaching" to substrate, giving an impression that the organism is searching for food with the snout (Fig. 4D).

Synhymenium positioned only on ventral side, obliquely from right margin to apical end of snout (Fig. 4F, double-arrowheads), in which about 80 pairs of kinetosomes are closely packed.

Somatic cilia about 10 μm long. All ventral kineties terminating at synhymenium: preorally about 8 kineties curving around cytostome with 4-5 rows "broken" or separated by cytostome (Fig. 4F, arrowheads); postorally meridional, considerably more densely ciliated than dor-

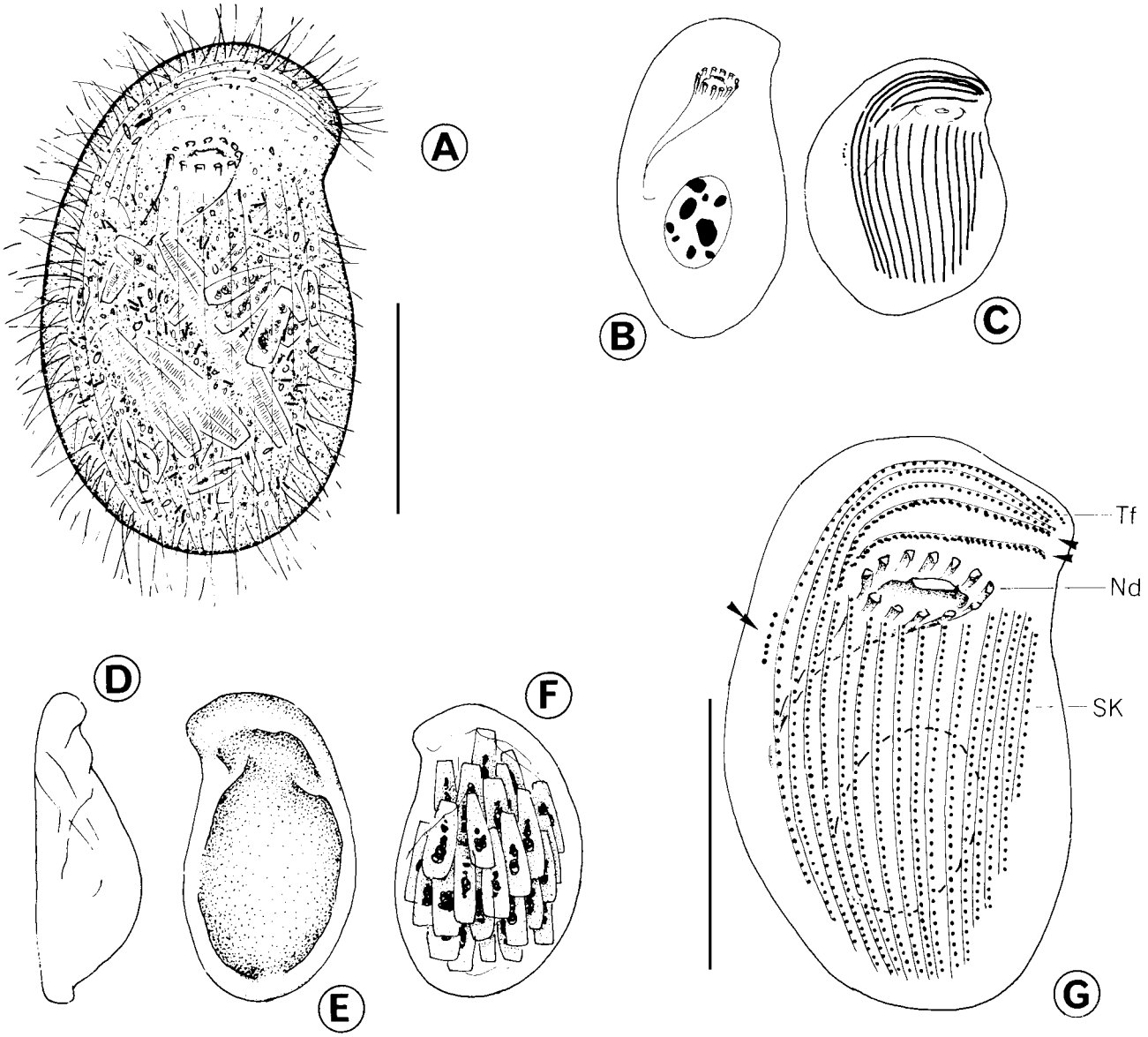

Figs 6A-G. *Chlamydonella* sp. from life (A, D-F) and after protargol impregnation (B, C, G). **A** - ventral view; **B, C** - ventral view, to show different body shapes and macronucleus; **D** - lateral view; **E -** dorsal view, to demonstrate the dorsal hump; **F** - dorsal view, showing a cell packed with large diatoms; **G** - ventral view of the infraciliature; arrowheads indicate the perioral kineties, while the double-arrowheads mark the external right equatorial kinety. Nd - nematodesmata, SK - left somatic kineties, Tf - terminal fragment of kinety. Scale bars - 20 μm

sal side. In snout portion, kineties appear to be continuous posteriorly with those on dorsal side (Figs 4F, G, double-arrowheads). On dorsal side, all kineties conspicuously loosely ciliated, extending whole dorsal side with anterior ends curved to left and converging in snout region (Fig. 4G).

Comparison. Considering the habitat, size and body shape, only one species in the genus *Orthodonella* can be compared with our new form, *O. hamata* (Gruber, 1884). However, the Antarctic species differs clearly from it in the number and position of contractile vacuoles (2 and positioned laterally on cell margin *vs*. 1, caudally

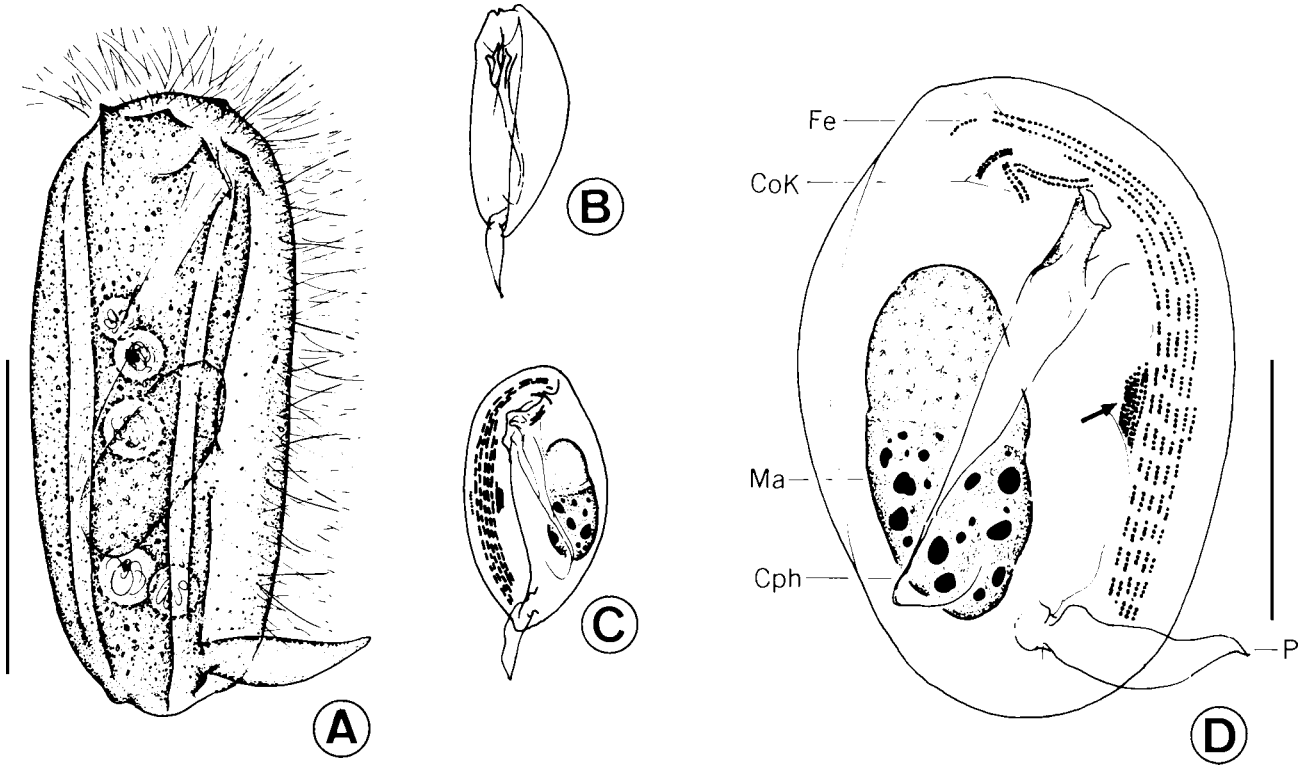

Figs 7A-D. *Dysteria calkinsi* Kahl, 1931 from life (A, B) and after protargol impregnation (C, D). **A** - right lateral view; **B** - left ventrolateral view, to show an ovoid-shaped cell; **C** - left lateral view, showing general infraciliature and nuclear apparatus; **D** - right lateral view of infraciliature, arrow indicates left equatorial field of kineties. CoK - circumoral kineties, Cph - cytopharynx, Fe - fragment of external right kinety, Ma - macronucleus, P - podite. Scale bars: A - 30 μm, D - 40 μm

positioned) (Ozaki and Yagiu 1941, Jankowski 1968, Wilbert 1986).

Genus *Aegyriana* gen. n.

This genus was originally erected by Deroux (1975) but no type species was fixed, hence it is a nomen nudum according to Art 13(b) of the ICZN (1985). To maintain stability, we re-establish it here.

Diagnosis for the new genus. Dorsoventrally flattened Dysteriidae with tail-shaped podite, oral structure reduced to 3 fragment-like kineties; preoral kineties arched to left; postoral kineties making no gap in median; one bald space present subcaudally, which is completely surrounded by kinetosomes and in which the podite is positioned; cytopharyngeal rods dominant.

Type species *Aegyriana oliva* (Claparède & Lachmann, 1858)

***Aegyriana paroliva* sp. n.** (Figs 5A-E)

Diagnosis for the new species. Marine metabolic *Aegyriana in vivo* 60-80 x 30-50 μm with 33-40 somatic kineties, of which the leftmost 10-15 evenly shortened posteriad; buccal basket prominent, consisting of *ca* 26-30 cytopharyngeal rods; single macronucleus oval in shape.

Description. Body shape variable, but generally elliptical or D-shaped, right margin convex, left slightly sigmoid or straight with posterior end broadly rounded or irregularly truncated, inconspicuous snout-like projection on anterior left (Figs 5A, C). Dorsoventrally rather thick, about 2:1 flattened, ventral flat, dorsal side strongly vaulted. Cytoplasm colourless or greyish, containing numerous small greasily shining globules and food vacuoles commonly with long pinnate diatoms, which renders cells highly opaque or even dark grey (Fig. 5A). No contractile vacuoles observed. Buccal basket genus-typical and considerably wide, nematodesmata (cytopharyngeal rods) conspicuous and toothed, directed leftwards. Macronucleus ellipsoid, about 20 x 15 μm in size, located in mid-body (Fig. 5C).

Ciliation basically on ventral side with densely spaced basal bodies. Preorally about 7 kineties arched to left

Table 2. Morphological comparison of some closely-related *Litonotus*-species, which inhabit marine or brackish water. Measurements in μm. Ma - macronuclei, SK - somatic kinety

Species	Size *in vivo*	No, SK on left side	No, SK on right side	Body shape	No, Ma	References
L. yinae	30-60	4-5	6-7	lanceolate, with narrowed posterior end, non-metabolic	2	Song 1991b
*L. lamella uninucleolata**	30-50	-	6	as above	1	Wilbert and Kahan 1981
*L. obtusus**	*ca* 60	-	5	as above	2	Borror 1963
*L. lamella**	40-200	5	10-16	lanceolate, with narrowed posterior end	2	Dragesco and Dragesco-Kernéis1986
L. antarcticus sp. n.	70-150	4-5	8-10	with broadly rounded posterior end, highly metabolic	2	present paper
L. emmerichi	60-90	4-5	5	with narrowed posterior end, non-metabolic	2	Petz *et al.* 1995

*Systematic identities not confirmed in the current table

margin of cell with some anterior-most kineties consistently shifted dorsally (Fig. 5B, SK); terminal fragment (Tf) composed of about 10 basal bodies, positioned on left frontal end of body. Perioral kineties likely in 3 fragments and separated from each other (very difficult to spot in our form since they are always on the margin of anterior end of cell, see Fig. 5E, double-arrowheads). On ventral side, kineties arranged as shown in Fig. 5E: anteriorly most kineties terminating beneath buccal region and making dominant bald area, some 10-15 of which are shortened posteriorly (Fig. 5E, arrows). About 8 kineties at posterior end "interrupted" by podite and hence forming one big bald area, right of which there are about 10 kineties, and *ca* 4 to the left.

Comparison. Only 2 species have been described in this genus: *Aegyriana oliva* (Claparède & Lachmann, 1858) and *A. minima* Deroux, 1975. The latter is small and has far fewer somatic kineties, and hence can be clearly separated from this new species (Deroux 1975). The big form, *Aegyriana oliva* is, according to redescriptions by Kahl (1930) and Deroux (1975), similar to our new form, it can be distinguished, however, in body shape (oval in outline and strongly vaulted or even folded like a *Dysteria in vivo*) and probably less-developed buccal basket (Deroux 1975).

Genus *Chlamydonella* Deroux in Petz *et al.* (1995)

According to the newly-defined diagnosis (Song and Wilbert 2000a), the genus *Chlamydonella* is characterized by: Lynchellids without plasmatic protrusions on ventral side; somatic kineties making no noticeable naked gap between left and right areas; perioral kineties continuous or slightly fragmented with leftmost rows parallel to each other, which are arched transversely; cytopharyngeal rods (nematodesmata) toothed. Macronucleus basically dimorphic. The form described here corresponds to this definition perfectly.

***Chlamydonella* sp.** (Figs 6A-G)

We have many well-impregnated specimens but have failed to observe some critical features such as the situation of the contractile vacuoles. Thus it has to be described as an uncertain species though we definitely believe that it represents a new member in this genus.

Description. Body size and shape slightly variable (30-60 x 20-30 μm in size, but usually smaller than 40 μm long); mostly oval with conspicuous snout-shaped projection on anterior left when viewed ventrally; both ends

Table 3. Morphometric characterization of *Metanophrys antarctica* sp. n. All data are based on protargol-impregnated specimens Measurements in µm

Character	Min	Max	Mean	SD	SE	CV	n
Body length	28	41	34.9	4.73	1.26	13.5	14
Body width	20	31	26.1	3.26	0.94	12.5	12
Length of buccal field	17	21	18.3	1.49	0.41	8.2	13
Length of macronucleus	15	19	16.7	1.60	0.61	9.6	7
Width of macronucleus	12	15	13.1	1.22	0.46	9.2	7
Number of macronuclei	1	1	1	0	0	0	>30
Number of somatic kineties	14	14	14	0	0	0	12
Number of kinetosomes in somatic kinety 1*	17	19	-	-	-	-	3
Number of kinetosomes in somatic kinety n*	18	19	-	-	-	-	3

* Paired kinetosomes counted as single.

Table 4. Morphometric characterization of *Scyphidia* sp. Data are either from life (*in vivo*) or based on protargol-impregnated specimens (*) Measurements in µm

Character	Min	Max	Mean	SD	M	n
Body length *in vivo*	74	115	95.5	12.0	96	33
Body width *in vivo*	31	43	36.9	3.7	36	33
Peristomial collar diameter *in vivo*	26	46	35.0	6.9	35	15
Scopula diameter *in vivo*	20	32	24.2	2.8	26	33
Length of macronucleus*	21	30	24.2	3.0	24	27
Width of macronucleus*	12	15	13.7	1.2	14	27
Length of micronucleus*	6	8	6.8	0.8	7	27
Width of micronucleus*	3	4	3.7	0.48	4	27
Distance between aboral ciliary wreath and scopula*	15	25	20.3	3.3	18	27

rounded (Figs 6A, E, F). Dorsoventrally about 1:2 flattened, ventral side flat, dorsal vaulted (Fig. 6D). Cytoplasm colourless to greyish, often containing numerous tiny granules and several to many different-sized diatoms (Figs 6A, F). Cytostome prominent, sub-apically located; buccal basket consisting of about 12 cytopharyngeal rods or nematodesmata (Nd in Fig. 6G), extending leftwards and posteriorly (Figs 6B, G). Contractile vacuoles not observed. One large ellipsoid macronucleus positioned in mid-body containing several large nucleoli (Fig. 6B). Micronucleus not recognizable.

Infraciliature as shown in Fig. 6G, 3 rightmost kineties extending preorally, with anterior portion curved to left margin; one terminal fragment (Tf) positioned on distal margin of cell. All other kineties (*ca* 11-14 in number) terminating at about cytostome level, making no suture posteriad. In addition to these "normal" kineties, one external right kinety which is fragment-like with about 6 basal bodies always recognizable in mid-body (Fig. 6G, double-arrowheads).

Oral structure consisting of two long rows of dikinetids, which are transversely arched preorally (Fig. 6G, arrowheads).

Remarks. The form described here is similar to its congener, *C. pseudochilodon* (Deroux, 1970), which was also isolated from the Antarctic area (Petz *et al.* 1995), but differs from the latter in smaller size (*vs.* 75 µm on average), differently humped dorsal side and the body shape (Deroux 1970, 1976; Petz *et al.* 1995).

Genus *Dysteria* Huxley, 1857

Much misinterpretation was/is involved in descriptions of the structure or position of organelles of these organisms. This genus is characterized by the highly bilaterally (*vs*. dorsoventrally flattened in most other groups) flattened body shape, hence all somatic ciliation is "squeezed" into a narrow region ventrally, while the

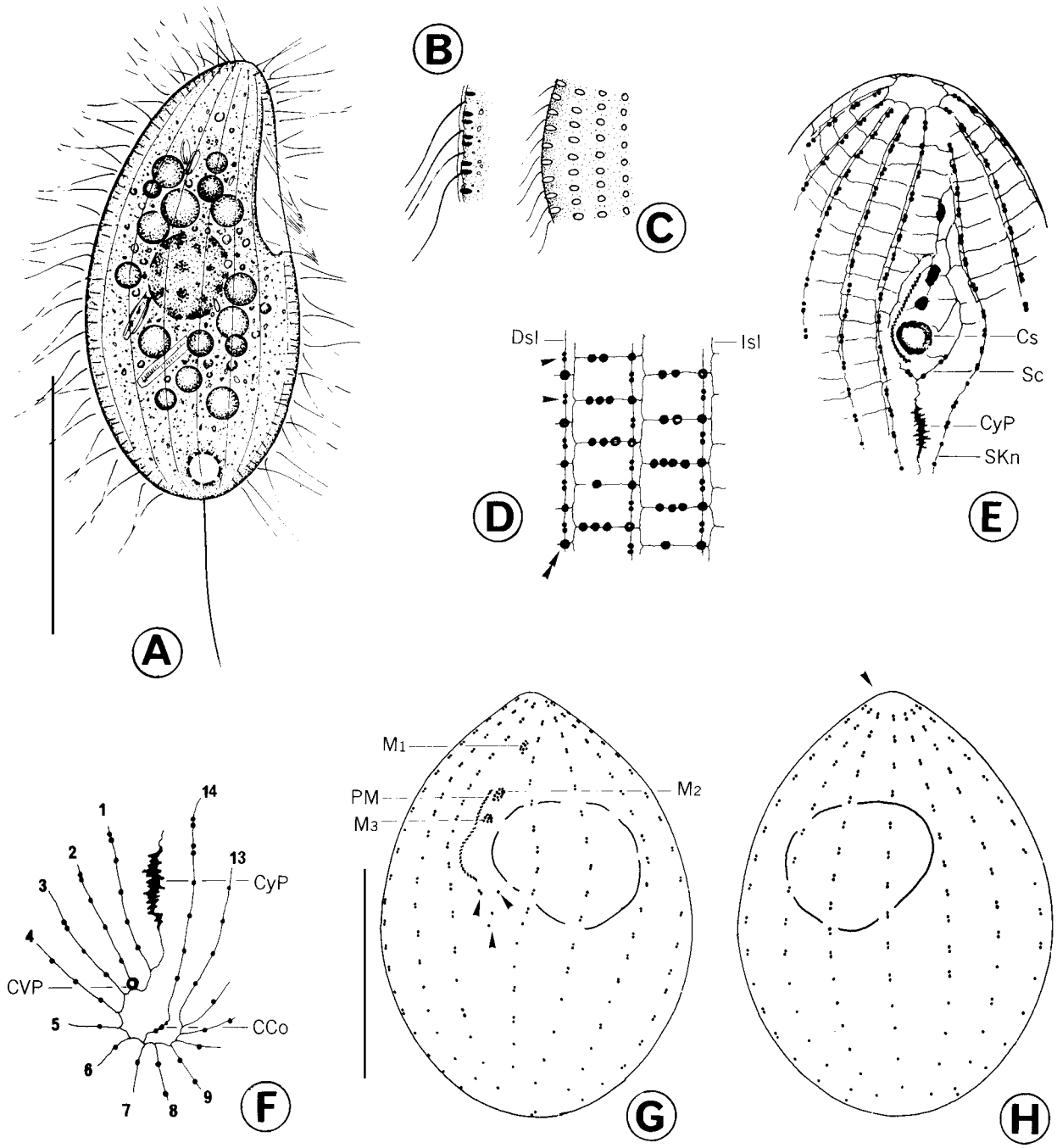

Figs 8A-H. *Metanophrys antarctica* sp. n. from life (A, B), after silver nitrate (D-F) and protargol (C, G, H) impregnation. **A** - right-lateral view; **B** - detail of cortex; **C** - to show the extrusomes after fixation; **D** - detail of silverline system, arrowheads indicate the basal bodies, double-arrowheads mark the extrusomes aligned in the direct silverline; **E** - ventral view of anterior portion, to show the silverline system and the buccal apparatus; note that the silverline makes a closed circle at anterior cell end; **F** - caudal view, to show the position of the CVP and the structure of the silverline around the caudal pole; **G, H** - ventral and dorsal view of infraciliature; arrowheads in G point to the scutica, and in H mark the pointed apex. CCo - caudal cilium complex, Cs - cytostome, CVP - contractile vacuole pore, CyP - cytopyge, Dsl - direct silverline, Isl - indirect silverline, M_{1-3} - membranelles 1-3, PM - paroral membrane, Sc - scuticaus, SKn - somatic kinety n. Scale bar - 20 µm

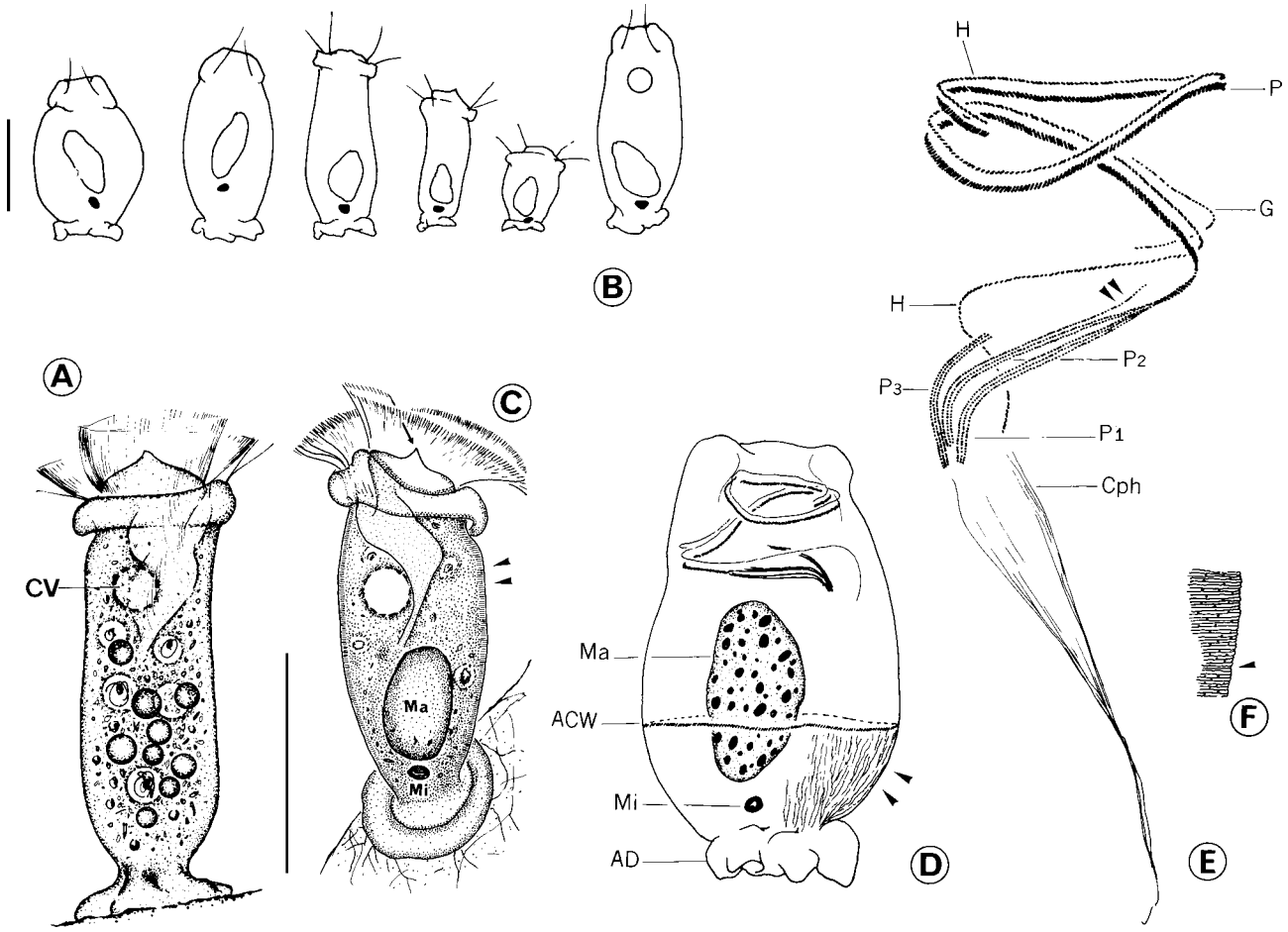

Figs 9A-F. *Scyphidia* sp. from life (A-C), protargol (D, E) and silver nitrate (F) impregnation. **A-C** - to show zooids with different body sizes and shapes; arrow in C indicates the peak of the disc; arrowheads mark the finely striped pellicle; **D** - general view, to demonstrate the infraciliature and nuclear apparatus; arrowheads indicate the argentophilic fibres; **E** - oral apparatus; arrowheads mark the separated row of the polykinety 2; **F** - detail of silverline system, arrowheads point to the aboral ciliary wreath. ACW - aboral ciliary wreath, AD - attaching disc, Cph - cytopharynx, CV - contractile vacuole, G - germinal row, H - haplokinety, P - polykinety, Ma - macronucleus, Mi - micronucleus, P_{1-3} - peniculi 1-3. Scale bars - 40 µm

left and right field of somatic kineties are positioned together (the latter are reduced to left equatorial field with densely packed, fragment-like kineties).

Dysteria calkinsi Kahl, 1931, (Figs 7A-D, 24)

Description. *In vivo* about 30-50 x 20-25 µm. Body bilaterally about 1:2-3 flattened. From side view, cells slender and more or less quadrilateral with 2 moderately conspicuous longitudinal furrows; anteriorly with some irregularly positioned ridges (Fig. 7A). When viewed ventrally, right side flat while left arched (Fig. 7B). Podite (attachment organelle, P) about 15 µm long, distally pointed, posteriorly on narrow ventral side. Cytoplasm colourless or slightly greyish, containing several large food vacuoles (likely with flagellates). Cytostome ventrally at anterior end, diagonally oriented, with inconspicuous nematodesmata (cytopharyngeal rods) extending dorsad (Fig. 7D, Cph). Contractile vacuoles not observed. Macronucleus (Ma) about in mid-body, *ca* 25 x 15 µm in size, characteristically dimorphic: anterior half with numerous fine nucleoli, while many large granules of nucleoli visiable in posterior half (Figs 7C, D).

Movement genus-typical, very quiet, slowly crawling and slightly thigmotactic. Infraciliature as shown in

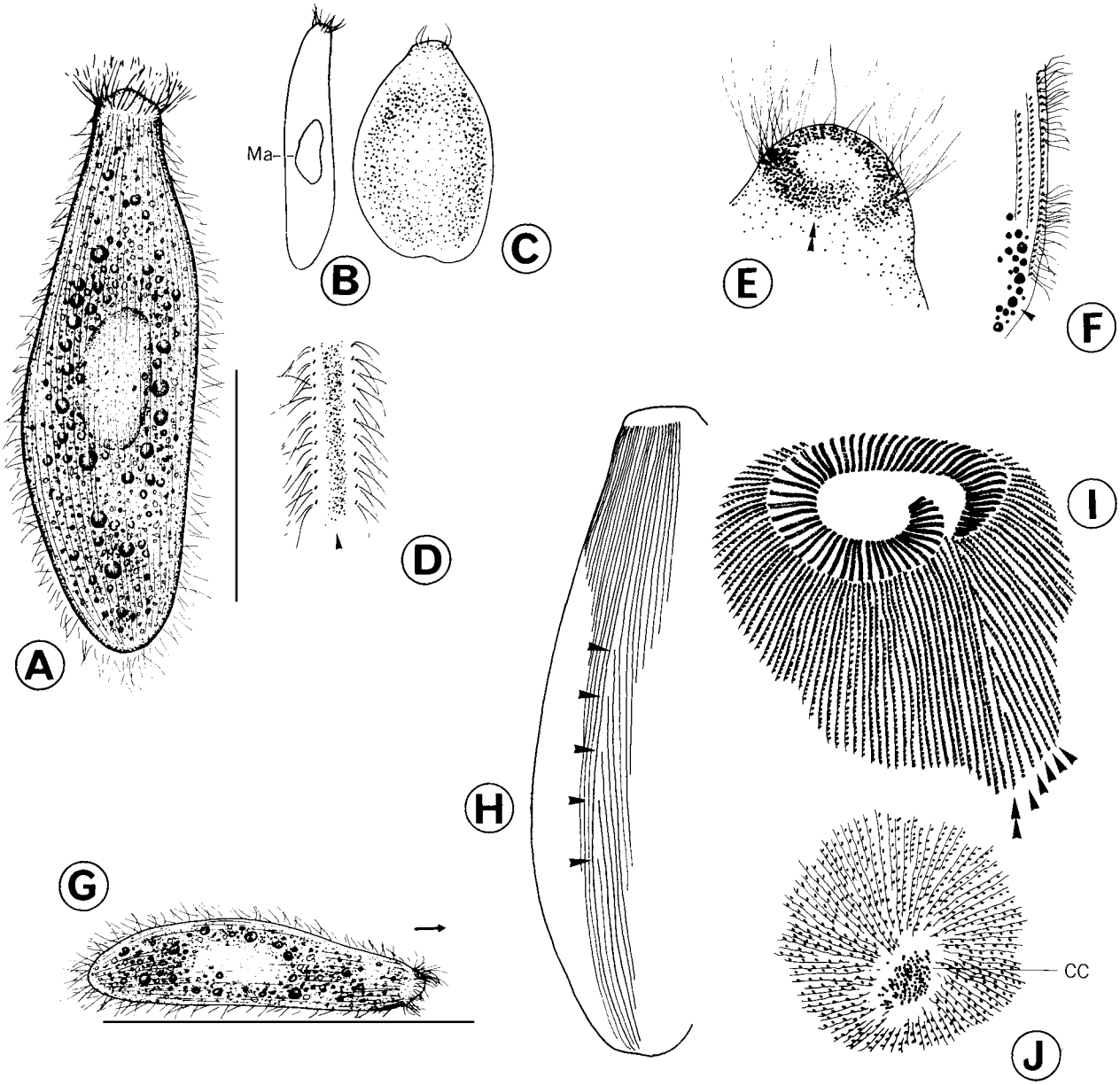

Figs 10A-J. *Heterostentor coeruleus* gen. n., sp. n. from life (A-E, G) and after protargol impregnation (F, H-J). A - a typical individual; **B, C** - to show extending and contractile forms; **D** - detail of pellicle, arrowhead indicates the pigments; **E** - anterior portion, note the pigments condense beneath the buccal apparatus (double-arrowheads); **F** - portion of cortex, arrowhead marks the granules beneath the pellicle; **G** - to demonstrate a cell gliding on substrate; **H** - to show the somatic kineties, arrowheads mark the shortened anterior end of some kineties which make the "suture". **I** - anterior part of cell, to show the adoral zone of membranelles, note no definite cytopharynx present; arrowheads mark the shortened kineties which form the suture, while the double-arrowheads indicate the somatic kinety No. 1; **J** - caudal view, to demonstrate the close-set caudal cilia. CC - caudal cilia, Ma - macronucleus. Scale bars - 120 µm

Fig. 7D: when viewed from right side, "right" filed of ciliature composed of (consistently !) 5 densely spaced kineties of variable length, formed by groups of *ca* 4 basal bodies, extending from anterior left to posterior right (Fig. 7D). To left of distal end of these kineties, one fragment of kineties (Fe) always present. In mid-body, about 6 short rows of densely packed basal bodies forming left equatorial field (arrow in Fig. 7D). Circu-

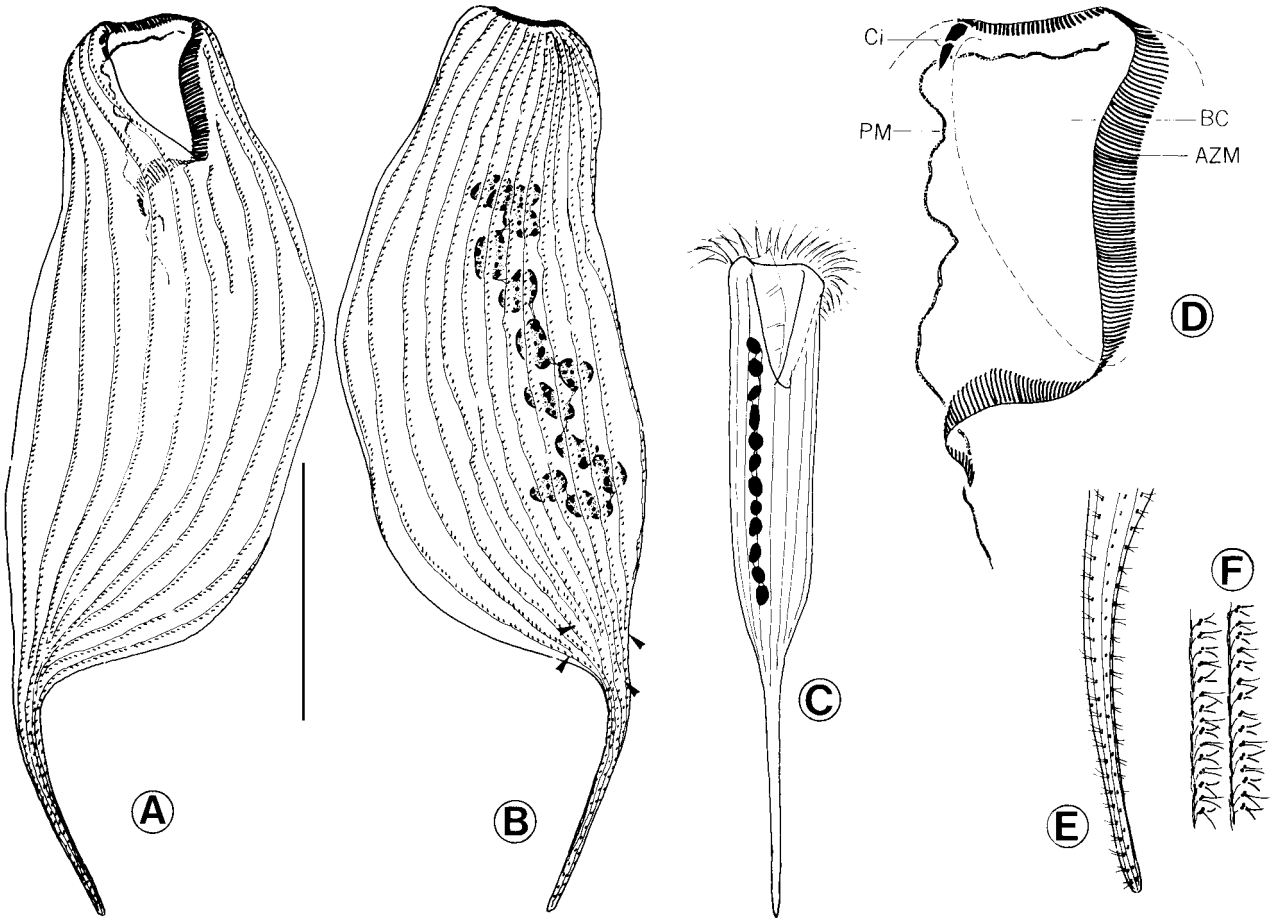

Figs 11A-F. *Condylostoma remanei* Spiegel in Kahl, 1932 from life (C) and after protargol impregnation (A, B, D-F). **A, B** - ventral and dorsal view of infraciliature, with arrowheads indicating the shortened somatic kineties; **C** - schematic diagram, to show "typical" body shape; **D** - detail of buccal apparatus; **E** - tail portion; **F** - to show the somatic kineties. AZM - adoral zone of membranelles, BC - buccal cavity, Ci - membranelles-like cirri, PM - paroral membrane. Scale bar - 100 μm

moral kineties (CoK) genus-typical, dorsally around cytostome (Fig. 7D).

Remarks. This species has never been reinvestigated using modern methods since it was described by Kahl (1931). We identify our population according to the size, body shape and the habitat (it was originally found in the Atlantic). The only point we cannot confirm: Kahl (1931) described it having 2 diagonally positioned contractile vacuoles, which were not detected in this Antarctic form (further observations needed).

It differs form *D. marina* in larger size (30-50 *vs.* 25 μm), slender body shape (*vs.* oval) and furrowed side view (*vs.* smooth) (Kahl 1931, Borror 1963).

Order Scuticociliatida Small, 1967

Genus *Cyclidium* O. F. Müller, 1786

Cyclidium varibonneti Song, 2000, (Fig. 36)

This Antarctic population was found in great numbers and resembles very closely that in the original report (Song 2000), hence the identification is quite certain and a further description is unnecessary.

Genus *Metanophrys* De Puytorac *et al.*, 1974

According to the new definition (Song and Wilbert 2000b), the genus *Metanophrys* is distinguished by: (a) possessing a *Parauronema*-like buccal apparatus (2- or more-rowed membranelle 1, the paroral membrane extending anteriorly to about the middle of the

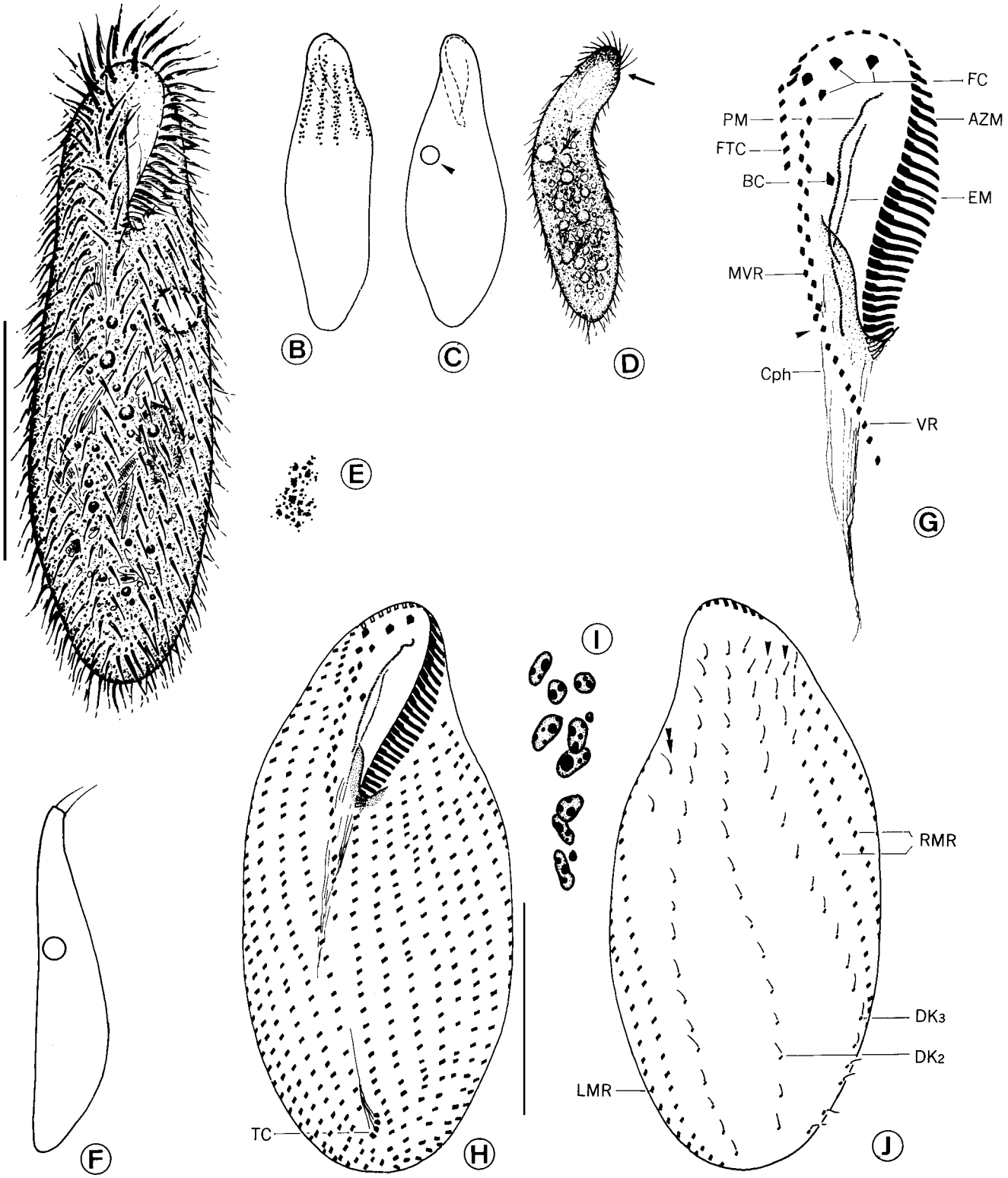
B
C
D
E
FC
PM
AZM
FTC
BC
EM
MVR
Cph
VR
G
F
TC
H
I
RMR
DK3
DK2
LMR
J

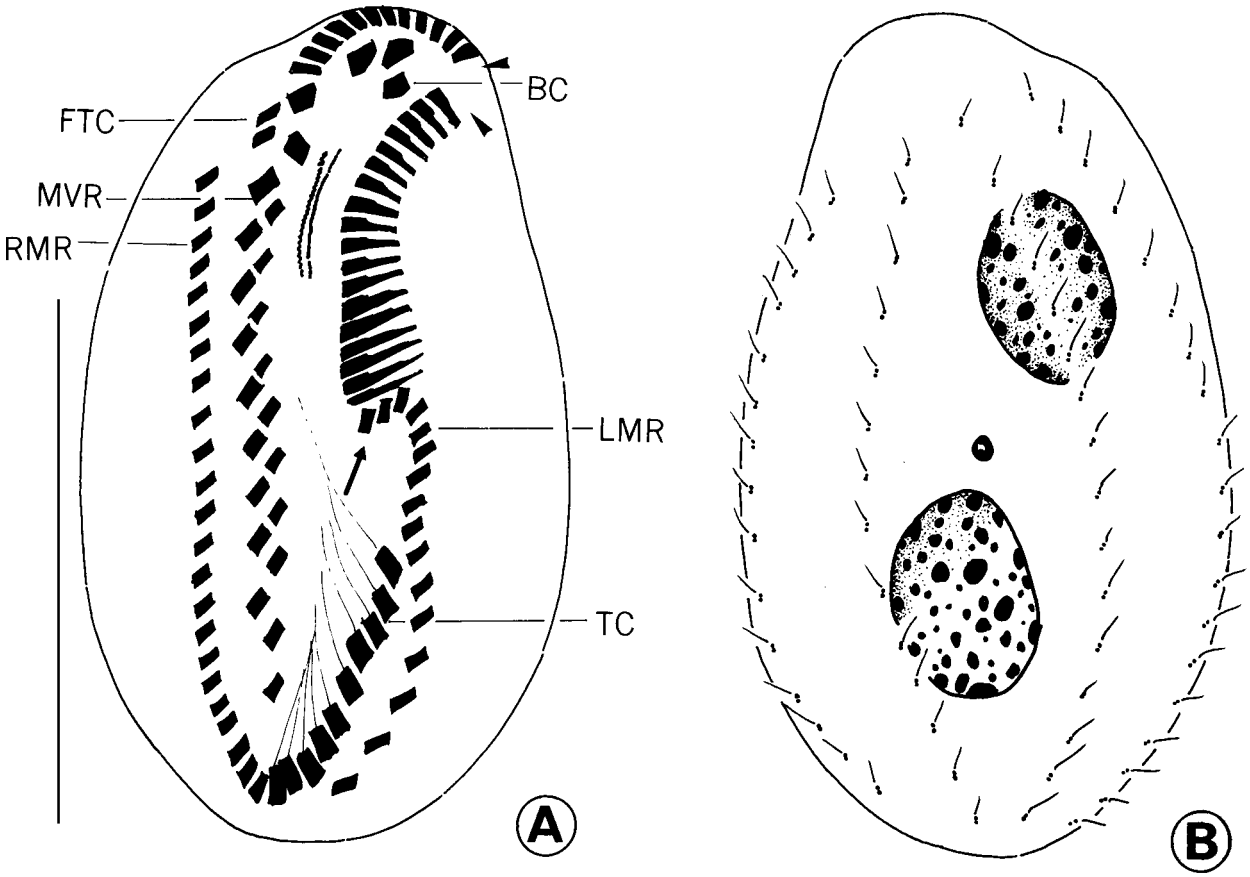

Figs 13A-B. *Holosticha diademata* (Rees, 1884) after protargol impregnation. **A, B** - ventral and dorsal view of the same specimen, to show the infraciliature and nuclear apparatus; arrowheads indicate the "gap" between the anterior and posterior part of adoral zone of membranelles, while the arrow marks the "hook-like" arrangement of cirri in left marginal row. BC - buccal cirrus, FTC - frontoterminal cirri, LMR - left marginal rows, MVR - midventral rows, RMR - right marginal rows, TC - transverse cirri. Scale bar - 30 μm

Figs 12A-J. *Metaurostylopsis rubra* sp. n., from life (A-F) and after protargol impregnation (G-J). **A-D** - to show different body shapes and arrangement of cortical granules (B); arrowheads in C indicate the contractile vacuole, arrow in D marks the densely arranged pigments at anterior end of cell; **E** - to show pigments beneath the pellicle; **F** - lateral view; **G** - detail of structure in buccal field, with arrowhead marking the position where the midventral rows and the ventral row are conjoined; **H, J** - ventral and dorsal view of infraciliature, with arrowheads indicating the fragment-like kineties anterior to the right marginal rows, while the double-arrowheads mark the "isolated" dikinetids; **I** - micronuclei. AZM - adoral zone of membranelles; BC - buccal cirrus; $DK_{2,3}$ - dorsal kinety 2,3; Cph - cytopharynx; EM - endoral membrane; FC - frontal cirri; FTC - frontoterminal cirri; LMR - left marginal rows; MVR - midventral rows; PM - paroral membrane; RMR - right marginal rows; TC - transverse cirri; VR -ventral row. Scale bars: A - 80 μm, H - 50 μm

membranelles 2), and (b) the pointed apex (i.e. with no conspicuous frontal plate). So the form we present here should be clearly assigned into this taxon.

***Metanophrys antarctica* sp. n.** (Figs 8A-H, 32-35; Table 3)

Diagnosis for the new species. Medium-sized marine *Metanophrys in vivo* 30-45 x 20-30 μm; body generally ovoid with slightly pointed apical end; one macro- and one micronucleus; oral field about 2/5 of cell length; buccal apparatus genustypical with distinctly small membranelles; 14 somatic kineties with *ca* 18 mono- and dikinetids each; single contractile vacuole terminally located; one prolonged caudal cilium.

Description. Cells *in vivo* mostly 30-40 x 20-25 μm, body shape oval to slender bag-shaped, circular in cross-section; apical end slightly pointed while posterior generally rounded. Ventral surface gently indented around buccal area, dorsally convex (Fig. 8A). Buccal field with shallow depression, about 40% of cell length. Pellicle rigid and slightly notched, below it densely spaced spindle-like extrusomes (*ca* 2 μm in length) (Fig. 8B), which after fixation usually appear thicker (Fig. 8C). Cilia

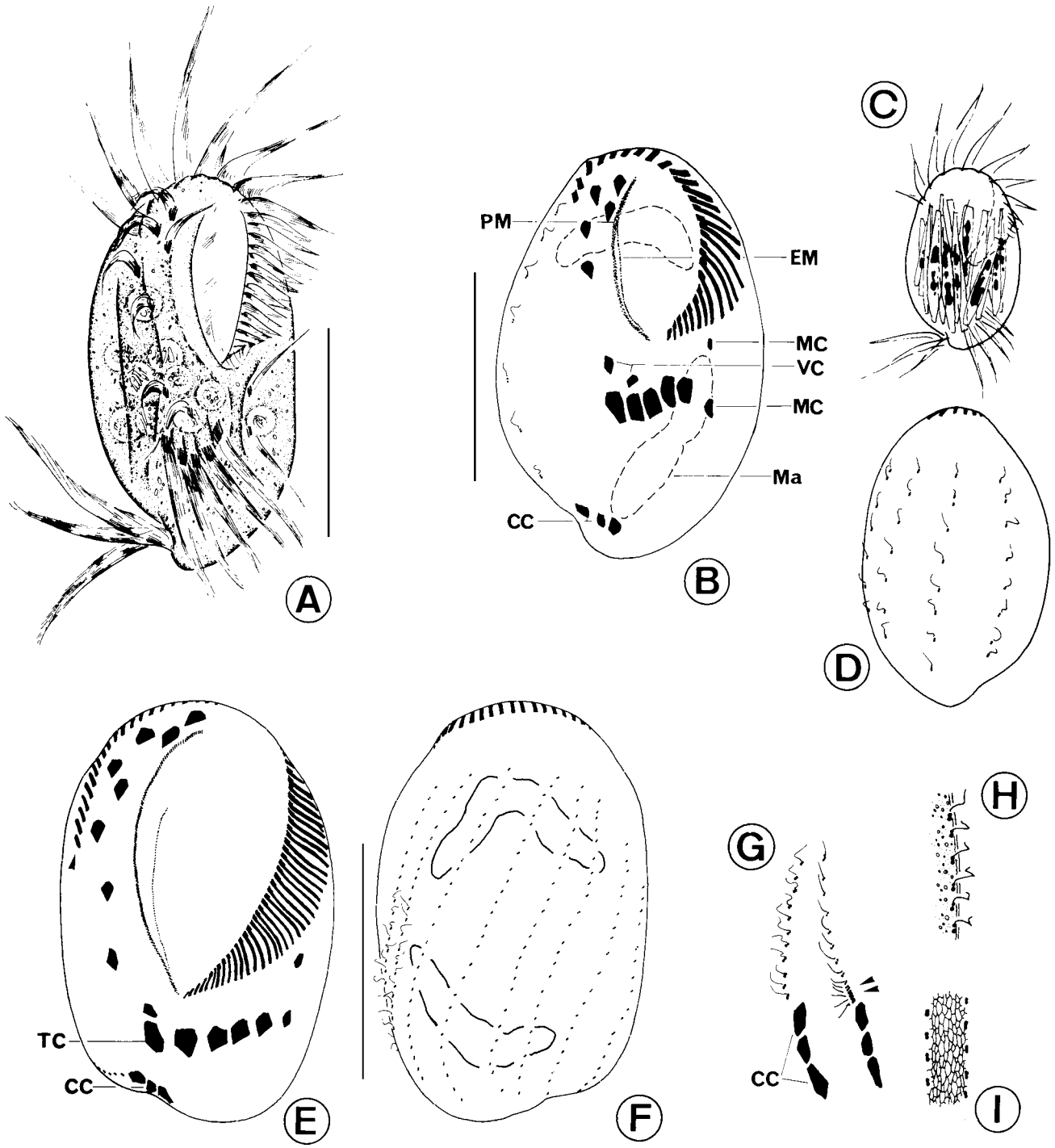

Figs 14A-I. *Diophrys oligothrix* Borror, 1965 (A-D) and *Diophrys scutum* Dujardin, 1842 (E-I) from life (A, C), silver nitrate (I) and protargol (B, D, E-G) impregnation. **A** - ventral view of a typical individual; **B, D** - ventral and dorsal view of infraciliature; **C** - to show a thick form full of digested diatoms. **E, F** - ventral and dorsal view of a specimen with ("abnormally" !) more than 7 frontoventral cirri (in the present figure, it is 9); **G** - detail of the caudal cirri and the rightmost kinety of an Antarctic population (left) and the populations from China (right); arrowheads indicate the fragment-like structure in the posterior end of the dorsal kinety; **H** - portion of cortex; **I** - silverline system on dorsal side. CC - caudal cirri, EM - endoral membrane, Ma - macronuclei, MC - marginal cirri, PM - paroral membrane, TC - transverse cirri, VC - ventral cirri. Scale bars: A, B - 40 μm, E - 90 μm

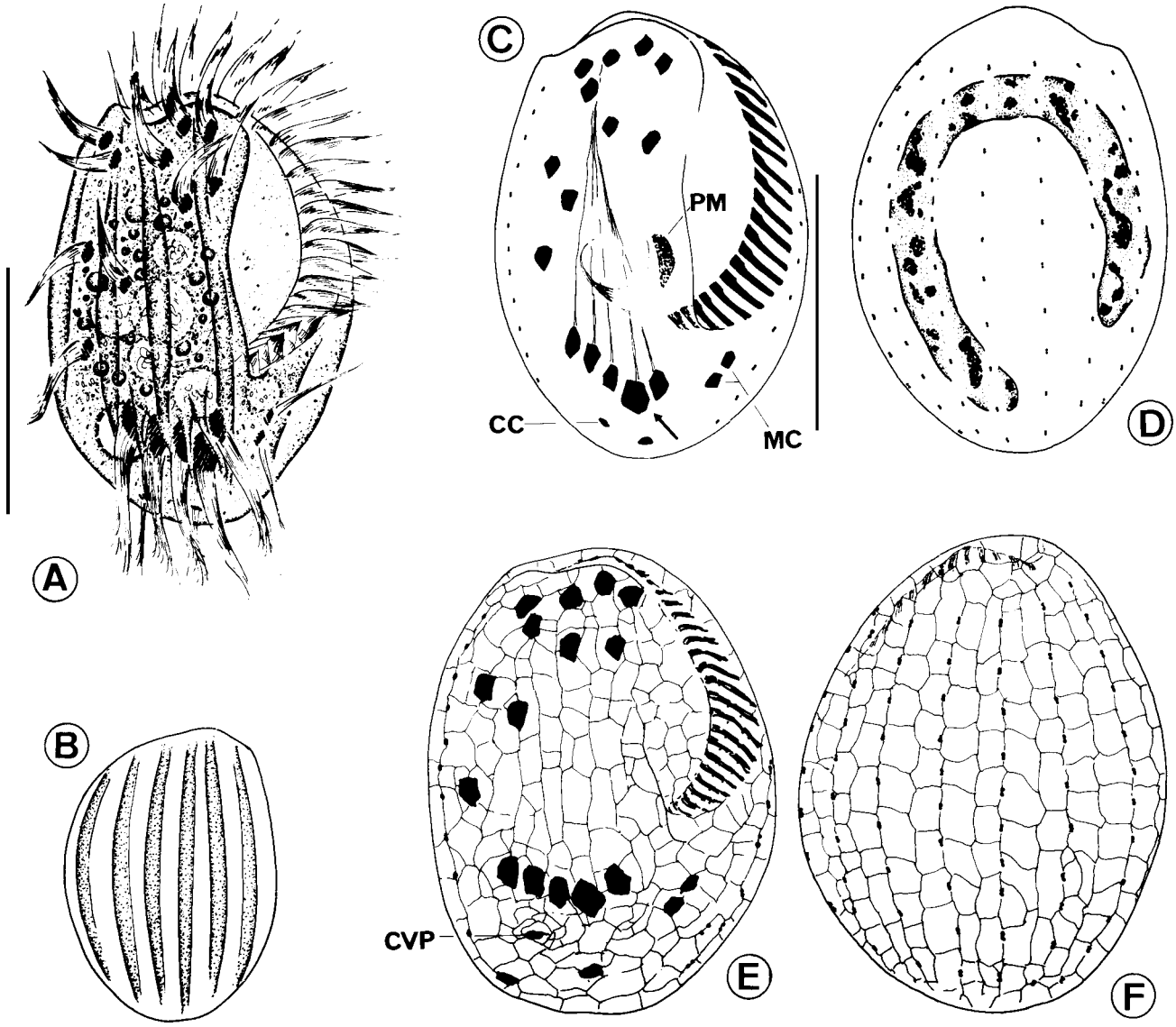

Figs 15A-F. *Euplotes balteatus* (Dujardin, 1841) Kahl, 1932 from life (A, B), protargol (C, D) and silver nitrate (E, F) impregnation. **A** - ventral view of a typical individual; **B** - dorsal view, to show the ridges; **C, D** - ventral and dorsal view of infraciliature; arrow in C indicates the enlarged transverse cirrus; **E, F** - ventral and dorsal view of the silverline system. CC - caudal cirri, CVP - pore of contractile vacuole, MC - marginal cirri, PM - paroral membrane. Scale bars - 30 μm

about 8 to 10 μm long, single caudal cilium *ca* 15 μm in length (Fig. 8A).

Cytoplasm colourless, often with several to many large shining granules (3-5 μm in diameter, inactive food vacuoles) and diatoms, which often render specimens rather dark. No food vacuoles observed. Contractile vacuole small, terminally located at posterior end of cell (Fig. 8A). One large oval macronucleus centrally located; micronucleus uncertain, possibly adjacent to macronucleus.

Infraciliature as shown in Figs 8G, H. Somatic kineties longitudinally arranged, extending over entire length of body, which are mainly composed of dikinetids throughout except the posterior 1/4 of each kinety. Each row

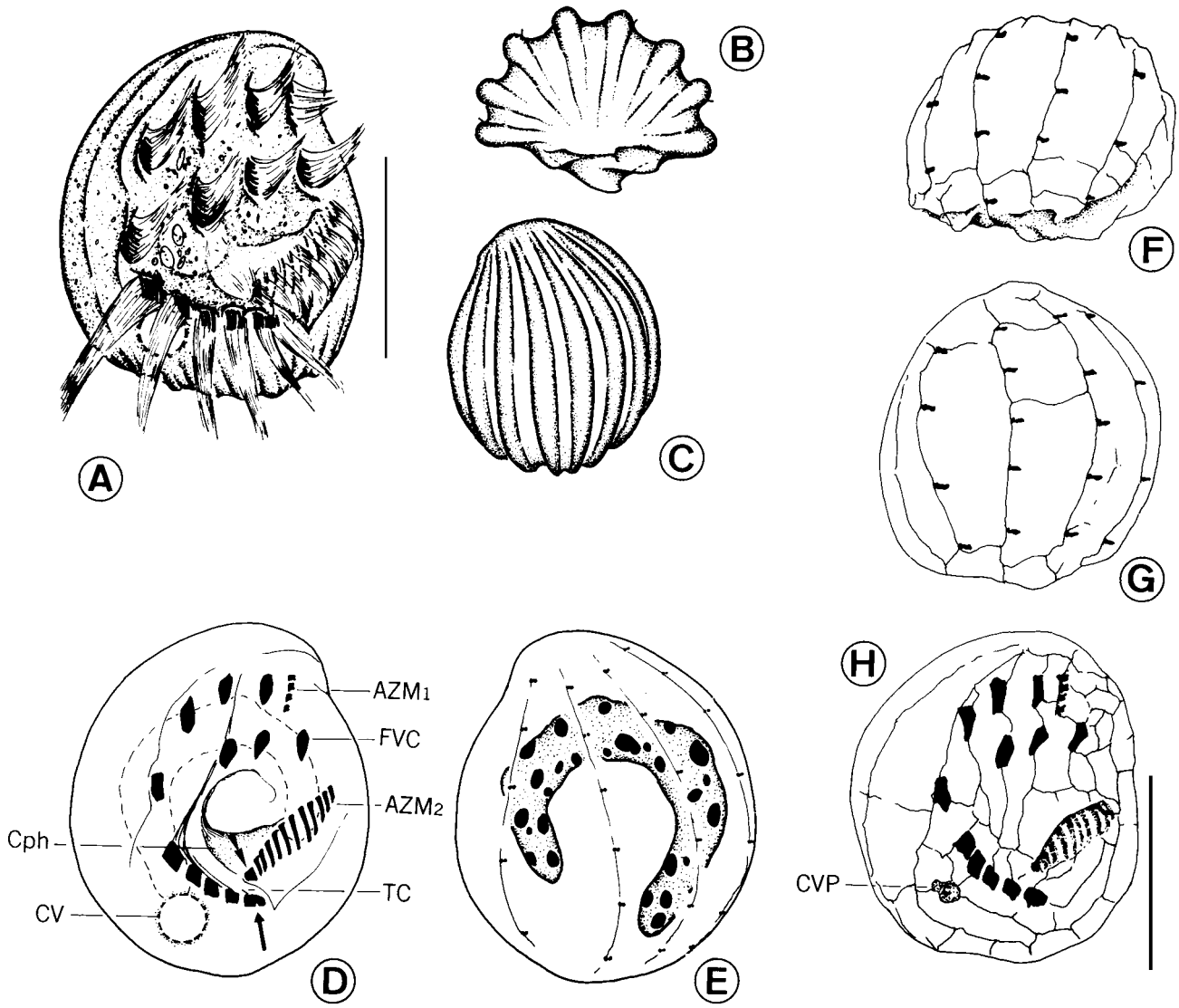

Figs 16A-H. *Aspidisca polypoda* (Dujardin, 1841) Kahl, 1932 from life (A-C), protargol (D, E) and silver nitrate (F-H) impregnation. **A** - ventral view of a typical individual; **B, C** - anterior and dorsal view, to show the ridges; **D, E** - ventral and dorsal view of infraciliature; arrow in D indicates the leftmost transverse cirrus, which often splits into several parts *in vivo,* while the double-arrowheads mark the paroral membrane; **F-H** - anterior, dorsal and ventral view of the silverline system. $AZM_{1,2}$ - adoral zone of membranelles 1, 2; Cph - cytopharynx; CV - contractile vacuole; CVP - pore of contractile vacuole; FVC - frontoventral cirri; TC - transverse cirri. Scale bars - 20 μm

with about 18 basal bodies (or basal body pairs). Anteriorly one small, rounded cilia-free apical area formed by kineties (arrowhead in Fig. 8H).

Buccal apparatus consisting of 3 membranelles (M1-3) and one short paroral membrane (PM) which extends to about the middle of membranelles 2. Membranelle 1 (M_1) small and likely 2-rowed, with about 6 kinetosomes; membranelle 2 (M_2) about equal in size to M1; membranelle 3 (M_3) smaller, close to M_2 (Fig. 8G). Paroral membrane with typical "zig-zag"

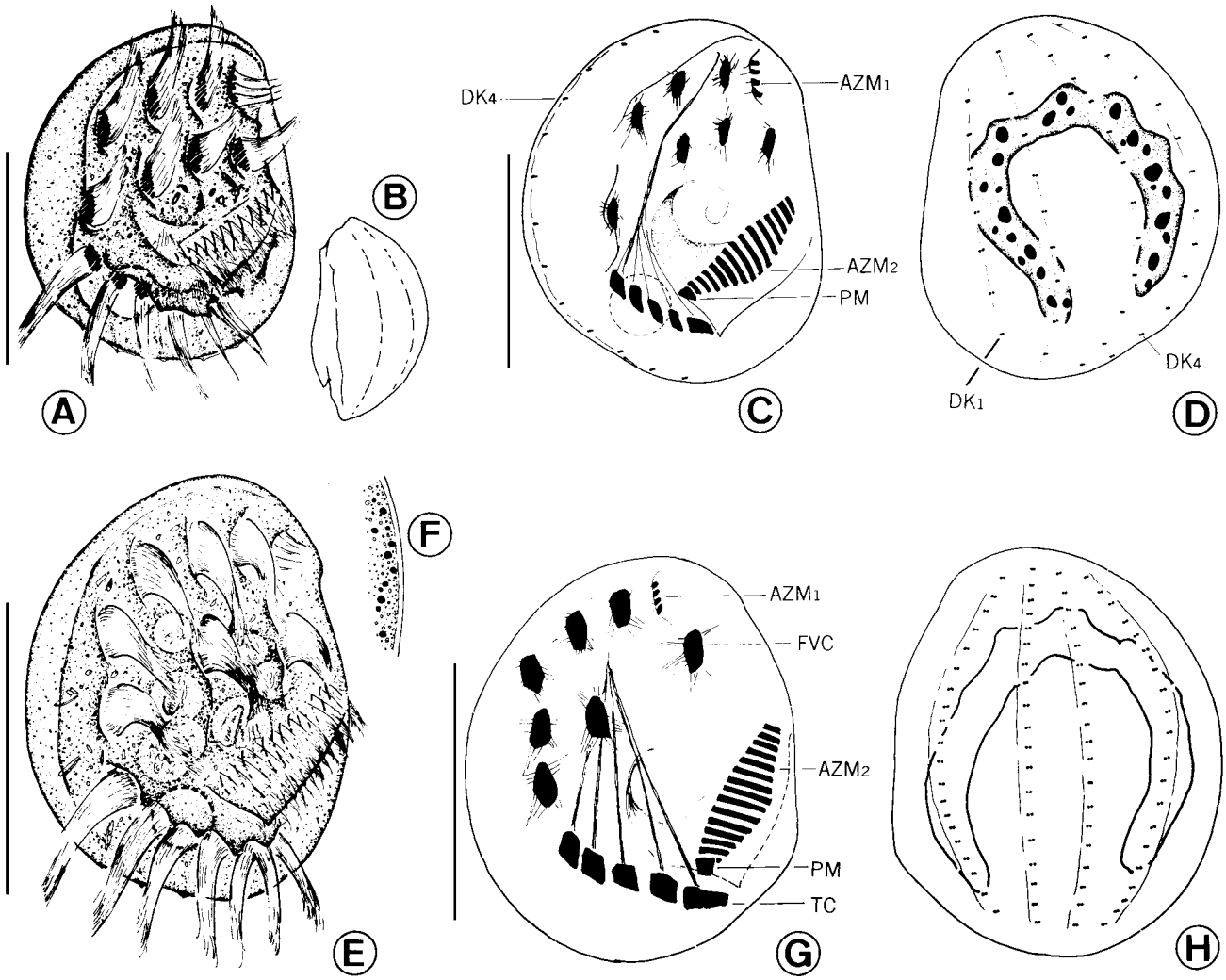

Figs 17A-H. *Aspidisca quadrilineata* Kahl, 1932 (A-D) and *Aspidisca crenata* Fabre-Domerque, 1885 (E-H) from life (A, B, E, F) and protargol impregnation (C, D, G, H). **A** - ventral view of a typical individual; B - lateral view to show the "smooth" ridges on dorsal side; **C, D - v**entral and dorsal view of infraciliature. **E** - ventral view of a typical individual; F - detail of the cortex, to show the dark granules beneath the pellicle; **G, H** - ventral and dorsal view of the infraciliature; note that the leftmost cirrus of the TC is considerably larger than others: *in vivo* it always "splits" into 3 cirri (see also the living situation in Fig. G). $AZM_{1,2}$ - adoral zone of membranelles 1, 2; $DK_{1,4}$ - dorsal kinety 1,4; FVC - frontoventral cirri; PM - paroral membrane; TC - transverse cirri). Scale bars: A, C - 20 µm, E, G - 40 µm

pattern (Fig. 8G). Scuticus (Sc) with about 3 pairs of basal bodies, sparsely arranged, posterior to cytostome (Fig. 8G, arrowheads).

Silverline system as shown in Figs 8D-F, apically one small silverline circle formed by kineties (Fig. 8E). Caudally leftmost kinety (SKn) crossing over caudal area and continuing on to caudal cilium complex (Fig. 8F). Caudal cilium complex (CCo) at posterior end, as seen in most other scuticociliates, consisting of 3 argentophilic granules (probably one basal body and 2 parasomal sacs), which are only revealed after silver nitrate impregnation (Fig. 8F). Extrusomes arranged in two ways: some of them between kinetosomes within direct silverline (double-arrowheads in Fig. 8D); others in groups of 1 to 4 situated between kineties, transversely connected by indirect silverline (Fig. 8D). Cytopyge (CyP) as short argentophilic slit between kinety 1 and n, irregularly shaped (Figs 8E, F). Contractile vacuole pore (CVP) near posterior end of kinety 2 (Fig. 8F).

Discussion and comparison. Until now, the genus *Metanophrys* has contained only 3 species, *M. durchoni* Puytorac *et al.* 1974, *M. sinensis* Song & Wilbert, 2000,

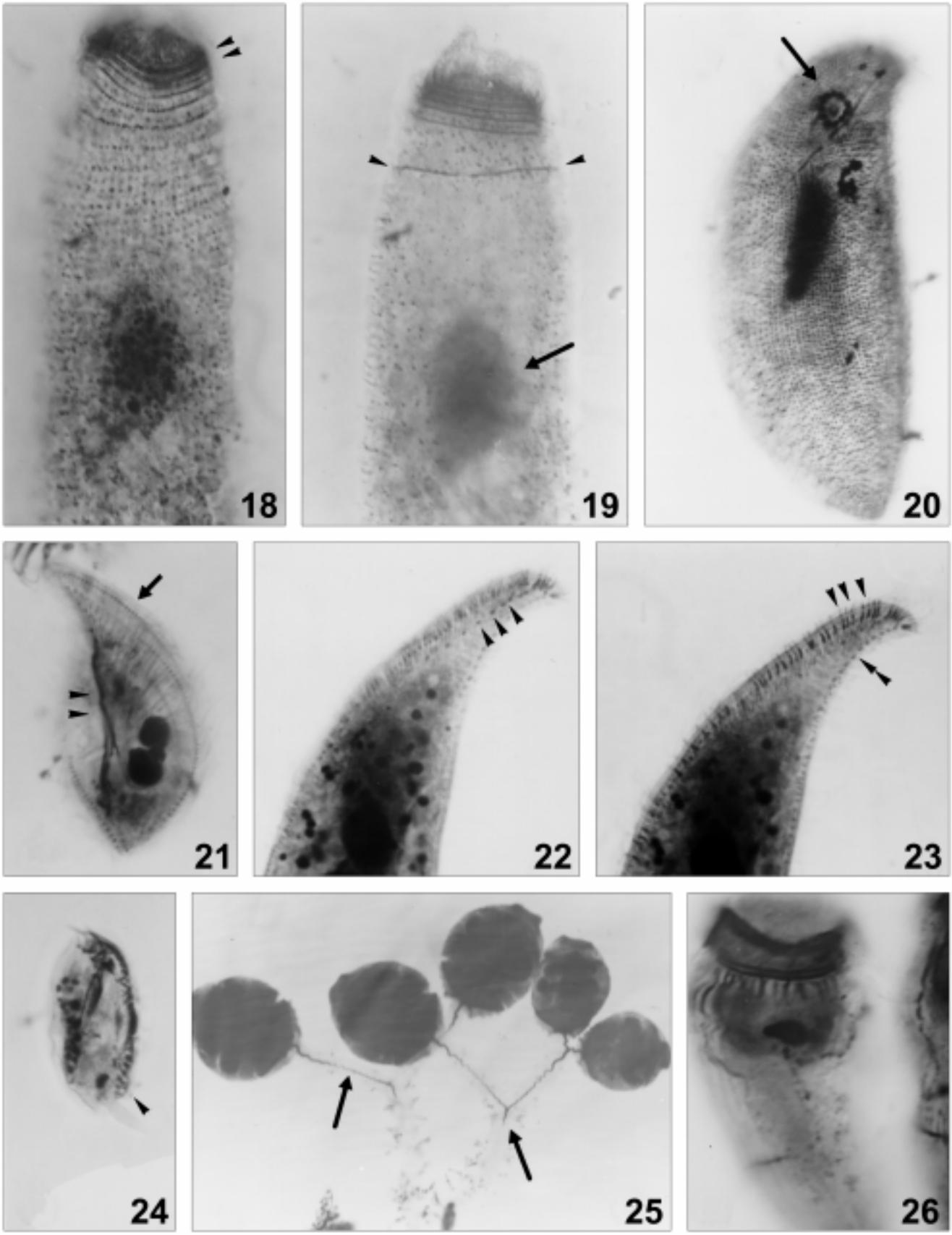
18
19
20
21
22
23
24
25
26

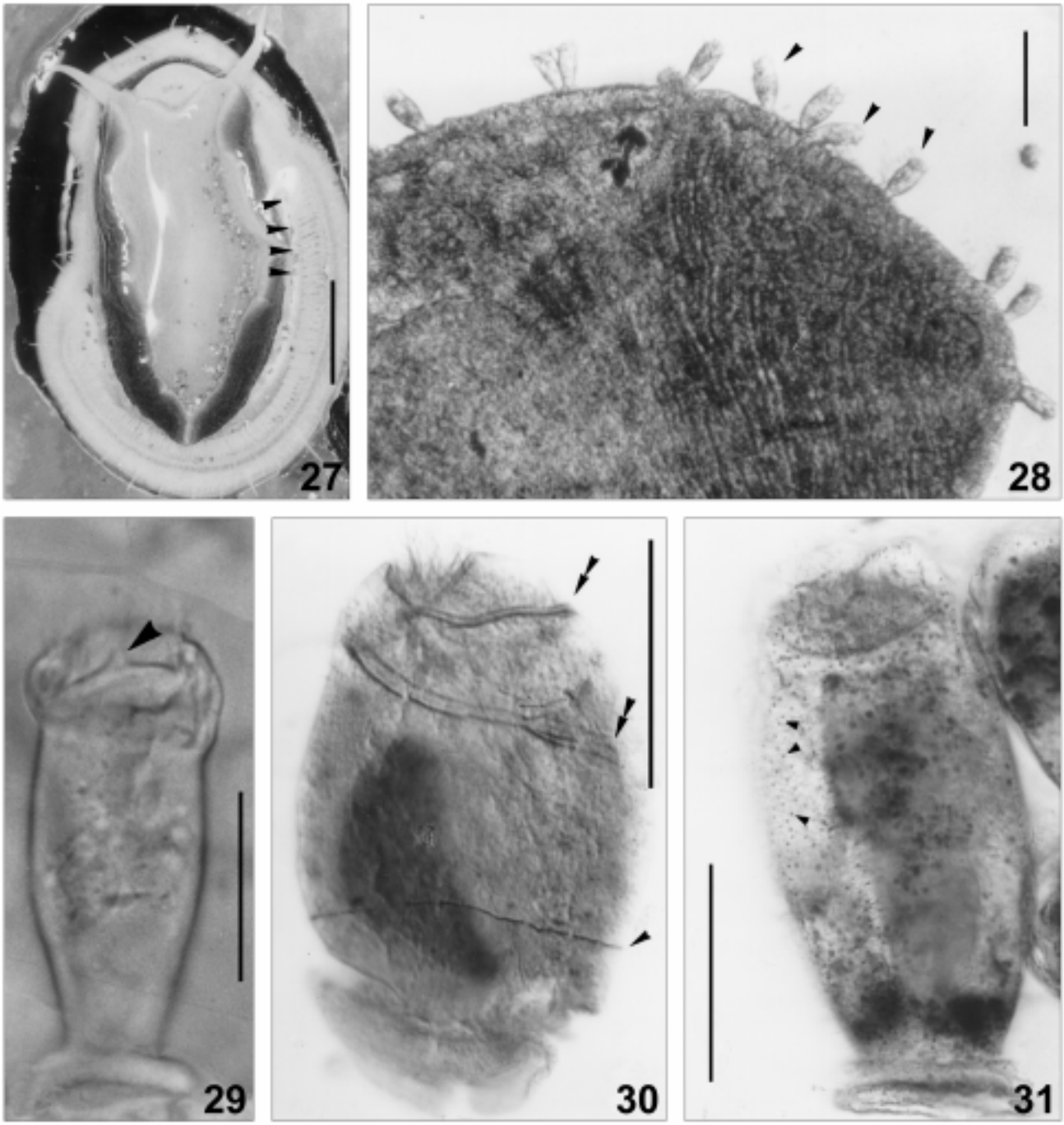

Figs 27-31. Photomicrographs of *Scyphidia* sp. **27** - ventral view of the host, *Nacella concinna*, with arrowheads marking the gills. **28** - zooids of *Scyphidia* sp. on the outer edge of a gill plate (arrowheads); **29** - a typical zooid *in vivo*. Arrow points to the peak on the perioral disc; **30** - protargol impregnated specimens, showing general infraciliature and nuclear apparatus; double-arrowheads indicate the peniculi, while the arrowhead marks the aboral ciliary wreath, **31** - silverline system after silver nitrate impregnation, note the pellicular pores between the close-set silverlines (arrowheads). Scale bars: **27**- 5 mm, **28** - 200 μm, **29-31** - 50 μm

Figs 18-26. Photomicrographs of *Metacystis* sp. (18, 19), *Orthodonella shenae* sp. n. (20), *Litonotus antarcticus* sp. n.(21-23), *Dysteria calkinsi* (24) and *Zoothamnium* sp. (25, 26) after protargol impregnation. **18, 19** - infraciliature of anterior portion; arrowheads in Fig. 18 indicate the double-rowed circumoral kineties, and in Fig. 19 mark the posterior-most perioral kinety; arrow in Fig. 19 ponts to macronucleus (arrow). **20** - ventral view of infraciliature; arrow indicates the cytostome. **21** - right view of infraciliature; arrowheads mark the fibres, while the arrow indicates the first perioral kinety; **22** - left view; arrowheads mark the 3rd perioral kinety; **23** - left view of the same specimen as in Fig. 22, to show extrusomes (arrowheads) and the dorsal brosse (double-arrowheads). **24** - to show the ventral kineties. **25** - four zooids, arrows mark the myoneme; **26** - general appearance of a zooid, note the argentophilic fibres extending all over the cell

and *M. elongata* (Biggar & Wenrich, 1932) Grolière *et al.* (1978). Our new species differs from *M. elongata* in body size (30-45 *vs.* 100-120 μm), number of somatic kineties (14 *vs.* 15-20) and structure of oral apparatus: the latter has highly developed, extremely long membranelles 1 and 2 (Grolière *et al.* 1978). *M. durchoni* has 2 contractile vacuole pores situated subcaudally within 2nd and 3rd somatic kinety, and a single-rowed membranelle 1 (Puytorac *et al.* 1974). Additionally, the silverline surrounding the caudal pole forms a small and in particular closed circle (misinterpretation ?) and is, therefore, distinctly different from those of the Antarctic organism. The species recently reported by the present authors, *M. sinensis*, is similar to this new species in size but can be identified definitely by lower number of somatic kineties (9-10 *vs.* 14), differently arranged extrusomes and the structure of membranelle 1: in the former membranelle 1 is much longer with *ca* 8 pairs of kinetosomes (Song and Wilbert 2000b).

Genus *Pleuronema* Dujardin, 1836

Pleuronema coronatum Kent, 1881, (Fig. 37)

This species was identified from protargol impregnated specimens. All morphometrical data correspond with the previous descriptions perfectly. For details see Dragesco (1968) and Song and Wilbert (1997).

Order Peritrichida Stein, 1859

Genus *Scyphidia* Dujardin, 1841

The family Epistylididae Kahl, 1933, to which *Scyphidia* belongs, comprises sessile peritrichs that either attach directly by way of the scopula or are fixed to the substrate by a non-contractile stalk. This family has been subdivided by Guhl (1979) into two subfamilies: (1) Epistylinae, with the diagnosis: oral region as a rule with distinctly set-off marginal ridge (= peristome with lip), the disk is not stalked, being continuous with the lip; brief description "epistyliform". (2) Opercularinae, which is characterized by: peristome without lip, disc can be absent and when present is usually stalked; brief description "opercullariform".

The traditional genus *Scyphidia* Dujardin, 1841 includes both epistyliform and opercullariform species. Hence it was divided into two genera by Guhl (1979): *Scyphidia* and *Scyphidiella* (for the opercullariform). In 1985, Jankowski included *Scyphidiella* in the genus *Scyphidia* but placed the epistyliform species originally assigned to *Scyphidia* by Guhl in a total of 4 genera according to the habitats and living styles: *Mantoscyphidia* Jankowski, 1980: reserved for species living on freshwater and marine mollusks; *Myoscyphidia* Jankowski, 1985 for species on aquatic plants and in the periphyton of ponds; *Speleoscyphidia* Jankowski, 1980: with one limnetic free-living species and *Riboscyphidia* Jankowski, 1980 for species living on marine and freshwater fishes (Jankowski 1980).

The classification of *Scyphidia* according to its hosts is definitely questionable, chiefly in view of the fact that many symphorionts do not exhibit the degree of host specificity required for such a system. For this reason we consider it unsuitable and maintain the systematic arrangement by Guhl (1979). Based on this new understanding, *Mantoscyphidia marioni* Van As *et al.*, 1998 should be transferred into *Scyphidia* as a new combination, *Scyphidia marioni* (Van As *et al.* 1998) comb. n.

The Antarctic form described here was found in large numbers on the gills of the Antarctic limpet *Nacella concinna* collected in the lower littoral at low tide and all its morphology was investigated in detail (i.e. living morphology, infraciliature and silverline system). Since some taxonomically reliable characters (i.e. the infraciliature and silverline system) are unavailable in most known congeners, which have been basically described using "classical" methods, while many other features (e.g. the body shape, size, position of the contractile vacuole or the appearance of the nuclear apparatus) overlap extensively among them, it is extremely difficult to recognize or to separate them (Cuénot 1891, Hirshfield 1949, Lom and Corliss 1968, Fish and Goodwin 1976, Van As *et al.* 1998). As a result, it is completely impossible for us to identify our species or even to compare it with its "related" forms.

In our opinion, this genus urgently needs a detailed revision and all "known" as well as uncertain species need re-confirmation or careful description/comparison before a definitive assignment is made. Hence, we treat our form as an "unrecognized" species here, whose taxonomic identification awaits further comparison and investigations.

***Scyphidia* sp.** (Figs 9A-E, 27-31, 61; Table 4)

Description. Zooids in extended state usually cylindrical or conical with prominent attaching "foot" on surface of gills, body about 70- 120 μm in length, when contracted, oval to broadly spindle-shaped (Figs 9B, C). Peristome with widely projecting collar. Peristomial disc slightly convex with a central peak (Fig. 29, arrowhead). Contractile vacuole large, below peristomial collar and dorsally positioned. Buccal cavity conspicuous; cytopharynx short, limited to the upper third of body. Pellicle delicately ringed and discernible only at high magnification. Endoplasm greyish, often with several

Table 5. Morphometric comparison of *Metaurostylopsis rubra* sp. n. (upper line), *M. marina* (Kahl, 1932) Song *et al.* (2001) (middle line) and *Holosticha diademata* (Rees, 1884) (lower line). All data are based on protargol-impregnated specimens. Measurements in µm

Character	Min	Max	Mean	SD	SE	CV	n
Body length	132	226	181.1	32.54	10.29	18.0	10
	86	120	107.1	9.20	2.06	9.3	20
	52	77	66.7	9.17	3.46	13.7	12
Body width	72	101	83.3	11.64	4.75	13.8	7
	38	60	47.0	5.80	1.85	12.2	20
	21	54	42.0	6.49	1.88	15.5	12
Length of buccal field	54	72	60.3	5.59	2.11	9.3	7
	35	46	40.6	2.90	0.67	7.1	19
	20	38	28.6	6.39	1.84	22.4	12
Number of adoral membranelles	35	46	38.9	3.76	1.19	9.7	10
	27	30	28.4	1.10	0.26	4.3	19
	21	33	28.1	3.81	1.21	13.6	10
Number of buccal cirri	1	1	1	0	0	0	>20
	1	1	1	0	0	0	25
	1	1	1	0	0	0	12
Number of frontal cirri	4	4	4	0	0	0	14
	4	4	4	0	0	0	25
	4	4	4	0	0	0	12
Number of frontoterminal cirri	5	8	6.2	0.98	0.30	15.9	11
	3	6	4.5	0.96	0.24	21.7	16
	2	2	2	0	0	0	13
Number of cirral pairs in midventral rows	8	11	9.5	1.04	0.31	11.0	11
	7	11	9.3	1.14	0.29	12.2	16
	7	10	8.7	1.03	0.31	12.4	12
Number of cirri in the ventral row	8	13	9.8	1.69	0.53	17.2	10
	4	7	-	-	-	-	5
	-	-	-	-	-	-	-
Number of left marginal rows	6	9	7.8	0.87	0.25	11.2	12
	3	5	4.1	0.57	0.14	14.1	16
	1	1	1	0	0	0	>30
Number of right marginal rows	6	7	6.3	0.49	0.14	7.8	12
	3	5	4.1	0.44	0.11	10.9	16
	1	1	1	0	0	0	>30
Number of transverse cirri	4	6	4.6	0.77	0.21	16.6	13
	5	9	6.8	1.00	0.24	15.2	17
	7	11	9.75	1.22	0.35	12.5	12
Number of cirri in left marginal row	-	-	-	-	-	-	-
	-	-	-	-	-	-	-
	12	16	14.3	1.49	0.43	10.4	12
Number of cirri in right marginal row	-	-	-	-	-	-	-
	-	-	-	-	-	-	-
	14	21	17.7	1.95	0.60	11.0	11
Number of dorsal kineties*	3	3	3	0	0	0	14
	3	3	3	0	0	0	16
	4	5	4.25	0.45	0.13	10.6	12

* Only the complete rows counted

large shining globules (inactive food vacuoles). Macronucleus variable in shape, slender to broad oviform, always positioned in posterior end of body.

This organism not very sensitive to stimulation, on isolated gills no formation of swarmers being induced (even after more than 2 weeks).

Infraciliature as shown in Figs 9D, E, haplokinety (H) und polykinety (P) spiral through about one and a half turns before entering vestibule (buccal cavity). As in other peritrichs, polykinety in buccal cavity differentiating three distinct peniculi (P_{1-3}), which finally spiral to reach the cytopharynx. Germinal kinety (G) begins far

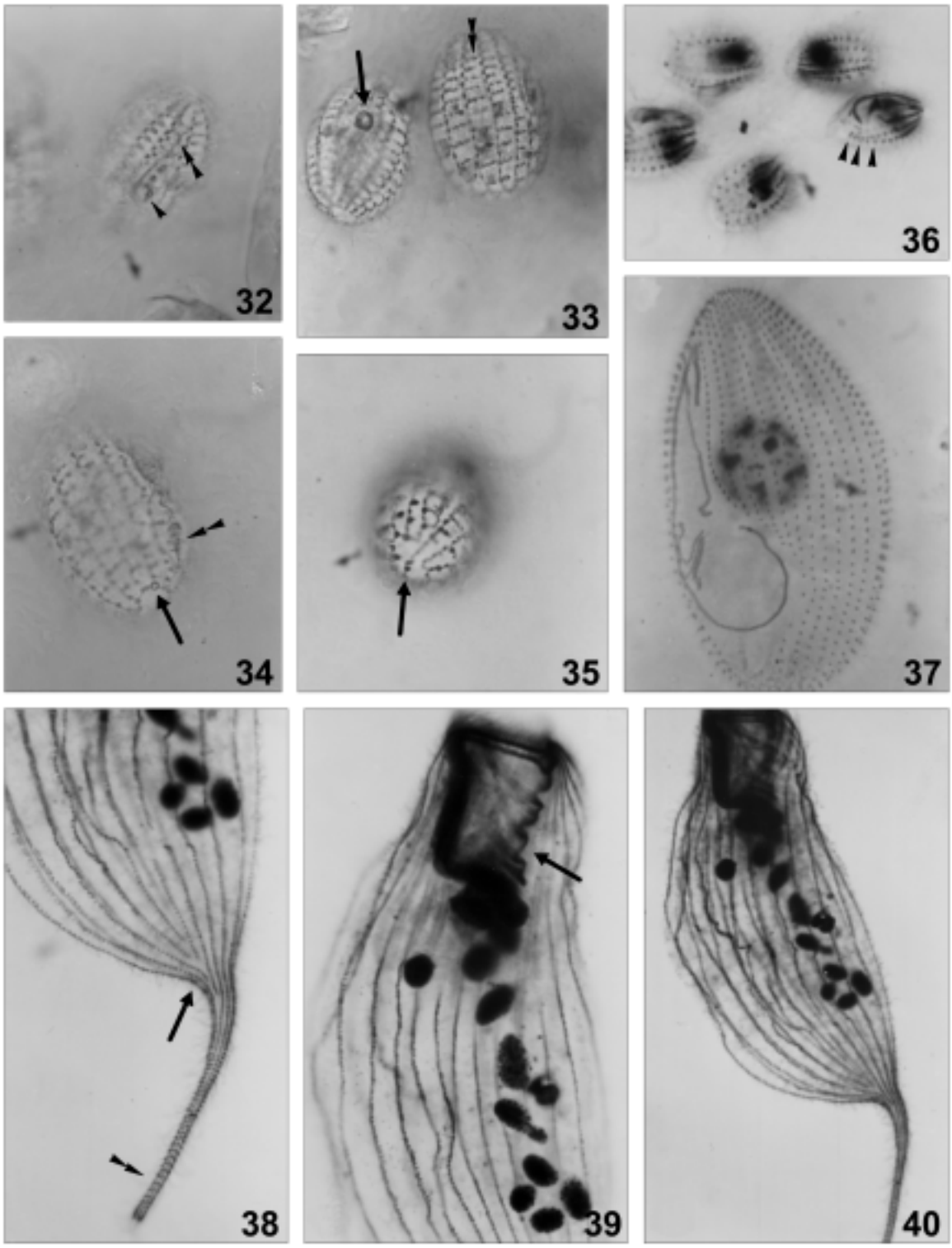

Figs 32-40. Photomicrographs of *Metanophrys antarctica* sp. n. (32-35), *Cyclidium varibonneti* (36), *Pleuronema coronatum* (37) and *Condylostoma remanei* (38-40) after silver nitrate (32-35) and protargol (36-40) impregnation. **32** - ventral view of silverline system; arrowhead marks the cytostome, while double-arrowheads indicate the membranelle 1; **33** - to show the arrangement of the extrusomes (double-arrowheads); arrow marks the cytostome; **34** - caudal-lateral view; arrow indicates the pore of contractile vacuole, while the double-arrowheads point to the cytopyge; **35** - caudal view, arrow marks the caudal-cilium-complex. **36** - general view of some individuals, arrowheads indicate the densely ciliated somatic kinety n-1; **37** - ventral view of infraciliature. **38** - posterior portion; arrow indicates the portion where the shortened kineties converge, double-arrowheads mark the long tail; **39** - anterior portion, arrow indicates the paroral membrane; **40** - general view from dorsal side

up in vestibule and parallel to haplokinety. In vestibule where the peniculi differentiate, G and H separate from the polykinety and run towards the opposite wall. Both peniculi 1 and 2 considerably longer than P3 (Fig. 9E). Aboral ciliary wreath (ACW) band-like, formed by short, diagonal kineties, each comprising *ca* 3 kinetosomes (Fig. 9C).

Silverline system striated type, very closely spaced less than 1μm between the individual lines, with numerous pellicular pores between silverlines (Fig. 9F). It resembles the silverlinesystem of *Scyphidia physarum* Lachmann, 1856, but the latter has a more widely spaced striation (Foissner and Schiffmann 1979)

Remarks. Our *Scyphidia* is possibly close to *Mantoscyphidia marioni* Van As *et al.*, 1998, which is also isolated as an ectocommensal organism from *Nacella* off South Africa, but has symbiotic flagellates (Van As *et al.* 1998). However, the two forms can be campared only on the basis of characters from life, for the latter was described without giving data or the infraciliature and silverline system. *Mantoscyphidia marioni* is smaller than the Antarctic form *in vivo* and differs from the latter in having symbiotic flagellates.

Other related symphorionts on marine mollusks are *S. hydrobiae* Kahl, 1933, 70 μm long, found in the Kiel Bay on tentacles and snout of *Hydrobia* species; *S. patellae* Cuénot, 1891, 30-50 μm in length, on the gills of *Patella vulgata*, Atlantic; *S. ubiquita* Hirshfield, 1949, 102 x 43 μm in size, on the gills and in the mantle cavity of the genera *Acmea, Lottia, Tegula, Fissurella, Littorina* and *Gibbula* (Hirshfield 1949, Lom and Corliss 1968, Fish and Goodwin 1976); *S. acanthophora* Fish & Goodwin, 1976, 108 x 37 μm, in the mantle cavity of *Gibbula umbilicalis* and *Monodonta lineata*, Irish Sea. For completeness, mention should also be made of the Atlantic species *S. scorpaenae* Fabre-Domergue, 1888, which is epizoic on the gills of *Scorpaena*, 53 μm long. Our Antarctic form differs from all these mentioned above in the combined characters of body shape and size. The peaked structure projecting above the disc can be found in either freshwater or marine species.

Genus *Zoothamnium* Bory de St Vincent, 1826

***Zoothamnium* sp.** (Figs 25, 26)

All colonies observed are rather senile and somewhat "abnormal" in stalk and myoneme structure, which render species identification difficult. Hence it is considered as an *incertae sedis*.

Zooids elongate, *in vivo* about 100 μm long with dominant double-layered peristomial border; pellicle smooth (at least at low magnification), endoplasm transparent. Contractile vacuole large, apically located. Macronucleus C-shaped, thick and transversely positioned. Colony large, stalk branching regularly dichotomous. There seems no differentiation of macro- and microzooids.

This species is fairly similar to the well-known *Zoothamnium duplicatum* Kahl, 1933 but larger in size and relatively slender (more elongated) in the shape of zooids (Song 1991a). Further investigations are definitely needed.

Order Heterotrichida Stein 1859

Genus *Heterostentor* gen. n.

Diagnosis. Slightly to strongly contractile, free-living Heterotrichina with elongated body shape; no conspicuous buccal cavity or cytopharynx; oral apparatus *Stentor*-like, restricted apically around small truncated frontal plate; without peristomial kineties, paroral membrane highly degenerated or absent; somatic ciliature with suture on ventral side.

Type species. *Heterostentor coeruleus* sp. n.

Etymology. The denomination "*Heterostentor*" (Hetero- Latin, different) indicates that this new genus is similar to the well-known taxon *Stentor.* Masculine gender.

Remarks. This new genus is characterized by the combination of the following traits: (1) without conspicuous buccal cavity; (2) structure of adoral zone of membranelles like that in *Stentor*, but has no peristomial kineties; (3) paroral membrane not present or highly degenerated when present and (4) free-living with elongated body shape.

***Heterostentor coeruleus* sp. n.** (Figs 10A-J, 41-44)

Diagnosis for the new species. Slightly asymmetric and contractile Heterotrichina with bright blue colour and elongate body shape; *in vivo* about 200-300 μm long with *ca* 50-70 membranelles in AZM which form a non-closed "6" pattern; no paroral membrane present; 100-120 somatic kineties in mid-body; one oval to ellipsoid macronucleus 60-80 x 30-40 μm in size; marine habitat.

Description. Body shape basically as shown in Fig. 10A, mostly elongated cylindrical to slightly fusiform, dorsoventrally somewhat flattened, length to width about 1:3-5; posteriorly narrowed to rounded tapering; anterior end narrowed and more or less head-like (similar to some prostomatids), oral bulge vaulted or slightly truncated (Figs 10A, G). Cells highly contractile but not sensitive to disturbance, hence *in vivo* observations, body shape almost constant, not metabolic or flexible (the contractility can be seen only after fixation). Pellicle as in some *Stentor*, rough with densely packed, dark-

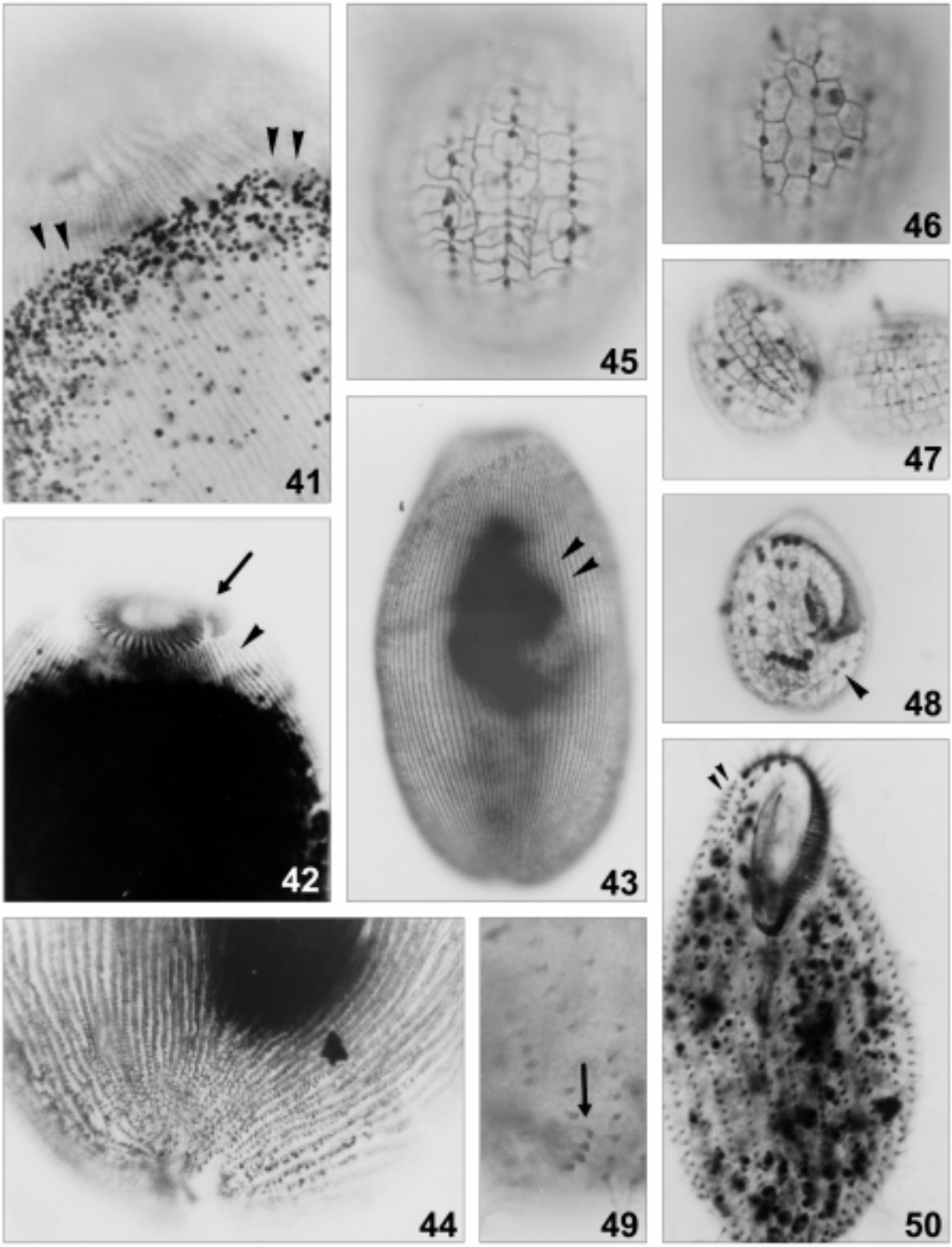

Figs 41-50. Photomicrographs of *Heterostentor coeruleus* gen. n., sp. n. (41-44), *Euplotes balteatus* (45-48) and *Metaurostylopsis rubrai* sp. n. (49, 50) after silver nitrate (45-48) and protargol (41-44, 49, 50) impregnation. **41** - anterior portion, arrowheads mark the dark argentophilic granules; **42** - anterior portion, to show the buccal apparatus (adoral zone of membranelles, arrow); note the suture on ventral side (arrowhead); **43** - general view of somatic ciliature, arrowheads mark the macronucleus; **44** - posterior portion. **45-47** - dorsal view, to show the irregular (45) and regular (46, 47) lattice structure; **48** - ventral view, arrow indicates the 2 close-set marginal cirri. **49** - posterior portion, to show the transverse cirri (arrow). **50** - general infraciliature on ventral side, arrowheads indicate the frontoventral cirri

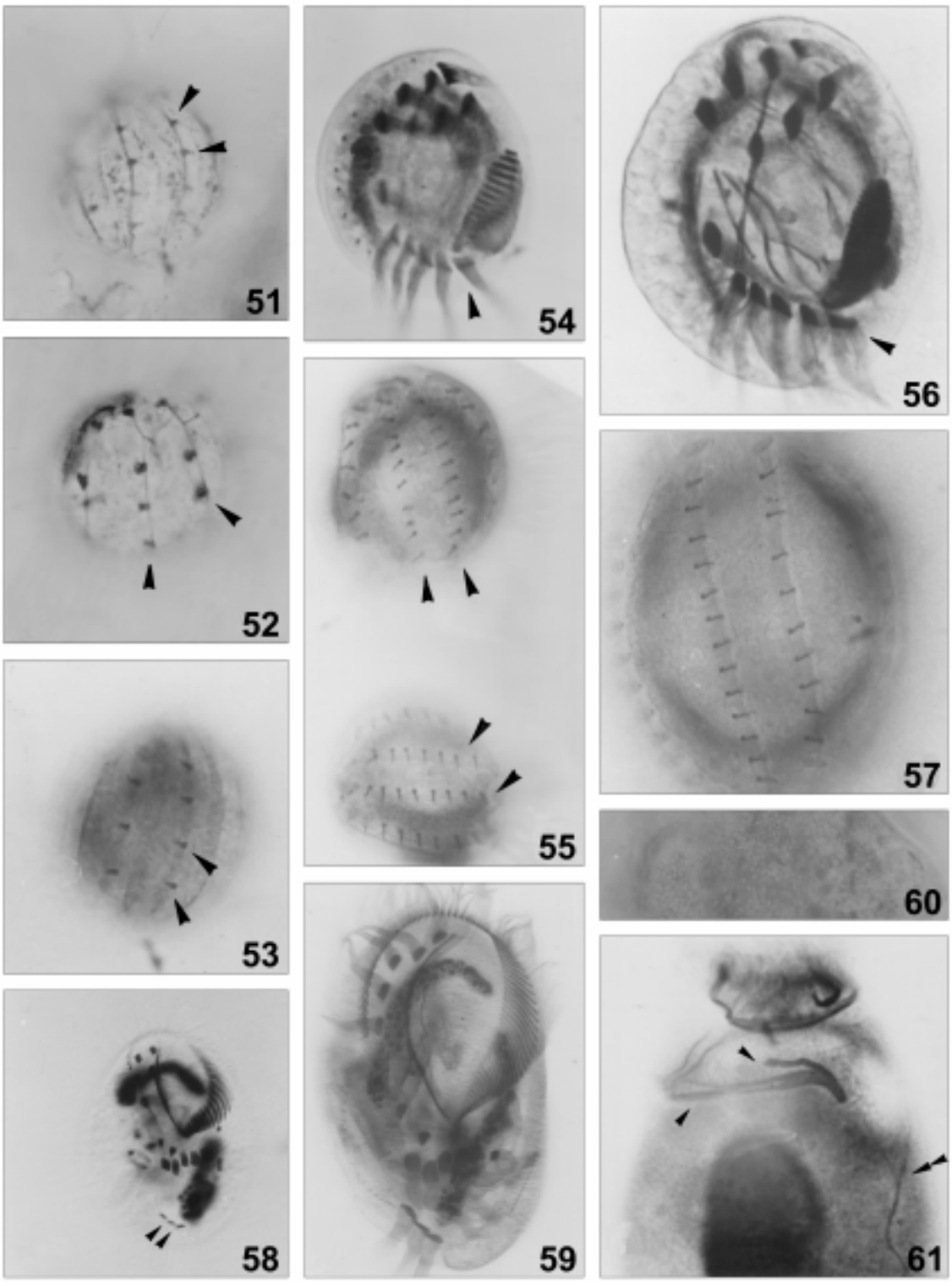

Figs 51-61. Photomicrographs of *Aspidisca polypoda* (51-53), *Aspidisca quadrilineata* (54, 55), *Aspidisca crenata* (56, 57), *Diophrys oligothrix* (58), *Diophrys scutum* (59, 60) and *Scyphidia* sp. (61) after silver nitrate (51, 52, 60) and protargol (53-59, 61) impregnation. **51, 52** - dorsal view, to show the silverline system; note the kinetids are loosely spaced (arrowheads); **53** - dorsal view, to exhibit the ribs and the loosely-arranged kinetids (arrowheads). **54** - ventral view, note the leftmost transverse cirri sharing the same base (arrowhead); **55** - dorsal view of two specimens, to show the densely spaced kineties (arrowheads). **56, 57** - ventral and dorsal view of infraciliature. **58** - ventral view, to show the general ciliature, arrowheads mark the caudal cirri. **59** - ventral view; **60** - dorsal view, to demonstrate the mesh-like silverline system. **61** - anterior portion, to show the buccal apparatus, arrowhead marks the peniculi, while double-arrowheads indicate the cytopharynx fibres

blue pigments between ciliary rows (arrowhead in Fig. 10D), which render the cell bright-blue (especially in some regions, e.g. anteriorly around/beneath adoral zone of membrane, where the pigments seem distinctively dense, double-arrowheads in Fig. 10E). Cytoplasm, due to thickness and numerous inclusions, completely opaque or even dark, often full of large lipid droplets; after protargol staining, always numerous black-coloured granules close to cortex (3-5 μm across) (Fig. 10F, arrowhead), which seem difficult to bleach during protargol impregnation (Fig. 10G). Macronucleus large, ellipsoid to elongate in shape, located in mid-body, appearing as one large transparent region in vivo (Fig. 10G); no micronucleus detected.

Cilia of membranelles about 20 μm long, in other somatic area *ca* 10 μm in length. Movement slow, gliding on substrate (Fig. 10G).

Oral apparatus as shown in Fig. 10I, base of membranelles *ca* 10-15 μm long with possibly 2 rows of kinetids. Adoral zone of membranelles (AZM) spiraling in a 6 shape, with small "gap" between the two ends, in the centre of which no kineties are present; hence a large, bald field is formed (BF in Fig. 10I). Buccal cavity possibly not present or very inconspicuous. Very unusually, no definite paroral membrane can be discerned (possibly severely degenerated ?) in our specimens.

Somatic kineties composed of densely packed dikinetids, generally both ciliated. Almost all kineties anteriorly terminating close to adoral zone of membranelles (Fig. 10I), while anteriorly on ventral side, some shortened kineties forming suture like that in *Stentor* (Fig. 10I, arrowheads). But sometimes in middle portion of cell (ventral side ? It is difficult to determine the "ventral" or "dorsal" side in this form), a few kineties shortened anteriorly terminating near right one and giving the appearance of one inconspicuous suture (arrowheads in Fig. 10H). Caudally a group of close-set basal bodies densely arranged (CC in Fig. 10J).

Comparison. Considering the body shape, cell colour, nuclear apparatus and especially the unique ciliature, no similar species can be compared with this new organism. However, since the buccal apparatus is really very unusual in structure, e.g. no paroral membrane has been recognized (non-present or degenerated ?), further studies will presumably be necessary.

Genus *Condylostoma* Bory, 1824

Condylostoma remanei Spiegel in Kahl, 1928, (Figs 11A-E, 38-40)

This species was *in vivo* merely insufficiently observed by us, therefore only a brief mention of its infraciliature can be given here (for further information, see Kahl 1932; Spiegel 1926; Villeneuve-Brachon 1940).

Description. The Antarctic population corresponds to the original very well (Spiegel 1926, Kahl 1928): cells colourless and rather transparent, about 500-800 μm long; body shape usually constant, cylindrical in body portion with one conspicuous, abruptly-narrowed long tail which is about 2/3 of body length. Buccal cavity dominant and genus-typical, about 30% of body length (Fig. 11C). Macronuclei with *ca* 12 ellipsoid nodules, beaded and slightly on right of body (Fig. 11G).

Somatic kineties composed of paired basal bodies, generally both ciliated with relatively short cilia (Figs 11A, F). About 22 somatic kineties, some of which terminate at the base of the tail (Fig. 11B, arrowheads). Kineties on ventral side more loosely arranged than dorsally.

Adoral zone of membranelles (AZM) conspicuous, proximal portion invaginated, consisting of more than 200 membranelles (Fig. 11D). At distal end of AZM, 2 to 3 membrane-like cirri apically on margin of buccal lip (Fig. 11D, Ci). Paroral membrane (PM) highly developed, on right of dominant buccal cavity, terminating posteriorly near cytopharynx (Fig. 11D).

Remarks. Differences from *Condylostoma longicaudata* Dragesco 1996: this species is in vivo considerably shorter (about 500-800 *vs*. 800-1600 μm in length), has relatively lower number of somatic kineties (22 *vs*. 27 on average) and in proportion longer buccal field compared with the body length (*ca* 1/4 *vs*. 1/6 of body length) (Dragesco 1996).

Order Hypotrichida Stein, 1859

Genus *Metaurostylopsis* Song, Petz & Warren, 2001

This newly-established genus *Metaurostylopsis* differs from other similar genera within the family Urostylidae (e.g. *Pseudokeronopsis, Thigmokeronopsis, Birojimia, Kahliella, Keronella, Australothrix*) by having several marginal rows on each side, which are generated completely from marginal cirral anlagen during morphogenesis, and by possessing both frontoterminal and clearly differentiated frontal cirri (Song *et al.* 2001).

***Metaurostylopsis rubra* sp. n.** (Figs 12A-J, 49, 50; Table 5)

Diagnosis for the new species. Large marine *Metaurostylopsis, in vivo* 150-300 x 50-90 μm with elongated body shape and brick-reddish cell colour; conspicuous cortical granules in rows on dorsal side;

6-7 right and 6-9 left marginal cirral rows; *ca* 40 adoral membranelles, 5-8 frontoterminal, 1 buccal and 4-6 transverse cirri; 8-11 midventral cirral pairs and one ventral row with about 8-13 cirri; constantly with 3 complete dorsal kineties; *ca* 100 macronuclear nodules; one contractile vacuole positioned anterior 2/5 of cell length.

Description. Body flexible and slightly contractile, *in vivo* mostly elongate or somewhat sigmoid, sometimes widest at posterior 1/3 of cell length with both anterior and posterior end narrowly rounded (Figs 12A-D). Ratio of length to width about 3:1, dorsoventrally flattened *ca* 2:1. Buccal cavity prominent, about 30 % of body length. Pellicle thin, cortical granules conspicuous, densely packed in irregular lines on dorsal side (Fig. 12B). Cytoplasm brick- to dark-reddish due to pigments which are fine and distributed throughout whole body and especially in the anterior cell end (Figs 12D, arrow; E). Endoplasm usually containing numerous different-sized shining globules (*ca* 2-5 μm across), flagellates, other ciliates and diatoms (Fig. 12A). Contractile vacuole large, located on left slightly above equatorial region of body. Macronuclear nodules oval to elongate, 5-8 μm long (Fig. 12I), each with several large nucleoli, scattered within body and almost impossible to spot *in vivo*.

Movement no specialities, crawling moderately quickly on debris or substrate.

Most cirri relatively fine, about 10-15 μm long, frontal cirri and membranelles *ca* 20 μm long. Consistently 4 enlarged frontal cirri (FC), which are continuous posteriorly with the midventral rows (MVR). Frontoterminal cirri (FTC) in short row between right end of adoral zone of membranelles and innermost right marginal cirral row (Fig. 12G). Single buccal cirrus (BC) relatively strong, situated beside mid-point of paroral membrane. Midventral cirral rows with *ca* 10 cirri, extending in zig-zag shape to about level of cytostome, posteriorly continuous with *ca* 10 unpaired ventral cirri (Fig. 12G). Transverse cirri located caudally, in gap between marginal cirral rows, which are basically fine and inconspicuous, projecting only slightly beyond posterior body margin (Fig. 12H). Commonly 8 left and 6 right marginal cirral rows, which are usually arranged obliquely from anterior right to posterior left, and some of which extend on dorsal side (Figs 12H, J).

Anterior portions of rightmost marginal rows always curving onto dorsal surface, where there are 3 complete dorsal kineties composed of 3 to 4 μm long cilia. Beside these kineties, commonly 2 to 3 fragment-like rows, each with about 1-4 paired kinetosomes anterior to rightmost marginal rows (Note: these "kineties" are not counted in Table 5 !). Not seldom some extra kinetosomes found inconstantly between kineties (double-arrowheads in Fig. 12J).

Adoral zone of membranelles (AZM) about 1/3 of body length in fixed specimens; bases of membranelles up to 12 μm long. Distal end of adoral zone of membranelles bending only slightly towards the right. Both paroral and endoral membranes (PM, EM) long and straight, almost parallel to one another. Pharyngeal fibres conspicuous after protargol impregnation, up to 50 μm long (Cph, Fig. 12G).

Comparison. There is only one known species in the genus, *Metaurostylopsis marina* (Kahl, 1932) Song *et al.* 2001. Compared with it, the new species can be distinguished *in vivo* by the larger size (150-300 *vs*. 80-120 μm), cell colour (brick-reddish *vs*. colourless) and body shape (elongated *vs*. oval). In addition, this new organism has a relatively higher number of ventral cirri (8-13 *vs*. 4-7), marginal rows on both sides (6-9 *vs*. 3-5) and adoral membranelles (35-46 *vs*. 27-30) (Table 5).

The reddish form described by Dragesco (1965) under the name of *Urostyla marina* Kahl, 1932 is possibly a population of this species, though his organism has fewer marginal rows on both sides (4 on the right and 3 on the left).

Genus Holosticha Wrzesniowski, 1877

Holosticha diademata (Rees, 1884), (Figs 13A, B; Table 5)

This well-known species is distinguished by the body shape and post-equatorial position of the contractile vacuole. Numerous specimens were found in our samples.

Considering the size and ciliature, the present population is highly variable in size (40-80 μm in vivo) with relatively rather strong cirri (Fig. 13A) and a higher number of marginal and mid-ventral cirri (see also Petz *et al.* 1995, called *H. pullaster*). Additionally, the adoral zone of membranelles is conspicuously separated into two parts with a large gap between them (arrowheads in Fig. 13A): anterior one with 8-12 membranelles, while the posterior one with 13-23.

As Hu and Song recently reinvestigated, this marine form differs from its closely-related freshwater congener, *H. pullaster* (Müller, 1773), in possessing cortical granules on the dorsal side, which appear absent in the latter (Foissner *et al.* 1991, Hu and Song 1999).

Petz *et al.* (1995) described an organism under the name *Holosticha pullaster* (Müller, 1773) from Antarctic that could be a population of this species though the number of paired cirri in the midventral rows seems

Table 6. Morphometric characterization of *Euplotes balteatus* (upper line) and *Diophrys oligothrix* (lower line). All data are based on protargol-impregnated specimens. Measurements in μm

Character	Min	Max	Mean	SD	SE	CV	n
Body length	40	66	48.8	4.65	1.34	9.5	12
	52	95	70.3	16.96	5.36	24.1	10
Body width	30	44	34.2	2.44	0.71	7.2	12
	30	67	46.5	14.80	4.68	31.8	10
Length of buccal field	29	42	32.9	2.54	0.73	7.4	12
	34	54	41.8	7.38	2.33	17.7	10
Number of adoral membranelles	27	33	30.2	2.15	0.68	7.1	10
	31	37	34.3	2.06	0.78	6.0	7
Number of frontoventral cirri	10	10	10	0	0	0	13
	7	7	7	0	0	0	11
Number of transverse cirri	5	5	5	0	0	0	14
	5	5	5	0	0	0	11
Number of left marginal cirri	1	2	1.9	0.34	0.09	18.2	16
	2	2	2	0	0	0	11
Number of caudal cirri	2	2	2	0	0	0	14
	3	3	3	0	0	0	11
Number of dorsal kineties	8	10	9.2	0.62	0.15	6.9	16
	4	5	4.4	0.50	0.10	11.4	23
umber of dikinetids in mid-dorsal rows	9	14	10.9	1.41	0.34	12.9	17
	-	-	-	-	-	-	-
Number of macronuclei	1	1	1	0	0	0	>30
	2	2	2	0	0	0	>20

somewhat lower and all ciliature appears relatively weaker. We consider these as population-dependent variation and suggest that the name, *H. pullaste*r be given to the freshwater form without cortical granules.

Genus *Uronychia* Stein, 1859

Uronychia binucleata Young, 1922

A few specimens of this species were found in protargol-impregnated slides. Both the morphology and infraciliature agrees perfectly with the redescriptions by previous authors (Curds and Wu 1983, Petz *et al.* 1995, Song and Wilbert 1997), so no further descriptions are needed.

Genus *Diophrys* Dujardin, 1841

Diophrys oligothrix Borror, 1965, (Figs 14A-D, 58; Table 6)

We agree with Borror (1965) and Czapik (1981) that *Diophrys oligothrix* Borror, 1965 is a valid species, which differs from the well-known *D. appendiculata* (Ehrenberg, 1838) Levander, 1894 in having the non-broken dorsal kineties, which extend continuously over the dorsal side instead of having a large gap in the equatorial region. Other features for *D. oligothrix* are: (a) paroral and endoral membrane parallel and closely located (*vs.* conspicuously separated); (b) basically 4 dorsal kineties (*vs.* mostly 5) and (c) usually slender (*vs.* more oval in shape) but larger (Song and Packroff 1997).

The Antarctic population agrees basically well with the original and subsequent descriptions (Borror 1965, Czapik 1981, Petz *et al.* 1995, Song and Packroff 1997). We thus supply only some additional data here.

Description. Cells *in vivo* about 60-80 μm long, usually more plump than the description given by Song and Packroff (1997), i.e. mostly oval to broadly oval with asymmetric posterior end: on right one prominent depression, where the caudal cirri transversely positioned (Fig. 14A).

Ciliary organelles in this population are relatively long, especially caudal cirri and some anterior membranelles which are conspicuously longer than others and spread stiffly (Fig. 14A). Buccal field about 1/2 of body length. 2 ridges on ventral side, one on right margin, another to left, relatively short and less dominant, posterior to cytostome (Fig. 14A). Cytoplasm grayish or colourless, often filled with several to many food vacuoles which render the cell completely opaque. This organism seems to feed preferably on flagellates and diatoms (Figs 14A, D). Consistently 2 elongated macronuclear nodules.

Behaviour and movement like a *Euplotes*, gliding without pause on substrate.

Both somatic and oral ciliature correspond perfectly to previous descriptions (Petz *et al.* 1995, Song and Packroff 1997). Compared with the China population, transverse cirri in the Antarctic form more anteriorly positioned. Mostly 4 (seldom 5) dorsal kineties with relatively longer cilia (about 5-7 µm) (Figs 14 B, D).

Diophrys scutum Dujardin, 1842 (Figs 14E-I, 59, 60)

Syn. *Diophrys magnus* Raikov & Kovaleva, 1968

Diophrys kasymovi Agamaliev, 1971

This species was also newly reinvestigated by Song and Packroff (1997) and hence no further complete descriptions are necessary. Here only some critical points will be mentioned.

Description. This species often exhibits some variability in ciliary pattern as observed by many previous authors. The number of the frontoventral cirri is "normally" 7, but not seldom 8 even 9 (Fig. 14E). The same situation has been also observed in the transverse and caudal cirri: in the former mostly 5, sometimes 6 (the surplus cirri might derive from the FVT-anlagen during the binary division rather than from the retained parental structure), while in the latter usually 3, less frequently 4.

The dorsal ciliature of the Antarctic population seems slightly different form the populations reported in previous work. The posterior end of the rightmost dorsal kinety is unlike that described for the China population, i.e. not fragment-like, but as "normal" dikinetids anterior to the caudal cirri (Fig. 14G).

Remarks. Raikov and Kovaleva (1968) described a new species form the Japan Sea, *Diophrys magnus*, which is characterized by slender body shape and two macronuclei with more or less moniliform shape and several micronuclei. We consider it conspecific with *D. scutum* because the number of micronuclei could have been misinterpreted (their organisms were impregnated by Chatton-Lwoff methods), and it is quite common in this species that the shape of body or macronuclei varies slightly.

According to Agamaliev (1971), the Caspian Sea species, *Diophrys kasymovi* Agamaliev, 1971 differs form *D. scutum* in having more frontoventral cirri (the author indicates that there are 6 transverse and 8 frontoventral cirri in the former). In our opinion, however, this is a very weak criterion because the number of transverse as well as frontoventral cirri changes frequently in *D. scutum* even within a clone culture according to the authors' knowledge. Hence we consider it as a junior synonym of the latter.

Genus *Euplotes* Ehrenberg, 1830

Eupotes balteatus (Dujardin, 1841) Kahl, 1932, (Figs 15A-F, 45-48; Table 6)

Syn. *Euplotes alatus* Kahl, 1932 (?)

E. quinquecarinatus Gelei, 1951 (?)

E. magnicirralus Carter, 1972 (?)

E. plicatum Valbonesi *et al.*, 1997 (?)

Since this species is highly polymorphic with extremely variations in size and other morphological features, we generalize the data obtained and give an improved definition here.

Improved diagnosis. Small to medium-sized marine *Euplotes in vivo* mostly 40-70 x 30-50 µm, 25-33 membranelles, 10 frontoventral, 5 transverse, 2 cau-

Table 7. Comparison of some small, morphologically-related marine *Euplotes*-species with silverline pattern of "double-*eurystomus*" on dorsal side and 10 frontoventral as well as 2 marginal cirri. Measurements in µm. AZM - adoral zone of membranelles, BB - basal bodies, DK - dorsal kineties, MC - marginal cirri, Mem - membranelles

Species*	Body size DK *in vivo*	No.	No., BB in mid-rows	No., mem in AZM	Feature of MC	References
E. balteatus	40-70	8-10	9-14	27-33	close-set	present paper
E. balteatus	30-150	8	11	25-30	widely separated	Tuffrau 1964a
E. balteatus	50	8	13-14	28-33	close-set	Agamaliev 1968
E. alatus	*ca* 40	8	*ca* 10 ?	*ca* 30 ?	widely separated	Borror 1968
E. quinquecarinatus	*ca* 60	9	*ca* 13 ?	*ca* 30 ?	widely separated	Borror 1968
E. magnicirratus	54**	8	13-17	*ca* 50	widely separated	Carter 1972
E. plicatum	42-55	10	14	22-25	widely separated	Valbonesi *et al.* 1997
E. rariseta	40-67	6	8-14	25-33	close-set	Petz *et al.* 1995

* The taxonomic identifications not confirmed in current table! ** Data probably from impregnated specimens? Data not given, he re counted from illustrations of the original authors.

Table 8. Morphometric characterization of *Aspidisca polypoda* (first line), *Aspidisca quadrilineata* (second line) and *Aspidisca crenata* (third line) All data are based on protargol-impregnated specimens

Character	Min	Max	Mean	SD	SE	CV	n
Body length in µm	25	37	30.8	2.83	0.89	9.4	10
	32	41	36.9	3.17	0.79	8.6	16
	50	64	59.2	4.64	1.47	7.8	10
Body width in µm	23	32	26.7	3.43	1.09	12.9	10
	26	36	31.6	3.22	0.81	10.2	16
	40	55	48.4	5.02	1.59	10.4	10
Number of membranelles in the first part of	4	4	4	0	0	0	9
the adoral zone of membranelles (AZM1)	4	5	4.2	0.38	0.10	9.0	13
	4	4	4	0	0	0	5
Number of membranelles in the second part of the	10	12	10.7	0.68	0.21	6.3	10
adoral zone of membranelles (AZM2)	12	14	13.2	0.83	0.23	6.3	13
	17	19	-	-	-	-	4
Number of frontoventral cirri	7	7	7	0	0	0	10
	7	7	7	0	0	0	21
	7	7	7	0	0	0	14
Number of transverse cirri*	5	6	5.6	0.51	0.13	9.6	15
	5	7	5.9	0.45	0.11	8.5	16
	5	7	5.4	0.67	0.19	12.3	10
Number of dorsal kineties	4	4	4	0	0	0	>20
	4	4	4	0	0	0	>20
	4	4	4	0	0	0	>15
Number of dikinetids in dorsal kinety 1	4	5	4.3	0.50	0.17	11.5	9
	7	10	8.4	1.01	0.27	12.1	14
	18	22	19.9	1.45	0.46	7.3	10
Number of dikinetids in dorsal kinety 2	5	6	5.7	0.54	0.17	8.8	9
	9	13	11.3	1.16	0.33	10.2	12
	18	24	21.3	2.15	0.65	10.1	11
Number of dikinetids in dorsal kinety 3	5	6	5.7	0.49	0.18	8.5	7
	11	14	12.4	1.02	0.27	8.2	14
	19	22	20.5	1.20	0.42	5.8	8
Number of dikinetids in dorsal kinety 4	5	7	6.3	0.68	0.21	10.7	10
	11	16	12.4	1.74	0.47	14.0	14
	19	24	21.6	1.97	0.59	9.1	11
Number of macronuclei	1	1	1	0	0	0	>20
	1	1	1	0	0	0	16
	1	1	1	0	0	0	>20

* According to the bases of cirri instead of the cirral number observed *in vivo* (see also text)

dal and two close-set marginal cirri; 8 to 10 dorsal kineties with *ca* 11 dikinetids in mid-rows; silverline system double-*eurystomus* type.

Description. Body shape generally oval, left convex, right straight with obliquely truncated posterior end (Fig. 15A). Dorsoventrally flattened about 2:1. At anterior region, dorsal surface more or less deck-like and stretching forwards, coving ventral part and distal end of adoral zone membranelles, which is clearly discernible after silver impregnation (Fig. 15E). 3-4 conspicuous ventral ridges between buccal field and right margin; ridges among transverse cirri short but prominent (Fig. 15A). On dorsal side about 6-7 longitudinal dorsal ridges extending over entire length of body, conspicuous *in vivo* (Fig. 15B). Cilia of cirri and membranelles *ca* 10-15 µm long. Cytoplasm colourless, containing many shining globules (*ca* 2-3 µm across) and food vacuoles with possibly flagellates or bacteria. Macronucleus inverted C-shaped. Contractile vacuole at level of transverse cirri (Fig. 15A).

Movement genus-typical, crawling on substrate, not fast and slightly jerking.

Infraciliature as shown in Figs 15C, D. Adoral zone of membranelles about 2/3 of body length, anteriorly terminating near right margin, where there is an inconspicuous spur-like projection on ventral surface. Paroral membrane (PM) small, new-moon-shaped, typically composed of "many" irregularly arranged kinetosomes; positioned beneath the buccal lip and hence generally revealed only by protargol impregnation (Fig. 15C). Considering the small size, most cirri - except marginal and caudal ones - rather strong (bases usually considerably large, especially in small individuals). Consistently 10 frontoventral cirri arranged in normal pattern; 5 transverse cirri posterior to cytostome, among which the second one from left is in most cells conspicuously stronger than the others (arrow in Fig. 15C). 2 left marginal cirri mostly closely spaced, cirri fine, *ca* 15 μm long. Consistently 2 fine caudal cirri near caudal margin. Dorsal ciliation as in most of its congeners, usually 2 dorsolateral kineties on margins of both sides (Figs 15C, E). On dorsal side, mostly 7 kineties extending over entire length of body, mid-dorsal rows with about 9-14 dikinetids (Fig. 15D).

Silverline system genus-typical ventrally; regular double-*eurystomus* type on dorsal side (Figs 15E, F).

Remarks. Though several revisions have been made in recent decades (Tuffrau 1960, Carter 1972, Curds 1975), species identification in this genus is always of very difficult because most species exhibit high variability (e.g. size, shape, number of kineties and other ciliary features) and many authors seem to (more or less) have overlooked these aspects. This confusion likely derives also from the fact that many "new" forms have been described only on the basis of populations with no further adequate comparison. In our opinion, more attention should be paid to confirming these known forms rather than, without reliable foundation, describing new species.

We identify our form by its size, appearance of adoral zone of membranelles, habitat and the basic ciliature on both ventral and dorsal side (Kahl 1932, Tuffrau 1964a, Curds 1975). The Antarctic population differs slightly, however, in the number of dorsal kineties (8-10 *vs.* 8), stronger cirri (*vs.* relatively finer or weaker) and the arrangement of the marginal cirri: in Tuffrau's redescription, the two marginal cirri seem far away from each other (Tuffrau 1964a). This species might be highly variable and indeed, we have frequently observed some "form-variants" with less-densely positioned marginal cirri or specimens with relatively finer frontoventral and transverse cirri. Therefore we believe that they should be conspecific.

Euplotes alatus Kahl, 1932 is possibly a junior synonym of *E. balteatus,* for according to Borror's redescription, it has 8 dorsal kineties and exhibits otherwise no great differences to separate it from the latter (Borror 1968). For the same reason, three other small marine forms, *Euplotes magnicirratus* Carter, 1972, *E. plicatum* Valbonesi *et al.*, 1997 and *E. quinquecarinatus* Gelei, 1951 might be also synonymized with *balteatus* (Table 7).

Euplotes bisculcatus Kahl, 1932 and another Antarctic form described by Petz *et al.* (1995), called *E. rariseta* possibly misidentified, are likely also similar to this species but the former has 9 frontoventral cirri and one marginal cirrus (Borror 1968) while the latter possesses only 6 dorsal kineties (Table 7), and hence should be separated from the current species.

Genus *Aspidisca* Ehrenberg, 1838

As in *Euplotes*, much disarray remains in this genus in terms of species identification (Kahl 1932, Dragesco 1960, Tuffrau 1964b, Wu and Curds 1979, Foissner *et al.* 1991). This confusion derives from many forms having been described on the basis of insufficient living observations. Other reasons include: (1) some features (e.g. spurs, ridges, number of transverse cirri) are indeed rather variable, and are easily overlooked in some cases but often, unfortunately, used as a reliable diagnostic character and (2) many authors devoted insufficient attention to comparing their populations with previous studies.

Aspidisca polypoda (Dujardin, 1841) Kahl, 1932 (Figs 16A-H, 51-53; Table 8)

This species is easy to recognize because of the presence of 7-8 conspicuous ridges on the dorsal side and its small size. Since no data about infraciliature available, redescriptions based on silver impregnated specimens are presented here.

New diagnosis. Small marine *Aspidisca* with generally oval body shape, *in vivo* about 25-35 x 20-30 μm; *ca* 8 distinctive ridges on dorsal side; no conspicuous spur-like protrusions on cell surface; generally 6 transverse cirri *in vivo;* constantly 7 frontoventral cirri; 4 dorsal kineties loosely ciliated, each with about 4, 5, 6, 6 dikinetids; 4 membranelles in AZM1 while 10-12 in AZM2. One macronucleus C-shaped.

Description. Specimens *in vivo* very similar in size and shape, outline generally as shown in Fig. 16A, triangle-shaped with slightly snout-like anterior end; broad-

est always behind mid-body, both margins evenly convex; anteriorly broadly narrowed, while posteriorly more or less notched because of the presence of dorsal ribs (Fig. 16A). Dorsoventrally only slightly flattened (about 3:2) with 8 dominant ridges, which are clearly visible even at low magnification (Figs 16B, C) Pellicle rigid, appearance of ventral side basically similar to its congeners. Cytoplasm colourless or greyish, often with several large food vacuoles (feeding likely on flagellates). Contractile vacuole small, right of median, posterior to transverse cirri. Macronucleus C-shaped, with large conspicuous nucleoli (Fig. 16E). Micronucleus not observed.

Movement moderately fast when compared with its body size, crawling on substrate without periods of resting.

Ciliary structure rather stable (Figs 16D, E; Table 7). Cilia of frontoventral cirri about 10 µm long, in typical pattern of genus. Transverse cirri relatively weak, *ca* 15 µm in length, subcaudally arranged in oblique row; right-most cirrus always splitting into two closely spaced ones (Fig. 16A), though united at the base (Fig. 16D, arrow). Anterior part of adoral zone of membranelles (AZM1) with consistently 4 membranelles, located in deep concavity, while posterior part (AZM2) with on average 11 organelles, beneath lid-like spur. Paroral membrane close to proximal end of AZM2 (double-arrowheads in Fig. 16D). Pharyngeal fibres curved anteriorly. Dorsal kineties with quite sparsely-arranged basal body pairs (4-6 pairs each, Table 8), each along dorsal ridge and generally extending from end to end of cell (Fig. 16E).

Silverline system as shown in Figs 16F-H, basically typical of genus, contractile vacuole pore prominent (Fig. 16H, CVP).

Remarks With the small size, marine habitat, general outline and the distinctive 8 dorsal ribs (ridges), this organism is easy to recognize.

Aspidisca quadrilineata Kahl, 1932, (Figs 17A-D, 54-55; Table 8)

To the authors' knowledge, no reinvestigations have been made since it was erected (Kahl 1932). Hence we present here a detailed redescription and an improved diagnosis based on our observations.

New diagnosis. Small marine *Aspidisca* with generally oval body shape, *in vivo* about 30-40 x 25-35 µm; with neither conspicuous dorsal ribs nor pronounced spur-like protrusions throughout; 6 transverse *in vivo* and 7 frontoventral cirri; 4 dorsal kineties densely ciliated, each with about 8, 11, 12, 12 dikinetids; 4-5 membranelles in AZM1 and 12-14 in AZM2. One macronucleus C-shaped.

Description. This species generally rather similar to *polypoda* except for the dorsal ridges. *In vivo* slightly larger, about 35 x 30 µm in size; outline tending to be more oval with anterior end only very slightly snout-like; broadest in posterior 1/3 of body, with both cell margins evenly convex; posterior end more broadly rounded than anterior (Fig. 17A). Dorsoventrally flattened about 1.5-2:1. Pellicle armed as last form, 4 inconspicuous dorsal ridges (Fig. 17B). Cytoplasm colourless and opaque, often full of tiny granules. Single contractile vacuole on right near transverse cirri. Macronucleus slightly notched anteriorly with conspicuous nucleoli (Fig. 17D). In our protargol impregnated specimens, no micronuclei revealed.

Movement as in last form, slow to moderately fast, gliding on substrate.

Ciliature as in last species (Figs 17C, D). Mostly 6 transverse cirri *in vivo* (we observed individuals with sometimes even 7 cirri, in which case the leftmost two often joined together); yet only 5 after impregnation (Fig. 17C). Fibres dominant, associated with transverse cirri, extending to about anterior margin of cell. Mostly 4 (seldom 5) membranelles in AZM1 and 12-14 in AZM2. Paroral membrane (PM) close to proximal end of AZM2 (Fig. 17C). Dorsal kineties with densely-arranged dikinetids (about 8-12 pairs each, Table 8) (Fig. 17D).

Remarks. In Wu and Curds' revision (1979), this species was treated, without giving any explanation, as a synonym of *Aspidisca polypoda*, but in view of the completely different living appearance (i.e. with *ca* 8 dominant dorsal ridges *vs.* inconspicuous 4 ribs; and the infraciliature on dorsal side: the number of dikinetids in each kineties, see Table 8), this form is doubtless a valid species.

This species might be similar to *Aspidisca aculeata* (Ehrenberg, 1838), which can be distinguished, however, by a conspicuous dorsal thorn and loosely ciliated dorsal kineties: each with about 4-8 (*vs.* 8-12) dikinetids according to the redescriptions by Kahl (1932), Borror (1965) and Agamaliev (1974).

Aspidisca crenata Fabre-Domergue, 1885, (Figs 17E-H, 56-57; Table 8)

Our Antarctic population corresponds to the previous descriptions by Kahl (1932) very well (having "7" transversale Cirren, Hinterrand ohne deutliche Zähne,

nur schwach gekerbt oder gewellt"). Though Kahl insisted that this organism has 3-4 inconspicuous furrows (instead of "ribs" as in our own observations), we believe that our identification is correct while the presence of ribs or furrows is entirely an observer-dependent expression.

New diagnosis. Medium-sized marine *Aspidisca* with generally oval body shape and smooth cell margin, *in vivo* about 50-65 x 40-55 μm in size, dorsally with 4 very inconspicuous ribs; 7 strong frontoventral cirri; basically 7 transverse cirri from life; 4 dorsal kineties densely ciliated, each with about 20, 21, 21, 22 dikinetids; 4 membranelles in AZM1 while 17-19 in AZM2; macronucleus C-shaped.

Description. Size of this Antarctic population *in vivo* about 50-65 x 40-55 μm, body elliptical with inconspicuous snout-shaped anterior end; broadest in about midbody, left and right margin evenly convex; both anterior and posterior end broadly rounded; dorsoventrally highly flattened (so in low magnification often appeared hyaline!). Ventral surface generally flattened with buccal lid covering adoral zone of membranelles. On dorsal side, always 4 dominant ridges (Fig. 13C). Buccal area with 1 distinct thorn-like projection (prostomial spur) on left subcaudally, which covers the AZM2. Pellicle rigid, beneath it always some tiny dark-gray granules (about 1μm across) sparsely distributed, which can be observed only at high magnifications from life (Fig. 17F). Cytoplasm hyaline and colourless with large food vacuoles. Contractile vacuole about in median, at level of transverse cirri. Macronucleus C-shaped (Fig. 17H).

Movement crawling on substrate, typical of the genus.

Ciliary pattern as shown in Figs 17G, H. Frontoventral cirri rather stiff and strong, cilia about 12-15 μm long; consistently 7 transverse cirri tightly arranged in oblique row, among which the base of the right-most always 3 cirri *in vivo* as in some other congeners (Fig. 17G). Fibres from transverse cirri strong and prominent, extending anteriorly. AZM1 in deep concavity, containing only 4 membranelles, while AZM2 on left margin, with about 18 membranelles. Paroral membrane (PM) small, often difficult to recognize (Fig. 17G). Pharyngeal fibres curved anteriorly. Kineties on dorsal side densely ciliated (Fig. 17H).

Remarks. Without knowing the infraciliature, the authors inappropriately synonymized *Aspidisca crenata* with *A. leptaspis* (Song and Wilbert 1997). According to the data obtained recently and our new observations, however, the former should be considered as a valid but separate species. It differs from the latter in having clearly fewer membranelles in the AZM1 (4-5 *vs.* 7-8) and the frontoventral cirri (consistently 7 *vs.* 7 plus one small cirrus) (Song and Wilbert 1997).

It seems quite common that many "large" species (over 50 μm in length) possess 7 transverse cirri and *ca* 20 membranelles in the posterior part of AZM, and, as noticed by many previous authors, the body shape, especially the spur - outline might be highly variable among them, hence species identification for these large forms remains a huge difficulty. This problem might be solved only when the infraciliature of all uncertain forms has been revealed.

Acknowledgements. These studies were supported by personnel and equipment funds from the Alfred Wegener Institute for Polar and Marine Research, Bremenhaven and by the Deutsche Forschunsgemeinschaft as part of the program "Antarctic Research with Comparative Studies in Arctic Regions" awarded to NW, and a visiting grant awarded to WS by "The Natural Science Foundation of China" (project No. 39970098). Our thanks are also to Dr. Alan Warren, The Natural History Museum, London for kindly supplying some literature.

REFERENCES

Agamaliev F. G. (1968) Materials on morphology of some psammophilic ciliates of the Caspian Sea. *Acta Protozool.* **6:** 225-244 (in Russian, English summary)

Agamaliev F. G. (1971) Complements to the fauna of psammophilic ciliates of the Western coast of the Caspian Sea. *Acta Protozool.* **8:** 379-407 (in Russian, English summary)

Agamaliev F. G. (1974) Ciliates of the solid surface overgrowth of the Caspian Sea. *Acta Protozool.* **13:** 53-82 (in Russian, English summary)

Agatha S., Spindler M., Wilbert N. (1993) Ciliated protozoa (Ciliophora) from Arctic sea ice. *Acta Protozool.* **32:** 261-268

Agatha S., Wilbert N., Spindler M., Elbrächter M. (1990) Euplotide ciliates in sea ice of the Weddell Sea (Antarctica). *Acta Protozool.* **29:** 221-228

Borror A. C. (1963) Morphology and ecology of the benthic ciliated protozoa of Alligator Habor, Florida. *Arch. Protistenkd.* **106:** 465-534

Borror A. C. (1965) New and little known tidal marsh ciliates. *Trans. Amer. Micros. Soc.* **84:** 550-565

Borror A. C. (1968) Systematic of *Euplotes* (Ciliophora, Hypotrichida); toward union of the old and the new. *J. Protozool.* **15:** 802-808

Carter H. P. (1972) Infraciliature of eleven species of the genus *Euplotes. Trans. Amer. Micros. Soc.* **91:** 466-492

Corliss J. O. (1979) The Ciliated Protozoa: Characterization, Classification and Guide to the Literature. 2nd ed. Pergamon Press, New York

Corliss J. O., Snyder R. A. (1986) A preliminary description of several new ciliates from the Antarctica, including *Cohnilembus grassei* n. sp. *Protistologica* **22:** 39-46

Cuénot L (1891) Infusoires commensaux des Ligies, Patelles et Arenicoles. *Rev. Biol. Nord France* **4:** 81-89

Curds C. R. (1975) A guide to the species of the genus Euplotes (Hypotrichida Ciliatea). *Bull. Br. Mus. Nat. Hist. (Zool.)* **28:** 1-61

Curds C. R., Wu I. C. H. (1983) A review of the Euplotidae (Hypotrichida, Ciliophora). *Bull. Br. Mus. Nat. Hist. (Zool.)* **44:** 191-247

Czapik A. (1981) La morphogenèse chez le cilié, *Diophrys oligothrix* Borror. *Acta Protozool.* **20:** 367-372

Deroux G. (1970) La série «Chlamydonellienne» chez les Chlamydodontidae (Holotriches, Cyrtophrdina Fauré,-Fremiet). *Protistologica* **6:** 155-182

Deroux G. (1974) Les dispositifs adhésives ciliaires chez les Cyrtophorida et la famile des Hypocomidae. *Protistologica* **10:** 379-396

Deroux G. (1976) Plan cortical des Cyrtophorida III. Les structures différenciatrices chez les Dysterina. *Protistologica* **12:** 505-538

Deroux G. (1978) The hypostome ciliate order Synhymeniida: from *Chilodontopsis* of Blochmann to *Nassulopsis* of Fauré-Fremiet. *Trans. Amer. Micros. Soc*. **97:** 458-469

Dietz G. (1964) Beitrag zur Kenntnis der Ciliatenfauna einiger Brackwassertümpel (étangs) der französischen Mittelmeerküste. *Vie Milieu* **15:** 47-93

Dragesco J. (1960) Ciliés mésopsammiques littoraux. Systématique, morphologie, écologie. *Trav. Stn. Biol. Roscoff* **122:** 1-356

Dragesco J. (1963) Compléments à la connaissance des ciliés mésopsammiques de Roscoff. II. Hypotriches. *Cah. Biol. Mar.* **4:** 251-275

Dragesco J. (1965) Ciliés mésopsammiques d'Afrique noire. *Cah. Biol. Mar*. **6:** 357-399

Dragesco J. (1968) Les genres *Pleuronema* Dujardin, *Schizocalyptra* nov. gen. et *Histiobalantium* Stokes (Ciliés holotriches hymostomes). *Protistologica* **4:** 85-106

Dragesco J. (1996) Infraciliature et morphométrie de cinq espèces de ciliés mésopsammiques méditerranéens. *Cah. Biol. Mar.* **37:** 261-293

Dragesco J., Dragesco-Kernéis A. (1986) Ciliés libres de l'Afrique intertropicale. *Faune Tropicale* **26:** 1-559

Dragesco J., Iftode F., Fryd-Versavel G. (1974) Contribution à la connaissance de quelques ciliés holotriches rhabdophores; I. Prostomiens. *Protistologica* **10:** 59-75

Fenchel T., Lee C. C. (1972) Studies on ciliates associated with sea ice from Antarctica 1. The nature of the fauna. *Arch. Protistenkd.* **114:** 231-236

Fish J. D., Goodwin B. J. (1976) Observations on the peritrichous ciliate *Scyphidia ubiquita* from the west coast of Wales and a description of an new species. *J. Zool. (London)* **179:** 361-371

Foissner W. (1984) Taxonomie und Ökologie einiger Ciliaten (Protozoa, Ciliophora) des Saprobiensystems. I: Genera *Litonotus, Amphileptus, Opisthodon. Hydrobiologia* **119:** 193-208

Foissner W. Schiffmann H. (1979) Morphologie und Silberliniensystem von *Pseudovorticella sauwaldensis* nov. spec. und *Scyphidia physarum* Lachmann, 1856 (Ciliophora, Peritrichida) *Ber. Nat. Med. Ver. Salzburg* **3/4:** 83-94

Foissner W. (1996) Faunistics, taxonomy and ecology of moss and soil ciliates (Protozoa, Ciliophora) from Antarctica, with description of new species, including *Pleuroplitoides smithi* gen. n., sp. n. *Acta Protozool.* **35:** 95-123

Foissner W., Blatterer H., Berger H., Kohmann F. (1991) Taxonomische und ökologische Revision der Ciliaten des Saprobiensystems - Band I: Cyrtophorida, Oligotrichida, Hypotricha, Colpodea. *Informat Bayer Land. Wasserwirt* **1/91:** 1-478

Fryd-Versavel G., Iftode F., Dragesco J. (1975) Contribution à la connaissance de quepques ciliés Gymnostomes. II. Prostomiens, pleurostomiens: Morphologie, stomatogenèse. *Protistologica* **6:** 509-530

Grolière C. A., Puytorac de P., Grain J. (1978) Ciliés endocommensaux de l'Oursin *Lytechinus variegatus* des cotes de Ciudad del Carmen (Mexique) (Abstract). *J. Protozool.* **25:** 554

Guhl W. (1979) Beitrag zur Systematik, Biologie und Morphologie der Epistylididae (Ciliata, Peritricha). *Arch. Protistenkd.* **121:** 417-483

Hartwig E (1973) Die Ciliaten des Gezeiten-Sandstrandes der Nordseeinsel Sylt. I. Systematik. *Abh math-naturw Kl Akad Wiss Mainz Mikrofauna Meer* **18:** 1-69

Hirshfield H. (1949) The morphology of *Urceolaria karyolobia,* sp. nov., *Trichodina tegula*, sp. nov., and *Scyphidia ubiquita*, sp. nov., three new ciliates from southern California limpets and turbans. *J. Morphol.* **85:** 1-28

Hu X., Song W.. (1999) On morphology of the marine Hypotrichous ciliate, *Holosticha diademata* (Ciliophora, Hypotrichida), with comparison of its related species. *J. Ocean. Univ. Qingdao* **29:** 469-473 (in Chinese, English summary)

ICZN (The International Commission on Zoological Nomenclature) (1985) International Code of Zoological Nomenclature. 3rd ed. Univ. California Press, Berkeley

Jankowski A. W. (1968) Taxonomy of the suborder Nassulina Jank., 1967 (Ciliophora, Ambihymenida). *Zool. Zh.* **47:** 900-1001 (in Russian, English summary))

Jankowski A. W. (1980) Une revue de la nouvelle systématique du phylum Ciliophora. *Trud. Zool. Inst. Akad. Nauk USSR* **94:** 103-121 (in Russian)

Jankowski A. W. (1985) Life cycle and taxonomy of genera of the groups Scyphidia, Heteroplaria, Zoothamnium and Cothurnia (Class: Peritricha*). Proc. Zool. Inst. USSR Akad. Sci.* **129:** 74-100

Kahl A. (1928) Die Infusorien (Ciliata) der Oldesloer Salzwasserstellen. *Arch. Hydrobiol.* **19:** 50-123

Kahl A. (1930) Urtiere oder Protozoa I: Wimpertiere oder Ciliata (Infusoria). 1. Allgemeiner Teil und Prostomata. *Tierwelt. Dtl.* **18:** 1-180

Kahl A. (1931) Urtiere oder Protozoa I: Wimpertiere oder Ciliata (Infusoria). 2. Holotricha. *Tierwelt. Dtl.* **25:** 181-398

Kahl A. (1932) Urtiere oder Protozoa. I: Wimpertiere oder Ciliata (Infusoria), 3. Spirotricha. *Tierwelt. Dtl.* **25:** 399-650

Kahl A. (1933) Ciliata libera et ectocommensalia. In: Die Tierwelt der Nord- und Ostsee (Eds. G. Grimpe and E. Wagler) **23:** 29-146

Kahl A. (1935) Urtiere oder Protozoa I: Wimpertiere oder Ciliata (Infusoria). 4. Peritricha und Chonotricha. *Tierwelt. Dtl.* **25:** 651-886

Lom J. (1961) On the buccal apparatus of peritrichous ciliates. *Progr. Protozool. 1st Intern. Conf. Protozool. Prague* 91-95

Lom J., Corliss J. O. (1968) Observations on the fine structure of two species of the peritrich ciliate genus *Scyphidia* and their mode of attachment to the host. *Trans. Amer. Micros. Soc.* **87:** 493-509

Ozaki Y., Yagiu R. (1941) Studies on the marine ciliates of Japan, mainly from the Setonaikai (the inland sea of Japan) II. *J. Sci. Hiroshima Univ. (Ser B)* **9:** 159-180

Petz W.. (1994) Morphology and morphogenesis of *Strombidium kryalis* nov. spec. (Ciliophora, Strombidiida) from Antarctic sea ice. *Arch. Protistenkd.* **144:** 185-195

Petz W. (1995) Morphology and morphogenesis of *Thigmokeronopsis antarctica* nov. spec. and *T. crystalis* nov. spec. (Ciliophora, Hypotrichida) from Antarctic sea ice. *Europ. J. Protistol.* **31:** 137-147

Petz W., Song W., Wilbert N. (1995) Taxonomy and ecology of the ciliate fauna (Protozoa, Ciliophora) in the endopagial and pelagial of the Weddell Sea, Antarctica. *Stapfia* **40:** 1-223

Puytorac P. de, Grolière C. A., Roque M., Detcheva R. (1974) A propos d'un cilié *Philasterina* trouvé dans la cavité générale du polychète *Nereis diversicolor* O. F. Müller. *Protistologica* **10:** 101-111

Raikov I. B., Kovaleva V. G. (1968) Complements to the fauna of psammobiotic ciliates of the Japan Sea (Posjet gulf). *Acta Protozool*. **6:** 309-333

Song W. (1991a) Contribution to the commensal ciliates on *Penarus orientalis* II. (Ciliophora, Peritrichida). *J. Ocean. Univ.* Qingdao 21:45-55 (in Chinese, English summary)

Song W. (1991b) *Litonotus yinae* n. sp. (Protozoa, Ciliophora), a periphytic and commensal species from Qingdao. *Ophelia* **34:** 181-189

Song W. (2000) Morphological and taxonomical studies on some marine scuticociliates from China Sea, with description of two new species, *Philasterides armatalis* sp. n. and *Cyclidium varibonneti* sp. n. (Protozoa: Ciliophora: Scuticociliatida). *Acta Protozool.* **39:** 295-322

Song W., Packroff G. (1997) Taxonomische Untersuchungen an marinen Ciliaten aus China mit Beschreibungen von 2 neuen Arten, *Strombidium globosaneum* nov. spec. und *Strombidium platum* nov. spec. (Protozoa, Ciliophora). *Arch. Protistenkd.* **147:** 331-360

Song W., Wilbert N. (1989) Taxonomische Untersuchungen an Aufwuchsciliaten (Protozoa, Ciliophora) im Poppelsdorfer Weiher, Bonn. *Lauterbornia* **3:** 2-221

Song W., Wilbert N. (1995) Benthische Ciliaten des Süsswassers. In: Praktikum der Protozoologie (Ed. Röttger) Fischer Verlag, Stuttgart

Song W., Wilbert N. (1997) Morphological investigation on some free living ciliates (Protozoa, Ciliophora) from China Sea with description of a new hypotrichous genus, *Hemigastrostyla* nov. gen. *Arch. Protistenkd.* **148:** 413-444

Song W., Wilbert N. (2000a) Ciliates form Antarctic sea ice. *Polar Biol.* **23:** 212-222

Song W., Wilbert N. (2000b) Redefinition and redescription of some marine scuticociliates from China, with report of a new species, *Metanophrys sinensis* nov. spec. (Ciliophora, Scuticociliatida). *Zool. Anz.* **239:** 45-74

Song W., Wilbert N., Warren A. (1999) Three new entocommensal ciliates from digestive tract of sea urchins of the Weddell Sea, Antarctica (Protozoa, Ciliophora). *Polar Biol.* **22:** 232-240

Song W., Petz W., Warren A. (2001) Morphology and morphogenesis of the poorly-known marine urostylid ciliate, *Metaurostylopsis marina* (Kahl, 1932) nov. gen., nov. comb., with a description of the new genus *Metaurostylopsis* (Protozoa, Ciliophora, Hypotrichida). *Europ. J. Protistol.* (in press)

Spiegel A. (1926) Einige neue marine Ciliaten. *Arch. Protistenkd.* **55:** 184-190

Thompson J. C. (1972) Ciliated protozoa of the Antarctic Peninsula. In: Antarctic Terrestrial Biology (Ed. G. A. Llano). *Antarct. Res. Ser.* **20:** 261-288

Thompson J. C., Croom J. M. (1978) Systematics and ecology of ciliated protozoa from King George Island, South Shetland Islands. In: Biology of the Antarctic Seas VII (Ed. D. L .Pawson). *Antarct. Res. Ser.* **27:** 41-67

Tuffrau M. (1960) Revision du genre *Euplotes*, fondée sur la comparaison des structures superficielles. *Hydrobiologia* **15:** 1-77

Tuffrau M. (1964a) Le maintien des caractères spécifiques à travers le polymorphisme d'Euplotes balteatus Dujardin, 1841. *Arch. Zool. Exp. Gén.* **104:** 143-151

Tuffrau M. (1964b) La morphogenèse de bipartition et les structures neuromotrices dans le genre Aspidisca (Ciliés hypotriches). Revue de quelques espèces. *Cah. Biol. Mar.* **5:** 173-199

Valbonesi A., Luporini P. (1990a) Description of two new species of *Euplotes* and *Euplotes rariseta* from Antarctica. *Polar Biol.* **11:** 47-53

Valbonesi A., Luporini P. (1990b) A new marine species of *Euplotes* (Ciliophora, Hypotrichida) from Antarctica. *Bull. Br. Mus. Nat. Hist. (Zool.)* **56:** 57-61

Valbonesi A., Luporini P. (1990c) A new marine species of *Uronychia* (Ciliophora, Hypotrichida) from Antarctica: *Uronychia antarctica*. *Boll. Zool.* **57:** 365-367

Valbonesi A., Apone F., Luporini P. (1997) Morphology and biology of a new species of *Euplotes, Euplotes plicatum* sp. n. (Ciliophora: Euplotidae). *Acta Protozool.* **36:** 287-294

Van As L. G., Basson L., Van As J. G. (1998) Two new species of *Mantoscyphidia* Jankowski, 1980 (Ciliophora: Peritrichia), gill symbionts of limpets, from South Africa and the sub-Antarctic island, Marion. *Acta Protozool.* **37:** 101-111

Villeneuve-Brachon S. (1940) Recherches sur les ciliés hétérotriches: cinétome, argyrome, myonèmes. Formes nouvelles ou peu connues. *Arch. Zool. Exp. Gén.* **82:** 1-180

Wiencke C., Ferreyra G., Arntz W., Rinaldi C. (1998) The Potter Cove coastal ecosystem, Antarctica. *Ber. Polarforsch.* **299:** 1-326

Wilbert N. (1975) Eine verbesserte Technik der Protargolimprägnation für Ciliaten. *Mikrokosmos* **64:** 171-179

Wilbert N. (1986) Ciliates from saline lakes in Saskatchewan. *Symp. Biol. Hung.* **33:** 249-256

Wilbert N. (1995) Benthic ciliates of salt lakes. *Acta Protozool.* **34:** 271-288

Wilbert N., Kahan D. (1981) Ciliates of Solar Lake on the Red Sea shore. *Arch. Protistenkd.* **124:** 70-95

Wilbert N., Petz W., Song W. (1993) Observations on the ciliate community of the Antarctic sea ice and plankton (Ciliophora, Protozoa). *Ber. Polarforsch*. **121:** 89-90

Wu I. C. H., Curds C. R. (1979) A guide to the species of the genus *Aspidisca*. *Bull. Br. Mus. Nat. Hist. (Zool.)* **36:** 1-34

Received on 19th March, 2001; accepted on 5th January, 2002

Acta Protozool. (2002) 41: 63 - 77

ACTA
PROTOZOOLOGICA

Ultrastructure of *Tuzetia weidneri* sp. n. (Microsporidia: Tuzetiidae) in Skeletal Muscle of *Litopenaeus setiferus* and *Farfantepenaeus aztecus* (Crustacea: Decapoda) and New Data on *Perezia nelsoni* (Microsporidia: Pereziidae) in *L. setiferus*

Elizabeth U. CANNING[1], Alan CURRY[2] and Robin M. OVERSTREET[3]

[1]Department of Biology, Imperial College, London, U.K.; [2]Public Health Laboratory, Withington Hospital, Manchester, U.K.; [3]Department of Coastal Sciences, University of Southern Mississippi, Ocean Springs, Mississippi, U.S.A.

Summary. A new microsporidian species, *Tuzetia weidneri* sp. n. , is described from the skeletal muscle of the decapod crustaceans *Litopenaeus setiferus* and *Farfantepenaeus aztecus*. Fresh spores are pyriform, measuring 3.1 x 2.3 µm. All stages have unpaired nuclei. Meronts lie in direct contact with degenerate host cell cytoplasm but produce numerous small blisters at the surface. Multinucleate meronts divide by constriction into groups or chains of uninucleate products. Sporogony is initiated by deposition of a dense surface coat on the plasma membrane of uninucleate or multinucleate stages and fusion of blisters to enclose the sporont in a sporophorous vesicle (SV). Episporontal secretions in the SV are involved in the division of the sporont. During sporogonic division into chains of sporoblasts, the SV divides together with the body of the sporont, so that each sporoblast is enclosed in its own SV. Spores have a flattened anchoring disc that lies in the polar sac, membranous and spongiform regions of the polaroplast and 9-10.5 coils of the isofilar polar tube, around a posterior vacuole. The endospore layer of the spore wall is not thinned over the anchoring disc. The spore wall is adorned with a complex series of ridges. New data are presented on the spores of *Perezia nelsoni* (Sprague 1950) in *L. setiferus*. Of special interest is the polaroplast which is composed of an outer region of tightly-packed membranes in the form of a globule, which almost invariably completely encloses an inner region of loosely packed membranes. The isofilar polar tube, arranged in 8-10 coils angled around the large nucleus in the posterior half of the spore, passes through the membranes of the globular polaroplast near the periphery of the spore, then runs a curved course through the inner polaroplast and passes again through the globular polaroplast to join the anchoring disc. A polaroplast with one region completely enclosed by another has not been described previously.

Key words: *Farfantepenaeus aztecus*, *Litopenaeus setiferus*, Microsporidia, *Perezia nelsoni*, shrimps, taxonomy, *Tuzetia weidneri* sp. n., ultrastructure.

INTRODUCTION

Several microsporidian parasites have been described from shrimps (Crustacea, Decapoda), mostly infecting skeletal muscle and rendering the affected regions opaque white (those recorded before 1971 are listed by Sprague and Couch 1971). Infections may be associated with high mortalities, especially under intensive rearing conditions but, even in the absence of mortality, heavy infections render the shrimp unmarketable and inedible (Overstreet 1973).

Four of these microsporidia have been reported from the penaeid shrimps *Litopenaeus setiferus* (Linnaeus) and *Farfantepenaeus aztecus* (Ives). These are (1)

Address for correspondence: Elizabeth U. Canning, Department of Biology, Imperial College at Silwood Park, Ascot, Berkshire SL5 7PY, U.K.; Fax: +44-0207-594 2339; E-mail: e.canning@ic.ac.uk

Perezia nelsoni (Sprague 1950) Vivarès and Sprague, 1979 (synonyms: *Nosema nelsoni* Sprague 1950; *Nosema pulvis* Jones 1958; *Ameson nelsoni* (Sprague 1950) Sprague 1977); (2) *Thelohania* sp. of Kruse 1959 (also in *Farfantepenaeus duorarum* (*Penaeus duorara*) and considered by Kruse to agree well with *Thelohania duorara* Iverson and Manning 1959); (3) *Pleistophora* sp. of Baxter, Rigdon and Hanna 1970 (synonyms: *Pleistophora penaei* Constransitch 1970, nomen nudum; *Pleistophora penaei* Constransitch 1970 quoted by Couch 1978; *Pleistrophora penaei* of Couch 1983); (4) *Agmasoma penaei* (Sprague 1950) Hazard and Oldacre, 1976 (synonym: *Thelohania penaei* Sprague 1950). The gross appearances of infected hosts have been described by Overstreet (1973) and ultrastructural data are available for *P. nelsoni* (see Sprague and Vernick 1969, Loubès *et al.* 1977, Clotilde-Ba and Togubaye 1996) and *A. penaei* (see Hazard and Oldacre 1976, Clotilde-Ba and Togubaye 1994).

In the genus *Pleistophora* groups of uninucleate spores are formed by sequential division of a multinucleate sporogonial plasmodium within a persistent sporophorous vesicle derived from the surface coat of the sporogonial plasmodium (Canning and Hazard 1982). As part of a study of relationships of *Pleistophora*-like microsporidia from a range of vertebrate and invertebrate hosts, two samples of purified spores were provided by the Gulf Coast Research Laboratory, Ocean Springs, Mississippi for sequencing of the small subunit ribosomal DNA (16S rDNA) at Imperial College, London. The spores, dispersed and non-aggregated after purification, were believed to have been derived from infections of *Pleistophora* sp. and were referred to as *Pleistophora* sp. LS (from *L. setiferus*) and *Pleistophora* sp. PA (from *F. aztecus*) (Cheney *et al.* 2000). In the rDNA study the former sample was found, on sequence data, to be closely related to *Ameson michaelis*, a microsporidium from the crab *Callinectes sapidus*, the only other crustacean host included in the study. *Pleistophora* sp. PA fell into a polytomy with *Glugea atherinae*, *Loma* spp. and *Ichthyosporidium* sp., all parasites of fish. As this study had indicated that the shrimp microsporidia were unrelated to the true *Pleistophora* spp. from fish, an ultrastructural study was undertaken, using tissues from *L. setiferus* and *F. aztecus* infected with a microsporidium with loosely clumped spores as seen in fresh preparations. A second species in *L. setiferus* which gave rise to dispersed spores was also studied.

The results indicated that neither has the generic characters of *Pleistophora*. The microsporidian species with loosely clumped spores was identical in development and spore structure in *L. setiferus* and *F. aztecus*. The morphology has led us to assign it to the genus *Tuzetia* as a new species. This genus has not been reported previously from decapod crustaceans. The microsporidium with dispersed spores was identified as *Perezia nelsoni*. We present a description of the new genus and species as seen in both hosts and provide additional ultrastructural data on *P. nelsoni.*

MATERIALS AND METHODS

Specimens of *L. setiferus* and *F. aztecus* infected with the microsporidia were collected from Davis Bayou and Back Bay of Biloxi, Mississippi, USA. The shrimps were injected into the cephalothorax, hepatopancreas and abdominal musculature with Davidson's fixative (95% ethanol 33 ml, formaldehyde 220 ml, glacial acetic acid 115 ml, distilled water 335 ml) and immersed in the fixative for 3 days before processing tissues for embedding in Paraplast X-tra (53-54°C MP), sectioning at 4 μm and staining with Gill's haematoxylin and eosin (H. and E.). For electron microscopy (EM), small pieces of abdominal muscle and other tissues were fixed in Karnovsky's fixative, washed in 0.1 M cacodylate buffer, postfixed in 1% OsO_4 dehydrated in an ascending series of ethanol solutions and embedded in Spurr's resin *via* propylene oxide. Spores were observed fresh, in Giemsa-stained smears and in histological sections.

RESULTS

Prevalence

Fifty specimens each of *L. setiferus* and *F. aztecus*, collected from the coastal waters, were examined on a monthly basis for microsporidian infection. For several years infections have not exceeded 0.5%.

Tuzetia weidneri sp. n. in *L. setiferus*

Fresh spores (Figs 1, 2) were pyriform, measuring 2.8-4.7 μm (m = 3.31 ± 0.10 μm) x 0.9-3.7 (m = 2.27 ± 0.11 μm). On release from skeletal muscle the spores remained in loose clumps, reminiscent of *Pleistophora* spp. Stained spores (Fig. 3) often showed a dark circle at the broader end. In paraffin sections spores measured 2.2-3.2 μm (m = 2.69 ± 0.05 μm) x 1.4-1.9 μm (m = 1.67 ± 0.05 μm).

Lesions seen in histological sections (Fig. 6) were elongate in the direction of the myofibrils, tapering at the ends. Electron microscopy showed a sharp demarkation between intact muscle fibres (Fig. 8) and the lesions,

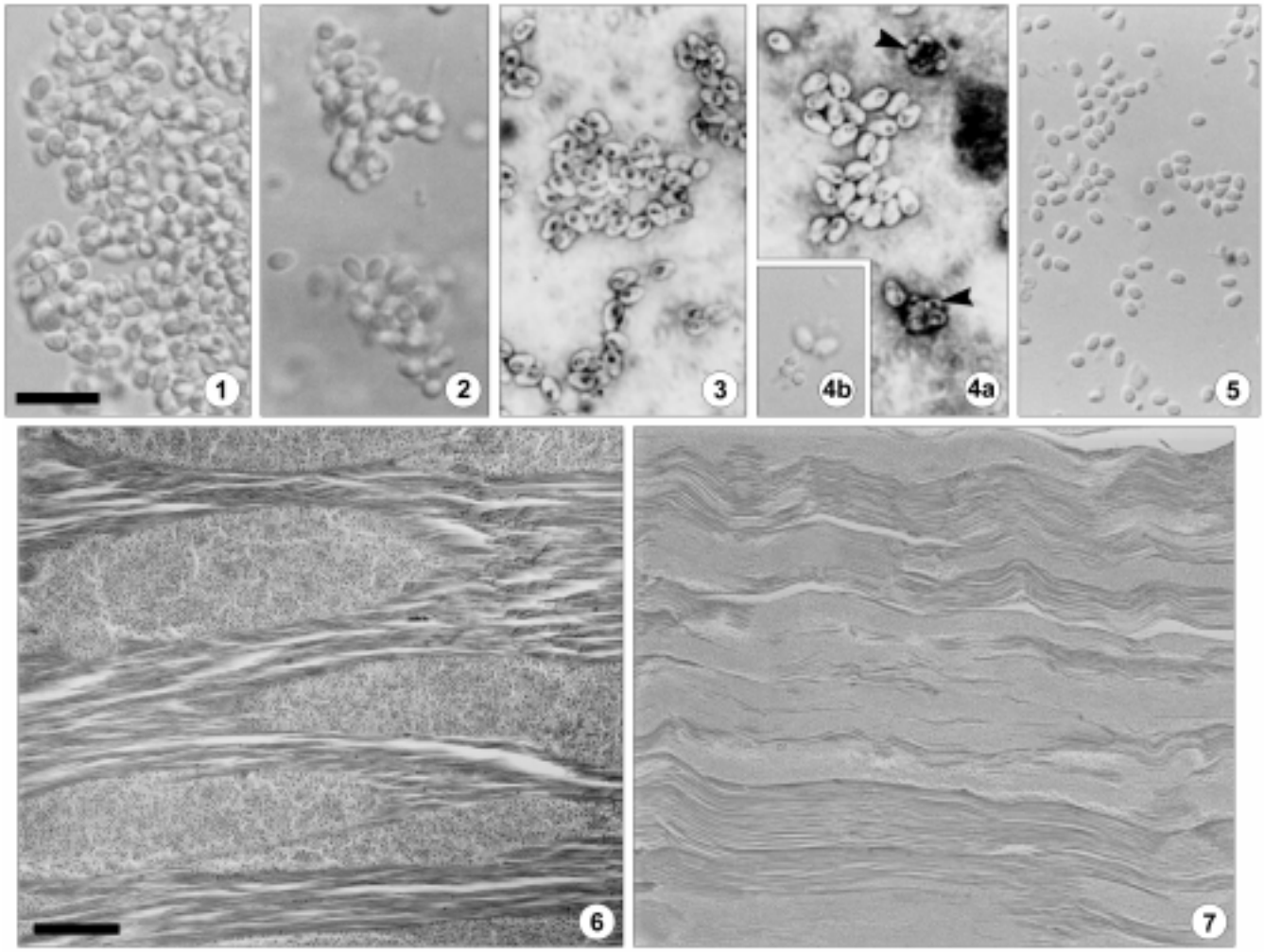

Figs 1, 2. Fresh, pyriform spores of *Tuzetia weidneri* sp. n., released from myocytes in loose clumps. Scale bar on Fig. 1 applies to Figs 2-5. **Fig. 3.** Stained spores of *T. weidneri*, showing darkly stained circle towards the posterior end. **Fig. 4. (a)** Stained spores of *T. weidneri* together with two sporophorous vesicles (arrowheads), each containing eight small spores of a presumed new species. **(b)** Fresh spores of *T. weidneri* adjacent to small spores of a presumed new species. **Fig. 5.** Fresh, ovoid spores of *Perezia nelsoni*, dispersed after release from myocytes. Scale bar - 10 μm (Figs 1-5). **Fig. 6.** Histological section of skeletal muscle of *Litopenaeus setiferus*, stained with H. & E. showing spore-packed lesions with tapering ends, due to *Tuzetia weidneri*. Scale bar on Fig. 6 applies to Fig. 7. **Fig. 7.** Heavily - infected muscle of *L. setiferus* stained with H. & E. showing extensive replacement of muscle fibres by *Perezia nelsoni*. Note more uniform appearance of the lesions than those caused by *T. weidneri*. Scale bar - 100 μm (Figs 6, 7)

which were packed with spores and stages of merogony and sporogony. Within the spore masses, there were a few bundles of frayed myofibrils in otherwise disorganised host cell cytoplasm, with abundant vesicles and occasional myocyte nuclei and cristate mitochondria. Chromatophores of the host produce a gross bluish-black colouration in response to infection.

Membrane systems were not well preserved within parasites apart from the nuclear envelope in some individuals. Meronts were multinucleate plasmodia bounded by a simple plasma membrane (Fig. 9). These became lobed, then elongate and divided by cytoplasmic contriction into groups or chains of multinucleate, binucleate, and ultimately, uninucleate products (Fig. 10). Nuclei contained dense mats of chromatin. Occasionally cytoplasmic preservation was good enough to reveal some cisternae of endoplasmic reticulum (Fig. 12). The surface of all merogonic stages was beset with a multitude of tiny blisters, some in contact with the plasma membrane (Fig. 9, insert), others detached and extended into the surrounding disorganised host tissue (Fig. 11). Division was effected by invagination between segments of cytoplasm containing nuclei. In the planes of division typical blisters were interspersed with larger,

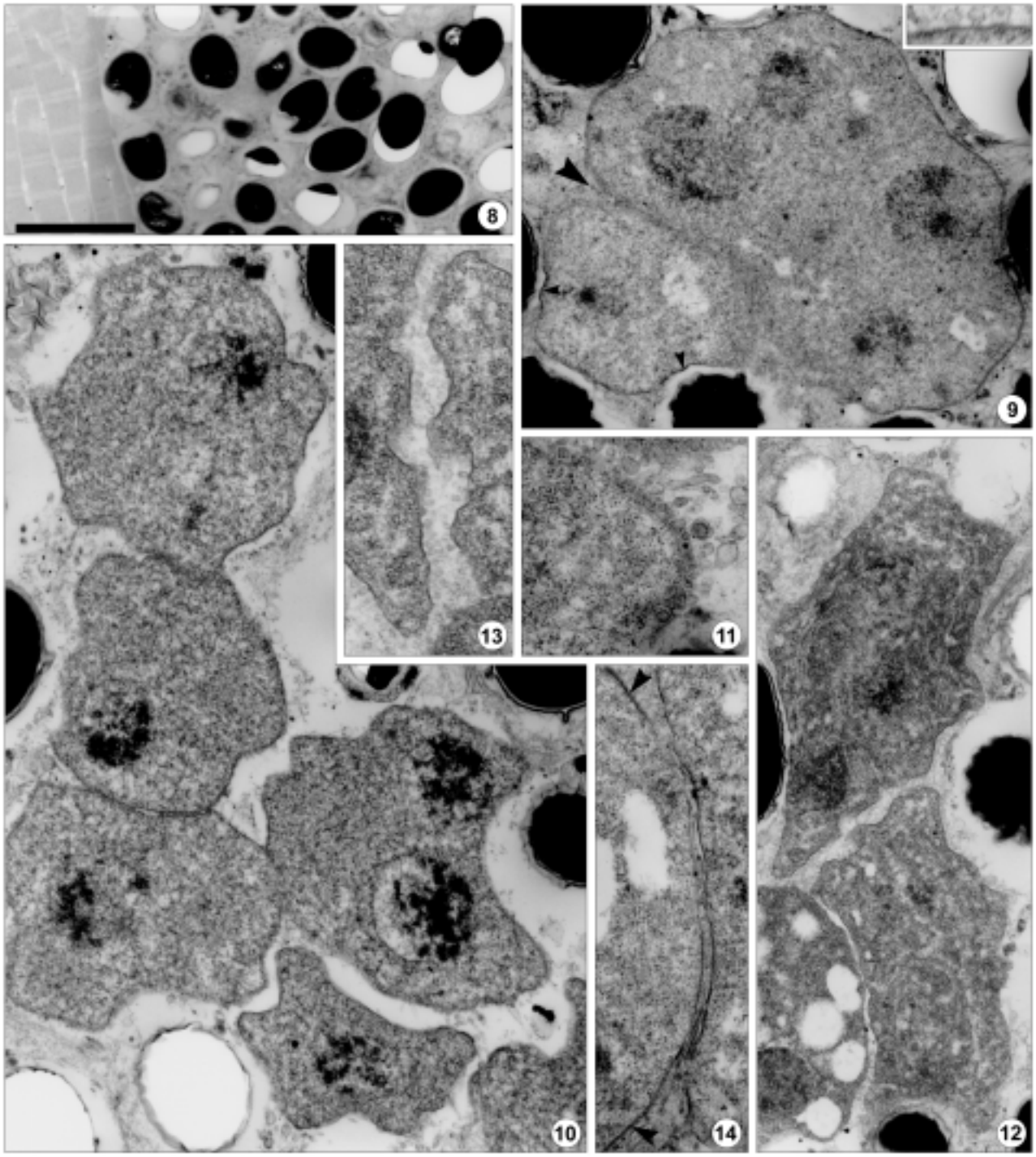

Figs 8-14. Electron micrographs of *Tuzetia weidneri* in skeletal muscle of *Litopenaeus setiferus*. Scale bar on Fig. 8 applies to all figures. **8.** Section at edge of lesion, showing intact muscle bordering spores in individual SVs, isolated in degraded host cell cytoplasm. **9.** Multinucleate meront at the onset of division: surface blisters are abundant in the division plane (arrowhead). Some areas show the first signs of deposition of surface coat (small arrowheads). The insert shows blister formation from the plasma membrane of a meront. **10.** Merogony in progress, giving rise to a chain of uninucleate products. **11.** Part of the surface of a multinucleate meront showing abundant attached and separate surface blisters. **12.** Newly separated products of merogony with restoration of surface blisters between the pair. **13.** Enlargement of part of Fig. 12 showing surface blisters. **14.** Division plane in merogony showing fusion of surface blisters and newly secreted tiny blisters (arrowheads). Scale bar: Fig. 8 - 4.0 μm; Fig. 9 - 0.2 μm and 0.06 μm (insert); Fig. 10 - 1.2 μm; Fig. 11 - 0.6 μm; Fig. 12 - 1.4 μm; Figs 13, 14 - 0.8 μm

elongate vesicles, and minute, apparently newly-formed blisters were present on the plasma membranes (Fig. 14). When daughter meronts were more widely separated, abundant new blisters were present between

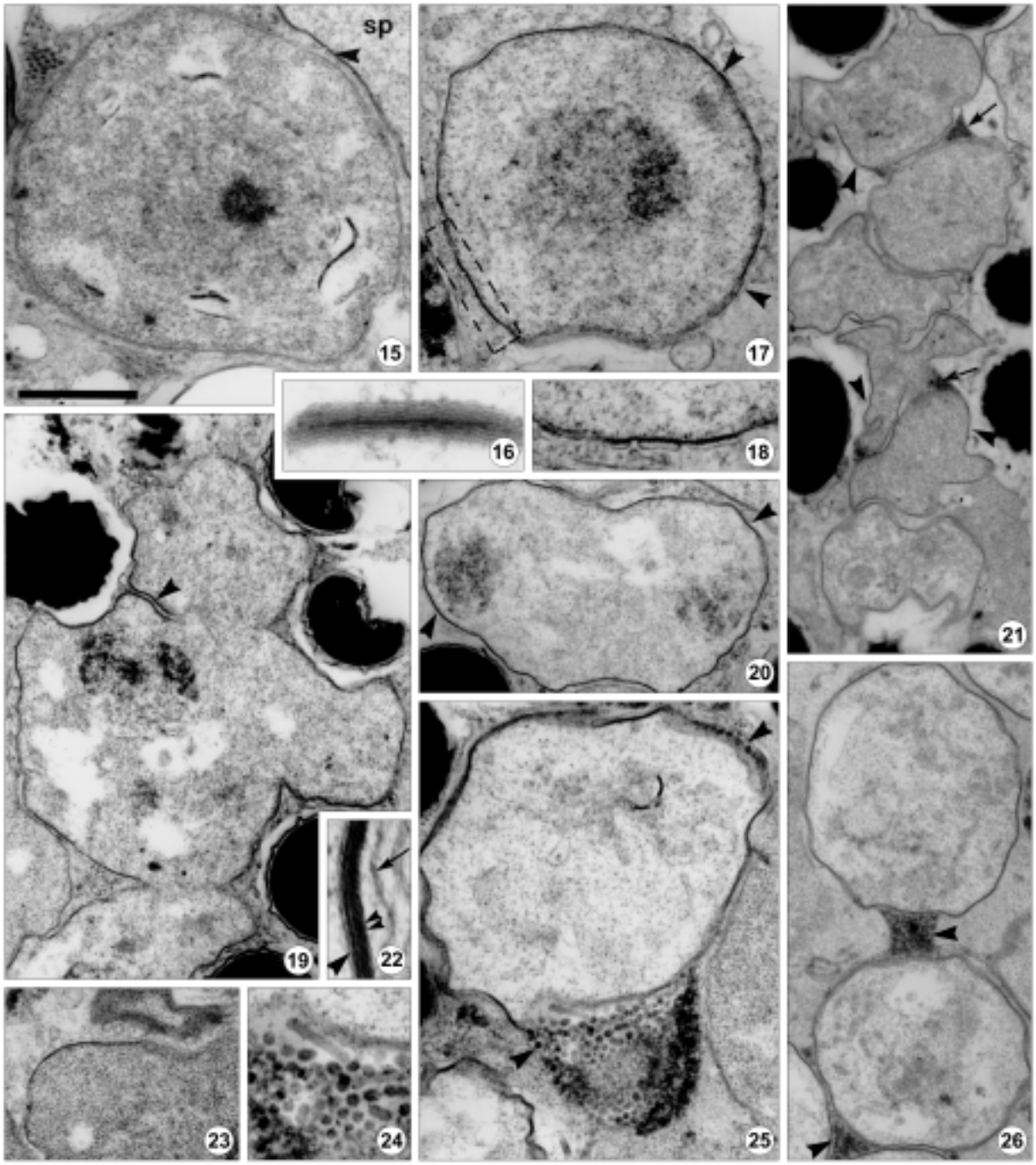

Figs 15-26. Electron micrographs of sporogony of *Tuzetia weidneri* in *Litopenaeus setiferus*. Scale bar on Fig. 15 applies to all figures. **15.** Incipient sporont, product of merogony, with several dense stacks of membrane in the cytoplasm. An adjacent sporont (sp) shows surface coat deposition and partial SV formation (arrowhead). **16.** Detail of membrane stack in sporont cytoplasm. **17.** Uninucleate sporont showing fusion of surface blisters during formation of SV (arrowheads). The boxed area is enlarged in fig. 18. **18.** Enlargement of boxed area of fig. 17 showing surface coat and fusion of blisters to form the SV. **19.** Division of sporont with moderately thick surface coat, while SV is incomplete: surface blisters are fusing in the division plane (arrowhead). **20.** Within a chain, a binucleate product of sporogony with well developed surface coat and complete SV (arrowheads). **21.** Chain of sporoblasts derived from sporogony. Individual SVs (not always clear) are indicated at arrowheads. Episporontal secretions lie in the division planes (arrows). **22.** Surface characteristics of mature sporont: the SV envelope (arrow) overlies the thick surface coat (small double arrowheads) on plasma membrane (arrowhead). The second SV belongs to an adjacent sporont. **23.** Part of the surface of an early multinucleate sporont showing deposition of surface coat prior to complete fusion of surface blisters. **24.** Enlargement of episporontal secretions from fig. 25. **25.** Sporont with complete SV and with episporontal tubules and globules accumulated in two patches (arrowheads). **26.** Formation of sporoblasts: accumulation of episporontal secretions (arrowheads) between sporoblasts during constriction of the SV envelope around individuals. Scale bar: Fig. 15 - 0.6 μm, Figs 16, 19, 20, 22, 26 - 1.2 μm; Figs 17, 23, 25 - 0.8 μm; Figs 18, 24 - 0.4 μm; Fig. 21 - 1.6 μm

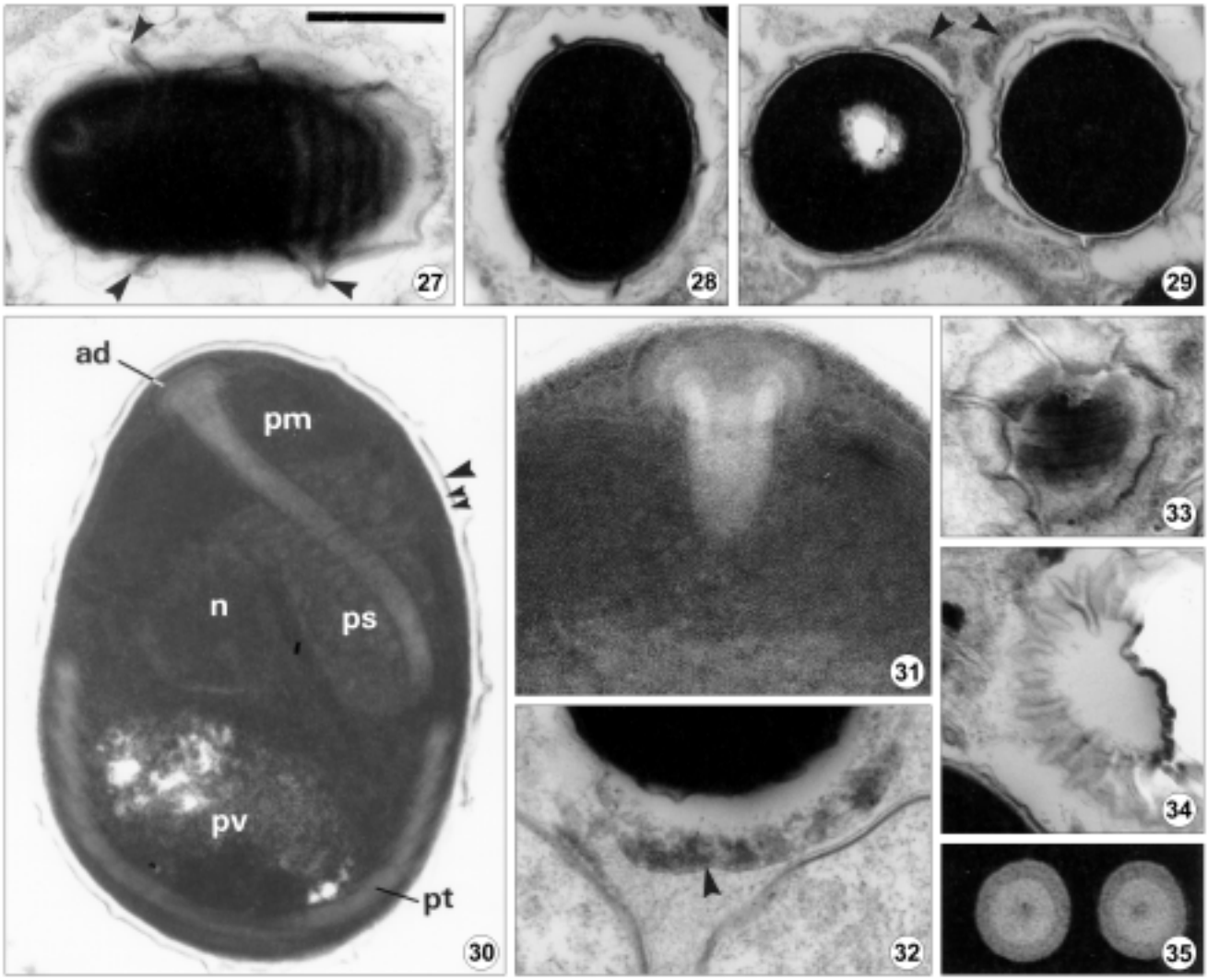

Figs 27-35. Electron micrographs of spores of *Tuzetia weidneri* in *Litopenaeus setiferus*. Scale bar on Fig. 27 applies to all figures. **27.** Longitudinal section of mature spore showing ridges of the spore wall (arrowheads) in contact with SV envelope. SV lacks episporontal secretions. **28.** Oblique section of mature spore, with ridged wall, in SV devoid of episporontal secretions. **29.** A pair of spores, possibly within a single SV containing degraded episporontal secretions (arrowheads). **30.** Mature spore showing exospore (arrowhead) with ridges, endospore (small double arrowheads), anchoring disc (ad), membranous polaroplast (pm), spongiform polaroplast (ps), polar tube (pt), nucleus (n) and posterior vacuole (pv). **31.** Detail of anchoring disc with several layers of differing density, into which the central tube of the polar tube spreads like a funnel. **32.** Part of SV containing a mature spore: the episporontal tubules and globules have been degraded (arrowhead) but not yet eliminated. **33, 34.** Sections of spores tangential to parts of the spore wall showing surface ridges, some of which are branched. Part of the polar tube is visible in Fig. 33. **35.** Transverse sections of polar tube coils showing concentric rings around a central core. Scale bar: Figs 27, 32-34 - 0.6 µm; Figs 28, 29, 35 - 1.0 µm; Fig. 30 - 0.4 µm; Fig. 31 - 1.8 µm

them (Fig. 13), possibly expanded from the tiny blisters seen in Fig. 14.

Uninucleate products of merogony, were incipient sporonts, and many showed stacks of membranes in the cytoplasm (Figs 15, 16) which persisted in some specimens during conversion to sporonts (Fig. 25)

Sporonts were recognised by the presence of an electron dense surface coat on the plasma membrane and a sporophorous vesicle (SV), which appeared to be formed by progressive coalescence of the blisters at the meront surface (Figs 17, 18). The initiation of sporogony was observed in both uninucleate (Fig. 17) and multinucleate (Fig. 19) products of merogony. These showed varied surface characters, parts of the surface being typical of meronts with a simple plasma membrane and abundant blisters and other parts covered with a thin surface coat and discontinuous SV envelope formed by coalescence of blisters (Fig. 23). When mature, the sporont surface coat was a 20 nm layer directly overlying the plasma membrane, outside of which was the

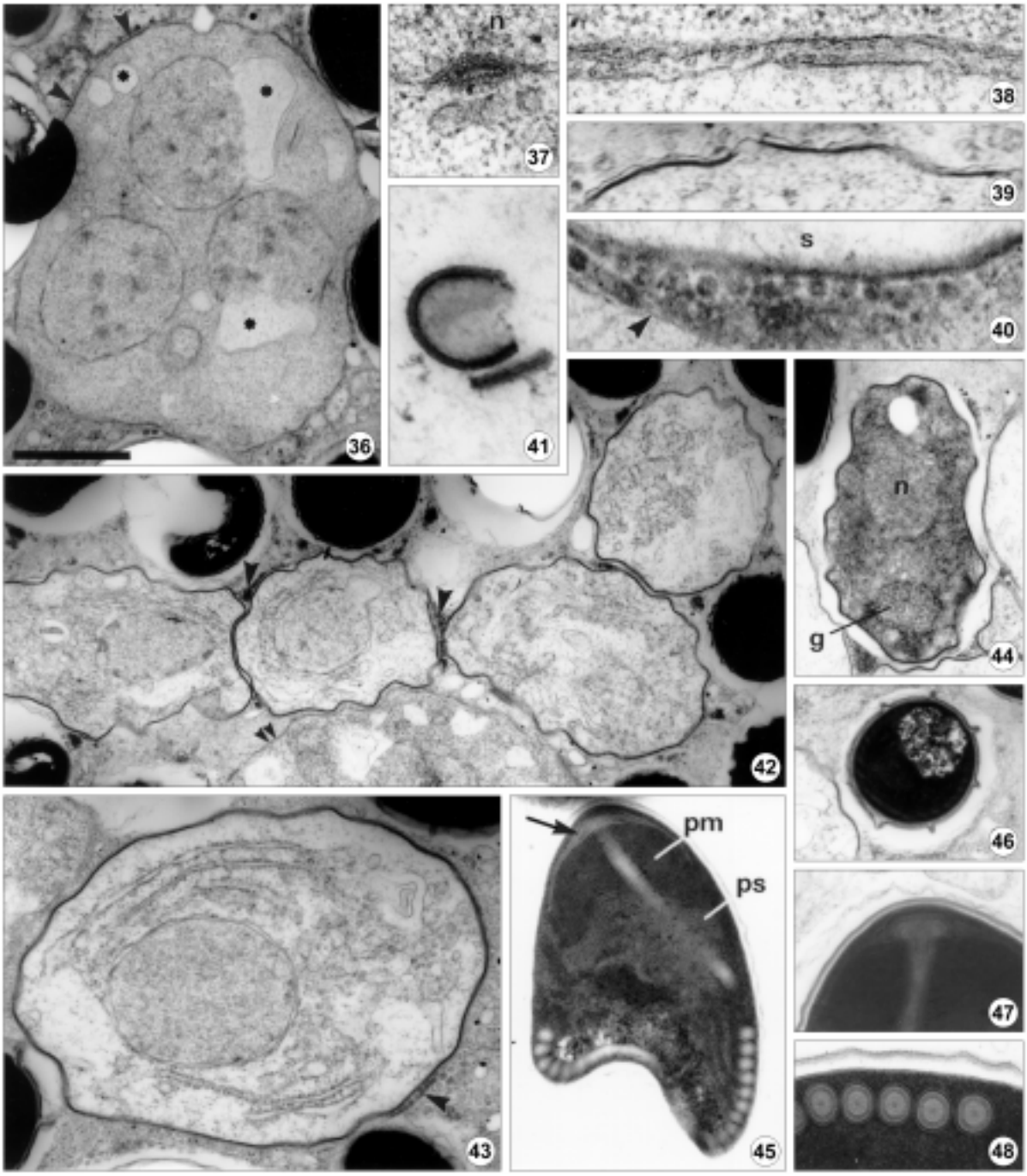

Figs 36-48. Electron micrographs of *Tuzetia weidneri* from skeletal muscle of *Farfantepenaeus aztecus*. Scale bar on Fig. 36 applies to all figures. **36.** Incipient sporont. Cytoplasmic vacuoles and expansions within the nuclear envelope*, containing a network of fine granules appear abnormal. The plasma membrane bears minute blisters (arrowheads). **37.** Spindle pole within the nucleus (n) of a multinucleate meront, showing electron dense discs and vesicles external to the spindle terminus. **38.** Division plane between products of merogony showing small blisters. **39.** Surface of developing sporont showing areas of unthickened plasma membrane and areas where the surface coat has been deposited and surface blisters have fused during formation of the SV. **40.** Surface of an early sporont (s) with episporontal secretions within the SV envelope (arrowhead). **41.** Stacks of membranes in the cytoplasm of an early sporont. **42.** Chain of uninculeate sporoblasts formed by constriction of a sporont. Episporontal secretions accumulate within the SV at the points of constriction (arrowheads). An adjacent meront has minute surface blisters (small arrowheads). **43.** Newly isolated sporoblast, with thick surface coat, enveloped in its own SV. Some episporontal secretions persist (arrowhead). **44.** Crenated sporoblast in SV. The nucleus (n) and Golgi vesicles (g) are visible. **45.** Mature spore showing exospore and endospore, polar sac (arrow) extending over membranous polaroplast (pm), polar tube running through spongiform polaroplast (ps) and coiling around the posterior vacuole. **46.** Section of a mature spore, passing through the posterior vacuole, showing ridged spore wall and SV devoid of secretions. **47.** Anterior end of mature spore showing anchoring disc with layers of differing density, through which the central tube of the polar tube opens like a funnel. **48.** Transverse sections of polar tube showing lucent and grey rings and double sleeve around a central core. Scale bar: Figs 36, 44 - 1.2 µm; Figs 37-41, 48 - 0.2 µm; Figs 42, 46 - 1.4 µm; Figs 43, 45, 47 - 0.8 µm

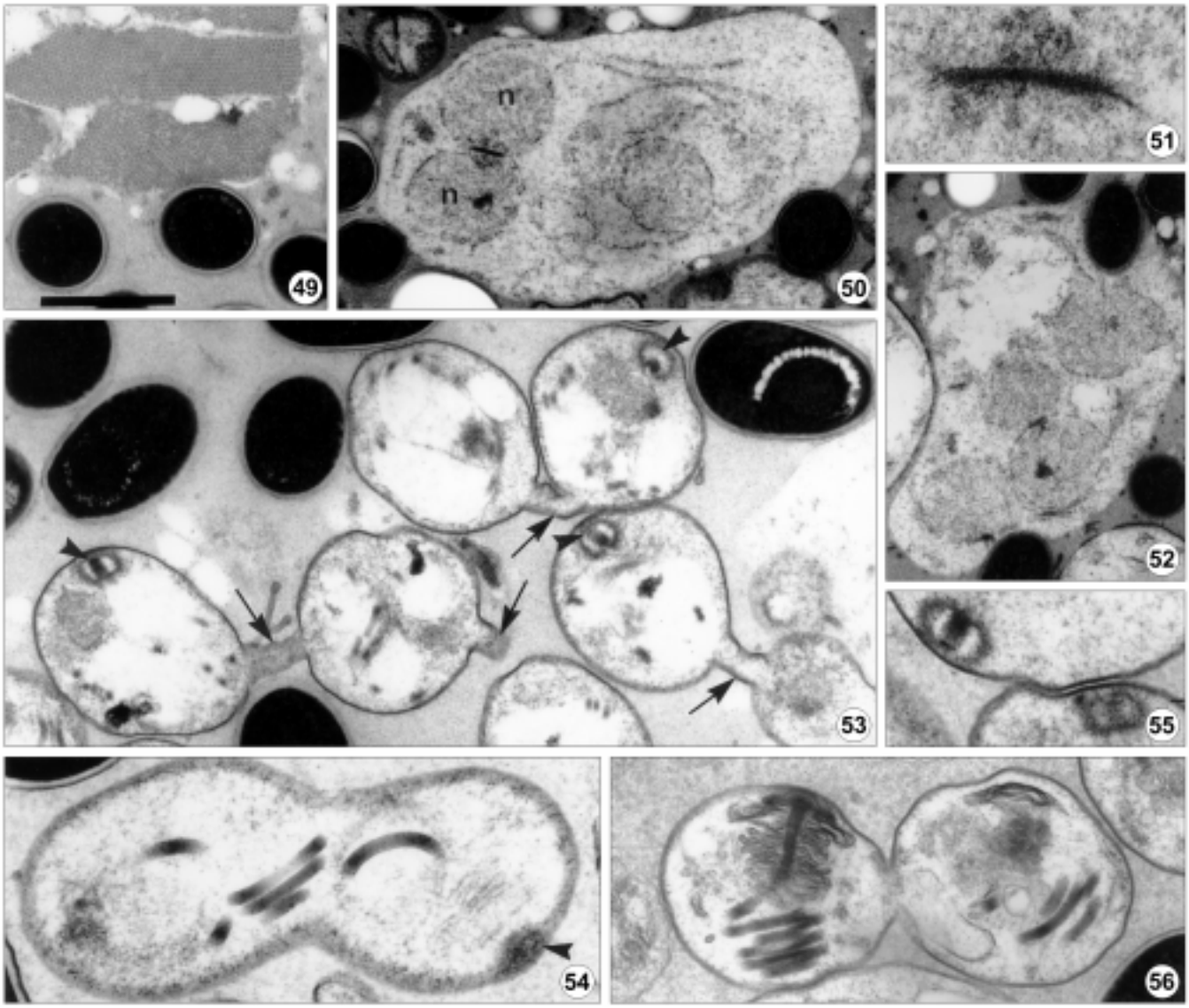

Figs 49-56. Merogony and sporogony of *Perezia nelsoni* in skeletal muscle of *Litopenaeus setiferus*. Scale bar on Fig. 49 applies to all figures. **49.** Intact muscle bundles, at the edge of skeletal muscle lesion and spores in an amorphous matrix of totally degraded muscle. **50.** Meront showing two nuclei (n) in diplokaryotic arrangement with very dense apposition of the four membranes of the nuclear envelopes. One nucleus of another pair is also visible. **51.** The very dense apposition of diplokaryotic nuclei in a meront. **52.** Separation of diplokaryotic nuclei in a meront in preparation for sporogony. **53.** Sporogonic division by binary or multiple fission. The sporoblasts are connected by narrow bridges (arrows). The developing anchoring discs are seen in three of the sporoblasts (arrowheads), in these cases directed away from the region of fission. **54.** Binary fission of a sporont showing coils of the polar tube near the constriction of the body and an anchoring disc at one pole (arrowhead). **55.** The point of separation of two sporoblasts showing the anchoring discs directed towards the plane of fission. **56.** Separation of two sporoblasts showing the long axis, indicated by the anchoring disc, polaroplast and polar tube, parallel to the plane of fission. Scale bar: Fig. 49 - 1.2 μm; Figs 50, 52 - 1.6 μm; Fig. 51 - 0.4 μm; Fig. 53 - 1.0 μm; Fig. 54 - 0.6 μm; Fig. 55 - 0.56 μm; Fig. 56 - 0.9 μm

SV envelope which measured 4.0 nm (Fig. 22). The SV envelope was separated from the surface coat by an irregular episporontal space (Fig. 22).

Once surface coat and SV formation had been completed, sporonts appeared less dense than meronts, with fewer ribosomes, and secretions were observed in the SV cavity (episporontal space). These took the form of 45-50 nm globules or short tubules with a slightly less dense centre (Figs 24, 25). Sporogonic divisions were by binary or multiple fission (Figs 19, 21), giving rise to groups or chains of uninucleate products, sometimes via binary fission of binucleate products within the chain (Fig. 20). The secretions in the episporontal space clearly had a role in the division process, as they were

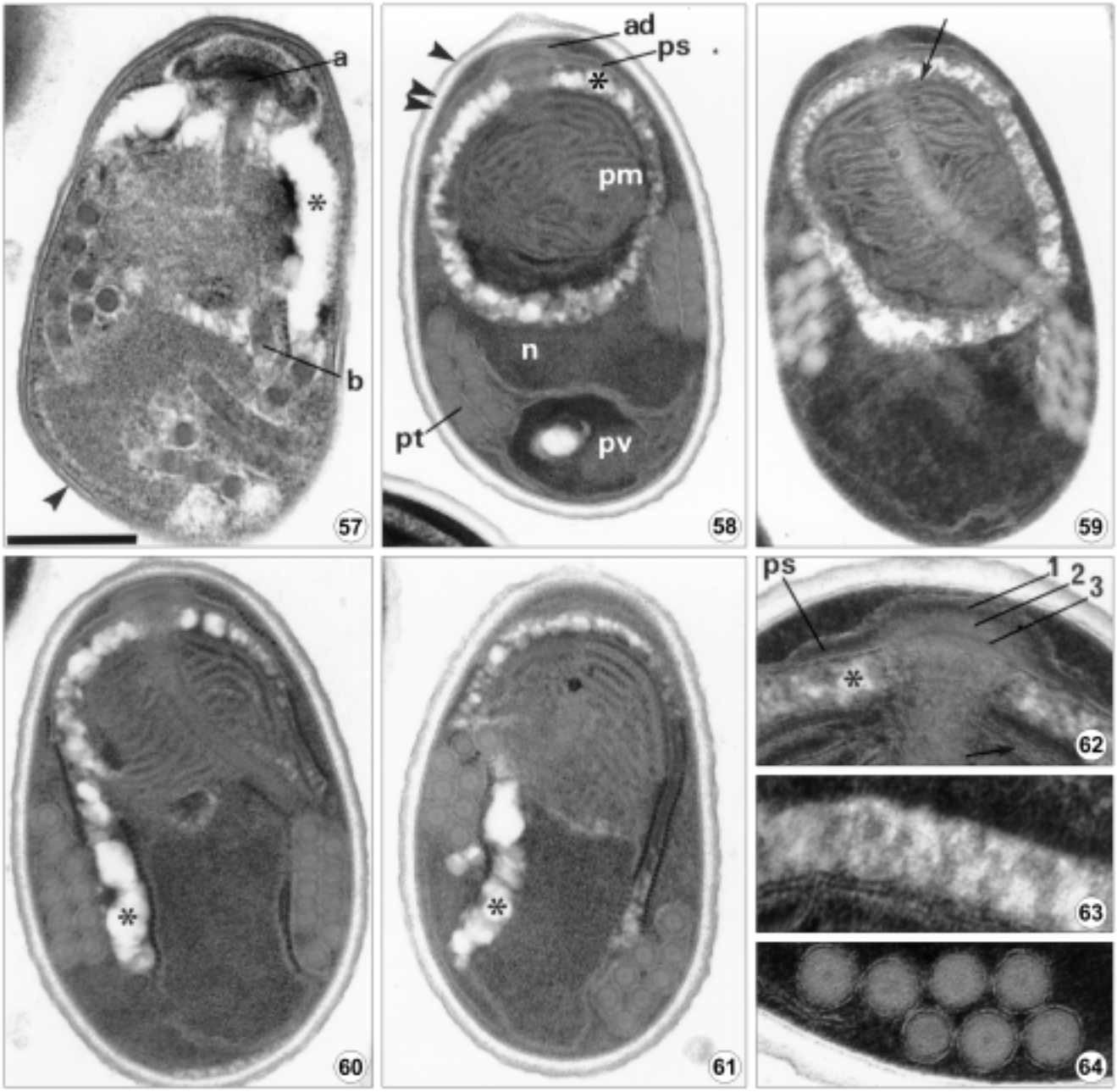

Figs 57-64. Spores of *Perezia nelsoni* in skeletal muscle of *Litopenaeus setiferus*. Scale bar on Fig. 57 applies to all figures. **57.** Immature spore with thick exospore (arrowhead) and minimal endospore layers of the wall. The outer polaroplast region* (appearing empty) forms a globular sac penetrated anteriorly by the polar tube for its attachment (a) to the anchoring disc and posteriorly at the point where the curved part of the tube joins the coil (b). **58.** Mature spore showing thick exospore (arrowhead), endospore (double arrowhead), anchoring disc (ad) within the polar sac (ps), outer region of the polaroplast in the form of a globule (*), inner polaroplast region of widely spaced membranes (pm), nucleus (n), polar tube coils (pt) and posterior vacuole (pv). **59.** Mature spore: section cut laterally to the median sagittal plane, showing the anterior part of the polar tube passing through the inner and outer polaroplast regions to unite with its coil. A few closely packed membranes lie at the anterior border of the inner polaroplast (arrow). **60.** Slightly oblique section of mature spore showing the anchoring disc, straight and coiled regions of the polar tube. The outer, lucent, component of the polaroplast (*) appears as an open structure surrounded by prominent polyribosomes. Compare with fig. 59. **61.** Mature spore: section cut laterally to the median sagittal plane so that the anchoring disc and straight part of the polar tube are not visible. The outer, lucent, component of the polaroplast (*) appears as an open structure surrounded by polyribosomes. **62.** Anterior end of mature spore: the endospore is not thinned over the anchoring disc, which has a dense anterior border (1) continuous with the polar sac (ps), a middle less dense region (2) and a fine inner layer (3) over the insertion of the polar tube. The polar tube passes through a narrow opening in the outer polaroplast region (*) in which traces of parallel membranes can be seen. A few membranes of the inner polaroplast (arrow) are tightly packed. **63.** Section through the outer region of a mature spore showing parallel membranes in the outer polaroplast region. **64.** Transverse sections through coils of the polar tube showing outer sleeve of two membranes and inner rings round a central core. Scale bar: Figs 57-61 - 0.4 μm; Figs 62, 64 - 0. 2 μm; Fig. 63 - 0.1 μm

present only in the narrow channels formed by constriction of the SV envelope between division products, before the final isolation of each sporoblast in its own SV (Figs 21, 26).

Sporoblasts matured into spores but the full sequence of events was not tracked. The episporontal secretions were broken down during spore maturation (Figs 29, 32) and were absent from most SVs containing mature spores. After maturation, each spore lay in its individual SV (Figs 27, 28). Occasionally a pair of spores appeared to be in the same SV (Fig. 29) but this may have resulted from breakdown of the SV in the heavy infection. The spores were pyriform (Fig. 30) although the posterior end had often collapsed during EM fixation (Fig. 8). The anchoring disc within the polar sac was slightly offset from the longitudinal axis and was separated from the spore wall by a 20 nm band of cytoplasm. The anchoring disc was composed of several layers decreasing in density in a posterior direction (Fig. 31). The polar tube abutted on to the last layer, while an inner component of the tube appeared to expand like a funnel through the layers (Fig. 31). The polar sac spread umbrella-wise over about half of the membranous region of the polaroplast. The polaroplast consisted of an anterior region of very tightly packed membranes occupying almost the width of the spore and about a fifth of its length, followed by a spongiform region which surrounded the polar tube during its course from a central to a peripheral position, and was thereby displaced laterally when viewed with the curve of the tube (Fig. 30). The nucleus lay alongside the spongiform polaroplast. The polar tube ran an oblique course through the two regions of polaroplast and formed 9-10.5 isofilar coils in a single layer in the posterior half of the spore, around a voluminous posterior vacuole containing flocculent material. In transverse section the coils of the polar tube showed a central dot surrounded successively by a lucent ring, a grey ring containing longitudinally running fibrils and two membranes (Fig. 35). The endospore measured 20-30 nm and was hardly thinned over the anchoring disc. The exospore was a 20 nm finely granular layer. The two layers were raised as complex branching and anastomosing system of ridges which appeared as protrusions in both longitudinal (Fig. 27), oblique (Fig. 28) or transverse sections (Fig. 29). Tangential sections across the spore surface revealed the complexities of the ridges (Figs 33, 34). At maturity spores usually lay free in the SV but in some cases the SV envelope made contact with the ridges on the spore wall (Fig. 27) and the episporontal space was usually devoid of secretions (Figs 27, 28). In heavily infected tissues many of the SV envelopes had broken down leaving spores dispersed in degraded host cell cytoplasm.

Tuzetia weidneri* sp. n. in *F. aztecus

Lesions in skeletal muscle were similar to those in *L. setiferus*, with total destruction of muscle fibres, leaving only remnants of cytoplasmic organelles. The bluish-black colouration of infected shrimps was observed as in *L. setiferus*. Preservation of parasite membrane systems was better than in *L. setiferus*, although large vacuoles containing an apparently abnormal network of fine granules were common in all stages. Some of these vacuoles were in the cytoplasm and others were clearly in part of the nucleus, lying internal to the nuclear envelope (Fig. 36). Centriolar plaques at spindle poles showed 2 or 3 associated external vesicles (Fig. 37). Surface blisters were less abundant but were present on meronts as a single layer and were involved in meront division (Fig. 38). Transition to sporogony involved secretion of the surface coat and progressive fusion of blisters to form the SV envelope (Fig. 39). Sporonts also exhibited the characteristic features of decreased electron density, aggregates of episporontal secretions in the SV (Fig. 40) and presence of multilamellar bodies in the cytoplasm (Fig. 41). Sporogonic divisions involved a series of fissions with the episporontal secretions positioned in the cytoplasmic fission planes (Fig. 42). Each sporoblast was finally enveloped in its own SV (Fig. 43). During maturation, sporoblasts showed a wavy or crenated outline, a single nucleus and a prominent Golgi apparatus of convoluted tubules in a posterior position (Fig. 44).

Spores, each lying in a persistent SV, were pyriform, often with the posterior end collapsed inwards (Fig. 45), and showed an anchoring disc with the same arrangement of layers (Fig. 47) as the species in *L. setiferus*, membranous and spongiform vesicular regions of polaroplast, the latter being laterally displaced (Fig. 45), around the polar tube along its curve toward the spore periphery. There was a single nucleus, 9 to 10.5 isofilar coils of the polar tube and a posterior vacuole with flocculent contents. Sections of the polar tube showed the same layers as in the parasites in *L. setiferus* (Fig. 48). The endospore measured 20 nm, with only slight thinning over the anchoring disc and the exospore

was a finely granular layer. The wall was raised into prominent ridges visible in all planes of section (Fig. 46).

Octosporous species

Among the masses of large spores of *T. weidneri*, much smaller spores measuring less than 2.0 x 1.0 µm were occasionally encountered (Fig. 4b). These had been released from groups of 8 in SVs (Fig. 4a). It is likely that these represent yet another microsporidian species infecting penaeid shrimps, rather than a stage of the *T. weidneri*, but their very rare occurrence prevented us from obtaining ultrastructural data.

Perezia nelsoni* from *L. setiferus

Fresh spores released from muscle were almost perfectly ellipsoid, measured 1.4-2.8 µm (m = 2.1 ± 0.07) x 0.9-1.9 µm (m = 1.22 ± 0.06) (N = 30) and were dispersed on release from muscle with no evidence of clumping (Fig. 5). Histological sections of skeletal muscle (Fig. 7) showed extensive lesions which appeared more homogeneous than those caused by *T. weidneri* (Fig. 6), probably because of the small spore size. Spores in sections measured 1.4-2.3 µm (m = 1.9 ± 0.4 µm) x 0.9-1.6 µm (m = 1.37 ± 0.04 µm). Data from light microscopy of this species in *F. aztecus* are similar. Electron microscopy showed that the lesions in skeletal muscle were packed with spores interspersed with developmental stages in an amorphous, homogeneous, finely granular background that formed a matrix virtually devoid of host cell organelles, indicating that the degradation of host cell cytoplasm was more complete than in lesions caused by *T. weidneri*. At the edges, the myofibrils were intact (Fig. 49) or only partially degraded. Infected hosts turned bluish-black.

Fixation of meronts and sporonts was poor, with clear spaces in the cytoplasm and minimal preservation of nuclear and cytoplasmic membranes. Meronts, in direct contact with the amorphous host cell matrix, were multinucleate, with simple plasma membrane and diplokaryotic nuclei (Fig. 50). In the plane of apposition of the diplokarya, the nuclear envelopes were exceptionally dense (Fig. 51). The nuclei separated from one another in preparation for sporogony (Fig. 52). After secretion of the electron dense surface coat on the plasma membrane sporonts underwent a series of divisions by binary or multiple fission (Fig. 53) to produce uninucleate sporoblasts. A number of these were connected by cytoplasmic bridges which were presumed to be temporary. Most micrographs suggested that pairs of sporoblasts were separated as mirror images with the anchoring discs directed away from the constricting cytoplasm and the coils of the polar tube close to the constriction (Figs 53, 54) but this arrangement could be reversed with anchoring discs near the division plane (Fig. 55). Arrangement of the anchoring discs, polaroplast membranes and polar tubes in some dividing stages indicated that the longitudinal axis could also be at right angles to the constriction (Fig. 56).

Preservation of immature (Fig. 57) and mature spores (Figs 58-61) was good except for the outer polaroplast membranes. The exospore was finely granular usually about 20 nm thick (Figs 58, 60) but sometimes only 10 nm (Fig. 62). The lucent endospore, about 25-35 nm thick, was only slightly thinned at the anterior end (Fig. 60). The anchoring disc was a flattened structure with its unit membrane separated by a 10 nm layer of cytoplasm from the plasma membrane (Figs 58, 62). The disc, made up of dense anterior and posterior layers with a middle, less dense layer, was continuous with the polar sac which extended over one third to one half of the polaroplast. The polar tube was inserted into the base of the anchoring disc. It then traversed the polaroplast obliquely towards the periphery. In the vast majority of spores, the outer part of the polaroplast in median sagittal sections appeared as a bright ring composed of granular material in a lucent background (Fig. 58). However, parts of the organelle showed traces of parallel membranes (Fig. 63). The ring structure appeared complete whether viewed in transverse or longitudinal section, even in sagittal sections lateral to the median, which showed the connection between the anterior part of the polar tube and the coils (Fig. 59). This outer part of the polaroplast was interpreted as a globular structure with a narrow anterior opening through which the polar tube passed to join the anchoring disc (Fig. 58). At the posterior end the membranes forming the globular polaroplast, were breached again by the polar tube where it passed between its curved section inside, and the coiled section in the posterior half of the spore (Fig. 59). Very occasionally the outer polaroplast was open to the rest of the spore (Figs 60, 61). Within the globular structure were typical polaroplast membranes, of which the 4-8 most anterior membranes, often visible on one side only (Figs 59, 62), were very closely packed and the remainder, almost filling the globule, were separated by a 25 nm dense matrix (Figs 58, 59).

The single large nucleus (Figs 58, 60, 61) lay immediately posteriad of the globular polaroplast and behind this was a posterior vacuole (Fig. 58), which was membrane-bound, with granular contents. The isofilar polar tube was arranged in a tight cluster of two layers of coils. Each showed a dense core and several layers

within a double membrane sleeve (Fig. 64). The number of coils ranged from 8 to 10. Prominent rows of ribosomes were sometimes seen along the borders of the "globular" polaroplast when present as an open structure and between the polar tube coils and the nucleus (Figs 60, 61).

DISCUSSION

Taxonomic considerations

***Tuzetia weidneri* sp. n.**

Baxter *et al.* (1970) briefly described a microsporidium which they named *Pleistophora* sp. in *L. setiferus* and *F. aztecus* and illustrated large "cysts" packed with spores, which were clear and persistent both in the dab smears and striated muscle sections. No measurements were given. Although there have been subsequent findings of *Pleistophora* in the same hosts (Constransitch 1970, Overstreet 1973), the species has not been named and there has been no formal description at light- or electron-microscopic levels. In the present ultrastructural study, it was clear that the microsporidia which developed in SVs did not belong to *Pleistophora*. Although the sporonts were multinucleate within SVs, the vesicles divided together with the sporont, so that each sporoblast lay in its own SV. Spores were thus loosely adherent in degraded host tissue, not aggregated in defined packets. Also, there was a tendency for the sporoblasts to be produced linearly, rather than in spherical groups. It is, thus, highly unlikely that the species we have described is the same as the *Pleistophora* sp. of Baxter *et al.* (1970) and we consider that it has not been described previously. Notable features of the mature SVs of *T. weidneri* were the absence of metabolic products (granules and tubules) and a complex pattern of ridges on the spore wall. Although *Pleistophora* sp. with persistent SVs as described by Baxter *et al.* (1970) has been found periodically in shrimp throughout the northern Gulf of Mexico (e.g. Overstreet 1973), it has not been collected by the authors off Mississippi for over 7 years.

Four genera, *Tuzetia*, *Janacekia*, *Alfvenia* and *Nelliemelba*, have been established for microsporidian species in which spores lie individually in SVs (Larsson 1983). The morphology of the microsporidia in *L. setiferus* and *F. aztecus* most closely fits the characters of *Tuzetia*, namely nuclei unpaired in all stages of development, meronts and sporonts dividing into a small number (2-8) of products, spores oval or pyriform, polar tube isofilar and exospore thin and without stratification. Most species of *Tuzetia* have evenly distributed, persistent narrow tubules, of unknown function, traversing the SV connecting the spore wall with the SV envelope. The tubular/spherical secretions in the *Tuzetia*-like microsporidia in *L. setiferus* and *F. aztecus* are not evenly distributed and their role appears to be linked with division of the sporont and disappear during spore maturation. We have tentatively assigned the species to the genus *Tuzetia* in spite of the difference which exists between the episporontal secretions and although the prominent system of ridges on the spore wall is a new feature for the genus. The only named species of *Tuzetia* that lacks episporontal tubules in mature SVs is *Tuzetia cyclopis* (Kudo 1921), named from the copepods *Cyclops fuscus* by Kudo (1921) and *Megacyclops viridis* by Loubès (1979). Spores of *T. cyclopis* are larger (4.2-4.7 x 2.7-3.0 μm) than those of *T. weidneri* and typically have 13 rather than 9-10.5 coils of the polar tube. For these reasons we have established *T. weidneri* as a new species. Also decapod crustaceans are new hosts for the taxon *Tuzetia*. As no difference was found in the *Tuzetia*-like microsporidia in their development and spore structure in *L. setiferus* and *F. aztecus*, material from both hosts is considered conspecific.

Taxonomic summary

***Tuzetia weidneri* sp. n.**

Type host: *Litopenaeus setiferus* (Linnaeus, 1767).

Other host: *Farfantepenaeus aztecus* (Ives, 1891).

Site of infection: striated muscle.

Type locality: Bayous associated with Mississippi Sound, Mississippi, U.S.A.

Diagnosis: nuclei always unpaired. Meront surface with a profusion of blisters which appear to be involved in division of the meront, usually into linear arrays of merozoites. Sporonts, which are enveloped by a fine sporophorous vesicle formed by fusion of the blisters at the surface of uninucleate or multinucleate stages, become rounded sporogonial plasmodia with a small number of nuclei. Sporonts become elongate and divide, together with the sporophorous vesicle, into linear arrays of sporoblasts each enveloped in its own sporophorous vesicle. Aggregates of globules and tubules secreted into the episporontal space are massed at the division planes

and are included in the sporophorous vesicles around sporoblasts. These secretions are degraded and disappear at spore maturity.

Spores are pyriform and measure 2.8-4.7 µm (m = 3.3 ± 0.1 µm) x 0.9-3.7 µm (m = 2.3 ± 0.1 µm) when fresh. Polaroplast has an anterior region of close-packed lamellae and a spongiform region around the posterior two thirds of the straight part of the polar tube. Polar tube is isofilar with 9-10.5 coils in a single rank close to the spore wall. Large posterior vacuole with flocculent contents. Spore wall ornamented with complex anastomosing ridges incorporating the endospore and the finely granular, non-stratified exospore.

Type material: resin blocks deposited in the University of Southern Mississipi Gulf Coast Research Laboratory Museum, Holotype - GCRL 2032 (from *L. setiferus*); paratypes GCRL 2033-2034 (from *L. setiferus*) and GCRL 2035-2037 (from *F. aztecus*)

Etymology: the specific name "*weidneri*" is proposed in honour of the contribution to microsporidiology of Professor Earl Weidner.

Perezia nelsoni

Perezia nelsoni was first described as *Nosema nelsoni* from *F. aztecus* collected from the Lousiana coast, USA (Sprague 1950). It has also been reported from *Litopenaeus setiferus* and *Farfantepenaeus duorarum* from coastal waters of the southern USA and from South Africa (summarised by Sprague and Couch 1971 and by Overstreet 1973) and later in *Parapenaeus longirostris* from the Mediterranean (Loubès *et al.* 1977), *Penaeus semisulcatus*, *Fenneropenaeus merguiensis* and *Penaeus esculentus* from Australia (Owens and Glazebrook 1988) and *Farfantepenaeus notialis* from Senegal (Clotilde-Ba and Togubaye 1995, 1996). The spore dimensions (measured fresh or fixed), provided by several authors are in accord with 2.5 x 1.5 µm given in the original description (Sprague 1950). The numbers of coils of the polar tube given by various authors are also within an acceptable range for a species i.e. 13 (Sprague 1977), 9-12 (Sprague and Vernick 1969), 8-13 (Loubès *et al.* 1977) and 10-11 (Clotilde-Ba and Togubaye 1995, 1996). In the present study the spore dimensions were 2.1 x 1.2 µm and the number of polar tube coils was 8-10. It is likely that *P. nelsoni* has a worldwide distribution, in a wide range of penaeid hosts but confirmation of this will rest with molecular studies.

Our studies of *P. nelsoni* have revealed merogonic stages with diplokarya and sporogonic stages with unpaired nuclei, in accord with the descriptions from *P. longirostris* (see Loubès *et al.* 1977) and *F. notialis* (see Clotilde-Ba and Togubaye 1996). However, we have been able to add more information on spore structure, the most interesting feature being the outer region of polaroplast, which in almost all of our specimens appeared as a globular sac composed of compact membranes enclosing the inner polaroplast, which in turn surrounded the straight part of the polar tube. In only two spores that we observed was the outer region seen to be open to the posterior part of the spore housing the nucleus and posterior vacuole. Although the outer polaroplast generally appeared mottled, with electron-dense and lucent parts, there were regions with traces of parallel membranes, and we have concluded that this part of the polaroplast had suffered fixation problems, disrupting the close-packed lamellae, thereby releasing the matrix that is normally enclosed by the membranes, and that the matrix had then become flocculent. We are fully in agreement with Clotilde-Ba and Togubaye (1996) that both polaroplast regions are composed of lamellae. These authors described the outer lamellae as being "anterior and lateral" but their illustrations clearly show the outer lamellae as encircling the inner, widely-spaced lamellae.

The closed sac appearance of the outer region is in accord with some images of *P. nelsoni* published by Sprague & Vernick (1969) i.e. Figs 4, 7, although unfortunately the enlargement (their Fig. 6), which might have shown whether the outer membranes are open or closed, does not extend to the posterior limit of the polaroplast. The organisation of the polaroplast of *P. nelsoni* is unusual but is similarly constructed in images of the closely-related species *Ameson michaelis* from crabs, *Callinectes sapidus* (see Sprague *et al.* 1968, Figs 10, 11 and Weidner 1970, Fig. 14d). Sprague *et al.* (1968) had first interpreted the outer polaroplast region as a fluid filled cavity and this appeared both closed (their Fig. 11) and open (their Fig. 12). This opinion was revised by Sprague and Vernick (1969) who proposed that it corresponded to the outer polaroplast zone of *P. nelsoni* and was thus a finely laminated structure. Weidner (1970) described the polaroplast of *A. michaelis* as spirally arranged. Larsson (1986) reviewed the range of polaroplast types in microsporidia. A polaroplast with a membranous inner component, enclosed by close-packed membranes forming a complete sac breached only by the polar tube, has not been described except in *Ameson* spp. and *P. nelsoni*.

Nosema nelsoni (Sprague, 1950) was transferred to the genus *Ameson* by Sprague (1977), then to *Perezia*

by Vivarès and Sprague (1979). The genus *Ameson* was established for *Nosema michaelis* by Sprague (1977) and differentiated from *Nosema* by its production of sporoblasts in chains from a moniliform multinucleate sporont, as opposed to production of sporoblasts in pairs from a binucleate sporont in *Nosema*. *Ameson* was placed in the family *Nosematidae* in the mistaken belief that sporoblasts (and presumably spores) were diplokaryotic (Sprague, 1977). This was later corrected (Vivarès and Sprague 1979). Two features, common to *A. michaelis* and *A. pulvis*, the latter species also from crabs (*Carcinus maenas*) described by Vivarès and Sprague (1979), are the outer region of compact polaroplast membranes and a layer of "bristles" covering the surface of sporoblasts and spores (Sprague *et al.* 1968, Vivarès and Sprague 1979). The transfer of *A. nelsoni* to *Perezia* was based on the absence of these bristle-like structures. However, the polaroplast of *Perezia lankesteriae* apparently lacks the outer region of close-packed membranes (Ormières *et al.* 1977) and, in this respect, *P. nelsoni* more closely resembles *Ameson* spp.

The present ultrastructural studies of *P. nelsoni* and *T. weidneri* have provided data which are in accord with the phylogenetic relationships of these species indicated by 16S rDNA sequences (Cheney *et al.* 2000). In their parsimony tree the species listed as *Pleistophora* sp. LS was most closely related to *A. michaelis*. As *Pleistophora* sp. LS has now been identified as *Perezia nelsoni*, the anomaly of a spieces thought to have SVs and *A. michaelis* without SVs within the same clade has been removed. Whether the presence or absence of hair-like projections on the spores carries sufficient weight to separate *P. nelsoni* on the one hand and *A. michaelis* and *A. pulvis* on the other hand into different genera is debatable, considering the extraordinary similarity in their merogonic and sporogonic stages and internal spore structure and given that they all parasitise decapod crustaceans. *Perezia lankesteriae*, a hyperparasite of the gregarine *Lankesteria ascidiae* in the ascidian *Ciona intestinalis*, may well be different but needs re-examination to reveal its mature spore structure.

The molecular study by Cheney *et al.* (2000) included the microsporidium, thought to be *Pleistophora* sp. from *F. aztecus*. This species, referred to as *Pleistophora* sp. PA, fell into a polytomy with *Glugea atherinae*, *Loma* sp., *Ichthyosporidium* sp. and *Loma acerinae*. In the present study it has been placed in the genus *Tuzetia* as *T. weidneri*, although it exhibited some morphological features not previously reported for the genus. No other species of *Tuzetia* has been examined for its 16S rDNA sequence so that the relationships of the type species *Tuzetia infirma* from the copepod *Cyclops fuscus* are unknown. *Janacekia debaisieuxi* is another species in which spores lie individually in SVs. It was split from the genus *Tuzetia* by Larsson (1983) because it is diplokaryotic in merogony and undergoes meiosis before producing uninucleate spores. *J. debaisieuxi* was found to be distant from *T. weidneri* (*Pleistophora* sp. PA) in the molecular study of Cheney *et al.* (2000). This adds credence to systematics which give weight to nuclear phenomena, especially diploidy and the occurrence of meiosis, in considering relationships among taxa (Sprague *et al.* 1992).

Acknowledgements. We thank Trish Rowland from Withington Hospital, Manchester for assistance with electron microscopy and Ronnie Palmer, Susan Plourde, Pam Monson, Kristine Wilkie, Marie Wright, Susan Carranza, Nate Jordan, Jody Peterson and Lex Galle (all from the University of South Mississippi) for collection and preparation of material from infected shrimps. The study was conducted in part under U.S. Department of Agriculture, Cooperative State Research Service Grant No. 98-38808-6019.

REFERENCES

Baxter K. N., Rigdon R .H., Hanna C. (1970) *Pleistophora* sp. (Microsporidia: Nosematidae): a new parasite of shrimp. *J. Invertebr. Pathol.* **16:** 289-291

Canning E. U., Hazard E. I. (1982) Genus *Pleistophora* Gurley 1893, an assemblage of at least three genera. *J. Protozool.* **29:** 39-49

Cheney S. A., Lafranchi-Tristem N. J., Canning E. U. (2000) Phylogenetic relationships of *Pleistophora*-like microsporidia based on small subunit ribosomal DNA sequences and implications for the source of *Trachipleistophora hominis* infections. *J. Eukaryot. Microbiol.* **47:** 280-287

Clotilde-Ba F.-L., Togubaye B. S. (1994) Ultrastructure and development of *Agmasoma penaei* (Microspora, Thelohaniidae) found in *Penaeus notialis* (Crustacea, Decapoda, Penaeidae) from Senegal. *Eur. J. Protistol.* **30:** 347-353

Clotilde-Ba F.-L., Togubaye B. S. (1995) Occurrence of microsporidia and gregarines in the shrimp *Penaeus notialis* from Senegal (West Africa). *Bull. Eur. Ass. Fish Pathol.* **15:** 122-124

Clotilde-Ba F.-L., Togubaye B. S. (1996) Complementary data on the cytology of *Perezia nelsoni* (Sprague, 1950) Vivarès and Sprague 1979 (Microspora, Pereziidae) found in *Penaeus notialis* (Crustacea, Decapoda) from Senegal. *Zool. Beitr. N. F.* **37:** 41-48

Constransitch M. J. (1970) Description, pathology and incidence of *Plistophora penaei* n. sp. (Microsporidia, Nosematidae), a parasite of commercial shrimp. Masters Thesis, Northwestern State University, Natchitoches, Louisiana

Couch J. A. (1978) Diseases, parasites and toxic responses of commercial penaeid shrimps of the Gulf of Mexico and South Atlantic coasts of North America. *Fish. Bull.* **76:** 1-44

Couch J. A. (1983) Diseases, caused by Protozoa. In**:** The Biology of Crustacea: Pathobiology, (Ed. A. J. Provenzano). Academic Press, New York, **6:** 79-111

Hazard E. I., Oldacre S. W. (1976) Revision of Microsporidia (Protozoa) close to *Thelohania*, with descriptions of one new family, eight new genera, and thirteen new species. U.S. Dept. of Agriculture Technical Bulletin No. 1530, 1-104

Kudo R. (1921) Microsporidia parasitic in copepods. *J. Parasitol*. **7:** 137-143

Larsson R. (1983) A revisionary study of the taxon *Tuzetia* Maurand, Fize, Fenwick and Michel, 1971 and related forms (Microsporidia, Tuzetiidae). *Protistologica* **19:** 323-355

Larsson R. (1986) Ultrastructure, function and classification of Microsporidia. *Prog. Protistol.* **1:** 325-390

Loubès C. (1979) Ultrastructure, sexualité, dimorphisme sporogonique des Microsporidies (Protozoaires). Incidences taxonomiques et biologiques. Thesis, Academie de Montpellier, Université des Sciences et Techniques du Languedoc, France

Loubès C., Maurand J., Comps M., Campillo A. (1977) Observations ultrastructurales sur *Ameson nelsoni* (Sprague, 1950) Microsporidie parasite de la crevette *Parapenaeus longirostris* Lucas consequences taxonomiques. *Rev. Trav. Inst. Pêches marit.* **41:** 217-222

Ormières R., Loubès C., Maurand J. (1977) Etude ultrastructurale de la Microsporidie *Perezia lankesteriae* Léger et Duboscq 1909, espèce-type: validation du genre *Perezia*. *Protistologica* **13:** 101-112

Overstreet R. (1973) Parasites of some penaeid shrimps with emphasis on reared hosts. *Aquaculture* **2:** 105-140

Owens L., Glazebrook J. S. (1988) Microsporidiosis in prawns from Northern Australia. *Aust. J. Mar. Freshw. Res.* **39:** 301-305

Sprague V. (1950) Notes on three microsporidian parasites of decapod Crustacea of Louisiana coastal waters. *Occ. Pap. Mar. Lab. Louisiana State Univ.* **5:** 1-8

Sprague V. (1977) Classification and phylogeny. In**:** Systematics of the Microsporida, Comparative Pathobiology (Eds. L.A. Bulla and T.C. Cheng). Plenum Press **2:** 1-30

Sprague V., Couch J. (1971) An annotated list of protozoan parasites, hyperparasites and commensals of decapod Crustacea. *J. Protozool*. **18:** 526-527

Sprague V., Vernick S. H. (1969) Light and electron microscope observations on *Nosema neloni* Sprague, 1950 (Microsporidia, Nosematidae) with particular reference to its Golgi complex. *J. Protozool.* **16:** 264-271

Sprague V., Becnel J. J., Hazard E. I. (1992) Taxonomy of phylum Microspora. *Crit. Rev. Microbiol.* **18:** 285-395

Sprague V., Vernick S. H., Lloyd B. J. (1968) The fine structure of *Nosema* sp. Sprague, 1965 (Microsporidia, Nosematidae) with particular reference to stages in sporogony. *J. Invertebr. Pathol.* **12:** 105-117

Vivarès C.P., Sprague V. (1979) The fine structure of *Ameson pulvis* (Microspora, Microsporida) and its implications regarding classification and chromosome cycle. *J. Invertebr. Pathol.* **33:** 40-52

Weidner E. (1970) Ultrastructural study of microsporidian development. I. *Nosema* sp. Sprague, 1965 in *Callinectes sapidus* Rathbun. *Z. Zellforsch.* **105:** 33-54

Received on 23rd July, 2001; accepted on 16th November, 2001

Acta Protozool. (2002) 41: 79 - 84

ACTA
PROTOZOOLOGICA

A New Suctorian, *Flectacineta isopodensis* (Protozoa: Ciliophora) Epibiont on Marine Isopods from Hokkaido (Northern Japan)

Gregorio FERNANDEZ-LEBORANS[1], Yukio HANAMURA[2] and Keizo NAGASAKI[2]

[1]Departamento de Biologia Animal I (Zoologia), Facultad de Biologia, Universidad Complutense, Madrid, Spain; [2]National Research Institute of Fisheries and Environment of Inland Sea, Ohno-cho, Hiroshima, Japan

Summary. Specimens of a suctorian ciliate were found as epibionts on the marine isopod *Excirolana chiltoni*. The small suctorians were loricate (10-17 µm long, 8-10 µm wide). The oval or bell-shaped body was covered completely by the lorica, which showed a rim curved outwards, with a lateral furrow. There were 5-9 capitate tentacles in an apical group that protruded through the opening of the lorica. The macronucleus was central. The micronucleus was located anterolaterally near the macronucleus. The contractile vacuole was central and behind the macronucleus. The stalk presented thin transverse striations. This is the first record of a suctorian on an isopod species of the suborder Flabellifera, which contains the majority of the marine isopods living in shallow waters.

Key words: Ciliophora, epibiont, *Flectacineta isopodensis* sp. n., suctoria

INTRODUCTION

An important number of protozoan ciliate species have been described as epibionts on crustaceans (Sprague and Couch 1971, Morado and Small 1995). The ciliate groups showing a larger number of species living on crustaceans are peritrich ciliates (Fernandez-Leborans and Tato-Porto 2000a), suctorian ciliates (Batisse 1994, Fernandez-Leborans and Tato-Porto 2000b), and chonotrich ciliates (Jankowski 1973, Fernandez-Leborans 2001). Ciliate epibionts have been found in many crustacean groups (branchiopods, cirripeds, copepods, mysids, amphipods, decapods).

Numerous suctorian species have been described living as epibionts on crustaceans (Collin 1912; Guilcher 1950; Batisse 1968, 1969, 1972, 1986, 1992; Evans *et al*. 1979; Hudson and Lester 1994; Fernandez-Leborans and Gomez del Arco 1996; Fernandez-Leborans *et al*. 1996, 1997; Zhadan and Mikrjukov 1996). The order Isopoda is one of the crustacean groups with basibiont species on which suctorian ciliates live, both in freshwater and marine environments; suctorian ciliates of the genera *Ophryodendron, Trichophrya, Acineta, Tokophrya* and *Stylocometes* having been found.

The suborder Flabellifera includes the genus *Excirolana*, in one of their species, *Excirolana chiltoni*, we have found numerous specimens of a suctorian

Address for correspondence: Gregorio Fernandez-Leborans, Departamento de Biologia Animal I (Zoologia), Facultad de Biologia, Pnta 9, Universidad Complutense, 28040 Madrid, Spain; E-mail: greg@bio.ucm.es

ciliate of the genus *Flectacineta*. The characteristics of these ciliates are described below.

MATERIALS AND METHODS

Specimens of *Excirolana chiltoni* (Richardson, 1905) were collected in the intertidal zone (at least >30 cm) of open sandy beaches of Hokkaido (Zenibako, Yufutsu, and Usu) (Fig. 1). Sampling was carried out with a hand-held net (30 cm mouth width, 0.74 mm mesh). All collection was done during daylight. Samples were fixed immediately with 5-10% seawater formalin and transferred later to 70% alcohol. The isopods were examined using a stereoscopic microscope. Epibionts were isolated and treated using the silver carbonate technique, according to the procedure described by Fernandez-Leborans and Castro de Zaldumbide (1986), neutral red and methyl green. Ciliate measurements were performed with an ocular micrometer. Samples for SEM (Hitachi S2460NA) observations were prepared following the procedure of Takayama (1981). Measurements were obtained considering 20% allowance for shrinkage due to fixation and staining (Montagnes *et al*. 1988).

RESULTS

The suctorians observed were small in size (10.3-17.2 μm in length; 8.6-10.8 μm in width), oval or bell-shaped (Figs 2-9). The body was surrounded completely by a lorica, which showed the rim curved outwards. The tentacles sticking out through the opening of the lorica. Laterally, the lorica presented a prolongation, as a furrow, which terminated in an acute angle. This furrow was 3.4-4.3 μm long, with a maximum width of 2-2.2 μm. There were 5-9 capitate tenctacles in a one apical group. The distal end of the tentacles had a diameter of 0.9-1.1 μm. The macronucleus was located centrally in the body, and was 3-4.5 in length and 2.5-3.8 μm in width. Near the macronucleus, laterally on the top was a micronucleus (0.6-0.9 μm diameter). The contractile vacuole, rounded, with 1.1-1.7 μm diameter, was located in the middle of the body, behind the macronucleus. The stalk was 8.9-25.2 μm in length, and its outer surface was covered by thin transverse striations. Inside the stalk, in several specimens, there was a central channel (Table 1).

Location on the basibiont. The suctorian ciliates were found in all pereiopods, directly attached to the surface, or on its setae. Ocasionally, several specimens were observed on the antennae. These ciliates were not found on the pleopods, buccal appendages or any other part of the body.

Taxonomic position. The ciliates observed are assigned to a new species, called *Flectacineta isopodensis,* in reference to the basibionts on which these suctorians were found.

The ciliates studied belong to the genus *Flectacineta* Jankowski, 1978 (subclass Suctoria Claparède & Lachmann 1958, order Podophryida Jankowski 1973, suborder Podophryina Jankowski 1973, family Paracinetidae Jankowski 1978) (Batisse 1994). Like the members of this genus, they were marine loricate ciliates, with a unique group of apical capitate tentacles. Thecostyle lorica rim is inverted at the apex (Curds 1987). Three species of the genus *Flectacineta* have been described: *F. livadiana* (Mereschkowsky, 1881) Jankowsky 1978, *F. dadayi* (Daday, 1886) Curds 1987, and *F. elegans* (Imhoff, 1883) (Curds 1987). The specimens studied differed from *F. livadiana* in the wide opening of the lorica, and in the position of the contractile vacuole (lateral in *F. livadiana*, in contrast it is located centrally behind the macronucleus in the ciliates observed). The specimens studied differed from *F. dadayi* in the location of the contractile vacuole and the presence of a lateral furrow of the lorica. Although *F. elegans* is the largest species of the genus, it had in common with the ciliates observed the union between the stalk and the lorica, which appeared with a ball-like shape in some specimens. However, *F. elegans* had a rectangular body, the lorica with a scalloped rim, and an apical contractile vacuole, characteristics that not found in the ciliates studied (Table 2).

Diagnosis of *Flectacineta isopodensis* sp. n. Small marine loricate suctorian ciliates (10.3-17.1 μm long, 8.6-10.8 μm wide). Oval or bell-shaped body, completely included in the lorica. Lorica with rim curved outwards, prolonged in lateral furrow. 5-9 capitate tentacles in an apical group. Centrally located macronucleus (3.0-4.5 x 2.3-3.7 μm). Micronucleus located laterally on the top near the macronucleus. Contractile vacuole (1.1-1.6 μm) central and posterior to the macronucleus. Stalk (8.9-25.2 μm) with thin transverse striations. Epibiont on the isopod *Excirolana chiltoni* (Richardson, 1905), (type locality: Hokkaido, Northern Japan).

DISCUSSION

Several suctorian species have been described as epibionts on isopods. *Ophryodendron multicapitatum* Kent, 1880 on *Idotea* Fabricius, 1798. *Trichophrya*

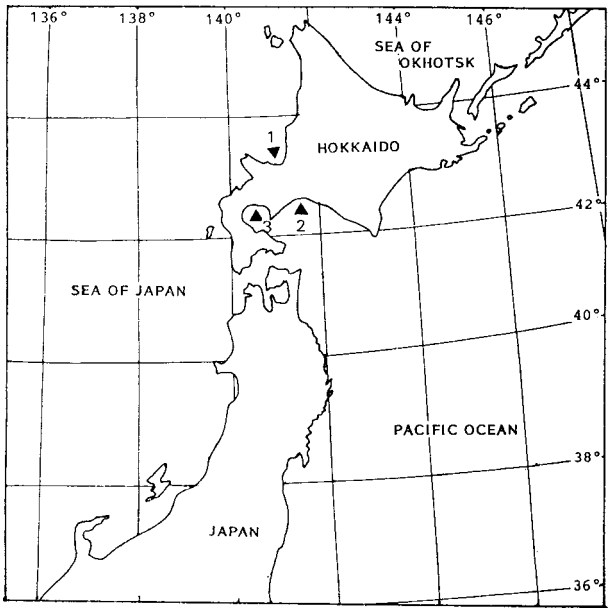

Fig. 1. Map showing the sampling sites. 1 - Zenibako, Otaru (city); 2 - Yufutsu, Tomakomai (city); 3 - Usu , Date (city)

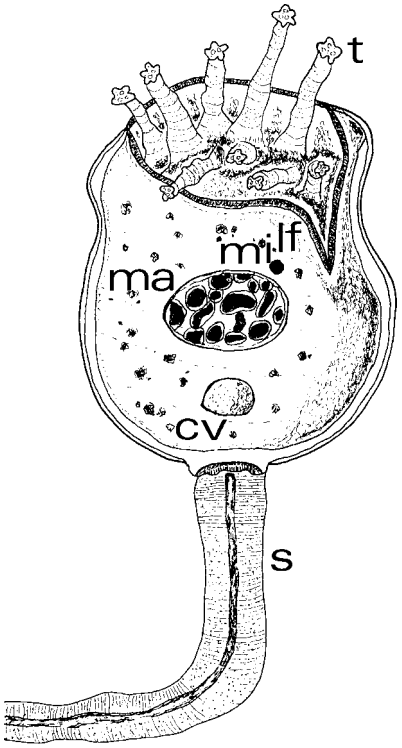

Fig. 2. Scheme of *Flectacineta isopodensis* sp. n. cv - contractile vacuole, lf - lateral furrow, ma - macronucleus, mi - micronucleus, s - stalk, t - tentacles

Table 1. Morphometric characteristics of *Flectacineta isopodensis* sp. n. (n: 42)

	Mean	SD	SE	Minimum	Maximum
Body length	14.36	1.97	0.62	10.32	17.16
Body width	9.29	0.62	0.21	8.64	10.80
Number of tentacles	7.44	1.42	0.47	5	9
Lorica opening max. width	8.30	0.68	0.19	7.65	10.10
Furrow length	3.74	0.36	0.11	3.38	4.32
Furrow max. width	2.08	0.03	0.01	2.04	2.16
Tentacle distal end diameter	1.02	0.05	0.02	0.91	1.09
Stalk length	14.43	3.83	1.10	8.90	25.20
Macronucleus length	4.08	0.41	0.13	3.02	4.54
Macronucleus width	3.27	0.31	0.10	2.52	3.78
Micronucleus diameter	0.75	0.08	0.03	0.64	0.92
Contractile vacuole diameter	1.33	0.15	0.05	1.13	1.68

* Measurements in µm. SD - standard deviation, SE - standard error

astaci Stein, 1859 on *Asellus* Geoffroy, 1762. *Acineta tuberosa* Ehrenberg, 1833 on *Idotea, Asellus* and *Microcerberus remyi* Chappuis, 1953. *Tokophrya lemnarum* (Stein, 1859) on *Asellus aquaticus* (Linnaeus, 1758). *Stylocometes digitatus* (Stein, 1859) on *Asellus aquaticus*. *Stylocometes stenaselli* (Matjasiè, 1963) on *Stenasellus virei* Dollfus, 1897. Up to now, the presence of suctorian epibionts on *Excirolana chiltoni* has not been described and, therefore, this is the first record of the existence of these ciliates as epibionts on the isopod. *Excirolana chiltoni*.

Excirolana chiltoni (Richardson, 1905) (Subphylum Crustacea, class Malacostraca, subclass Eumalacostraca, order Isopoda) belongs to the suborder Flabellifera.

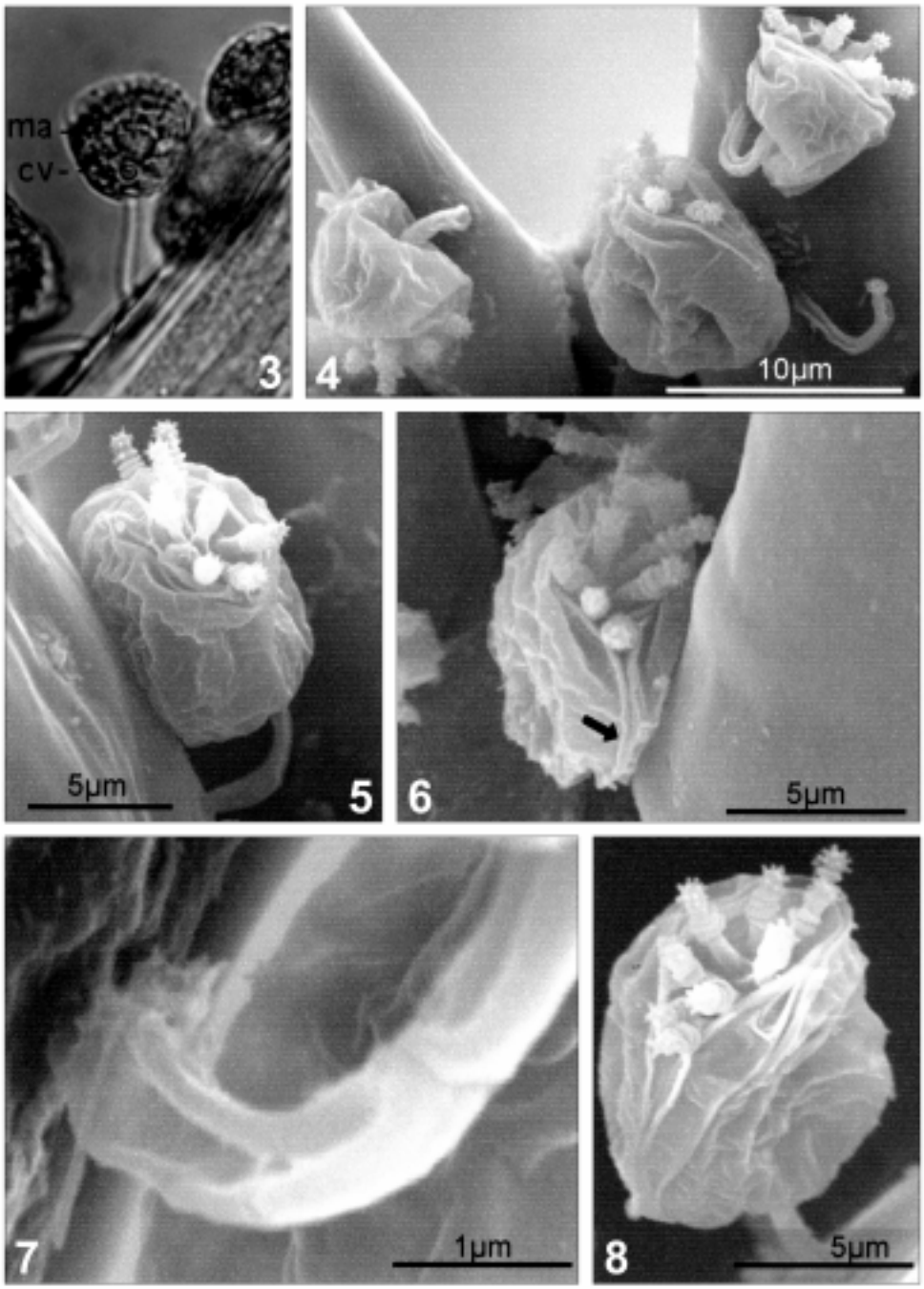

Fig. 3. *Flectacineta isopodensis* sp. n. Light micrograph of a specimen. cv - contractile vacuole, ma - macronucleus (x 1200). **Fig. 4.** Three specimens attached to the surface of a pereiopod and to a seta. The central channel of the stalk can be seen. **Fig. 5.** *F. isopodensis*. The anterior part of the body showing the opening of the lorica and the tentacles. **Fig. 6.** *F. isopodensis*. Anterior part of the body. The lateral furrow (arrow) can be seen. **Fig. 7.** *F. isopodensis*. A detail of the stalk showing its base and the central channel. **Fig. 8.** *F. isopodensis*. A lateral view of an specimen, showing the opening of the lorica, the tentacles and the stalk

Suctorian epibionts have not been found in the species included in this suborder, and the specimens studied corresponded to the first finding of suctorians in this suborder, which contains the main part of the marine isopod species living in shallow waters.

On the other hand, there is not sufficient morphological data to differentiate *Flectacineta livadiana* from *Flectacineta dadayi*, and thus there is a possibility that both species should be included in a unique species: *F. livadiana* (Mereschkowsky, 1881) Jankowski 1978.

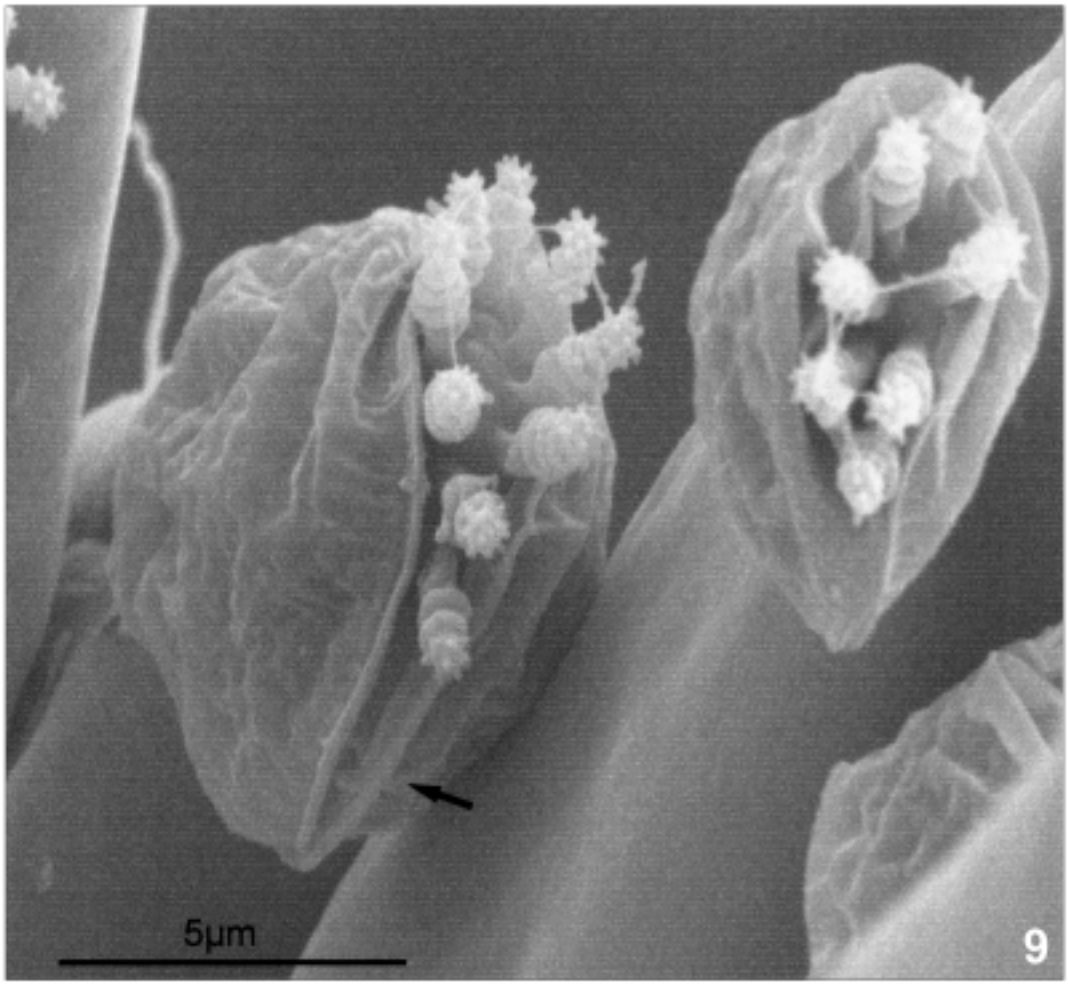

Fig. 9. *Flectacineta isopodensis*. Two specimens showing the opening of the lorica and the tentacles. The lateral furrow (arrow), and the rim curved outwards of the lorica can be seen

Table 2. Comparison between the different species of *Flectacineta*

	F. lividiana Jankowski, 1978	*F. dadayi* Curds, 1987	*F. elegans* Curds, 1987	*F. isopodensis* sp. n.
Size	30-80 µm	45 µm	70 µm	10.3-17.2 µm
Openinglorica	Small	Small	Small	Wide
Lorica with lateral furrow	No	No	No	Yes
Contractile vacuole position	Lateral	Lateral	Apical	Central posterior

F. livadiana and *F. dadayi* are epizoic on hydroids and marine algae. *F. elegans* has been found on the cladoceran *Bythotrepes longimanus* Leydig, 1860.

REFERENCES

Batisse A. (1968) Les ultrastructures squelettiques chez certains Thecacinetidae. *Protistologica* **4:** 477-492

Batisse A. (1969) Acinétiens nouveaux ou mal connus des côtes méditerranéennes françaises. I. *Ophryodendron hollandei* n. sp. (Suctorida, Ophryodendridae). *Vie Milieu* **20:** 251-278

Batisse A. (1972) Premières observations sur l'ultrastructure de *Trematosoma bocqueti* (Guilcher), Batisse (Ciliata, Suctorida). *Protistologica* **8:** 477-495

Batisse A. (1986) Acinétiens nouveaux ou mal connus des côtes méditerranéennes françaises: II. *Dendrosomides grassei* n. sp. (Suctorida, Ophryodendrina). *Protistologica* **12:** 11-21

Batisse A.(1992) Acinétiens nouveaux ou mal connus des côtes méditerranéennes françaises. 3. *Dentacinetides collini* gen. n., sp. n. (Suctoria, Ophryodendrina).*Vie Milieu* **42:** 295-306

Batisse A. (1994) Sous-Classe des Suctoria Claparède et Lachmann, 1958. In: Traité de Zoologie, (Ed. Masson) Paris, **2:** 433-473

Collin B. (1912) Etude monographique sur les Acinétiens. II. *Arch. Zool. exp. gén*. **51:** 1-457

Curds C. (1987) A revision of the Suctoria (Ciliophora, Kinetofragminophora) 5. The *Paracineta* and *Corynophrya* problem. *Bull. British Mus. nat. Hist. (Zool.)* **52:** 71-106

Evans M. S., Sicko-Goad L. M., Omair H. (1979) Seasonal occurence of *Tokophrya quadripartita* (Suctoria) as epibionts on adult *Limnocalanus macrurus* (Copepoda, Calanoida) in southeastern Lake Michigan. *Trans. American microsc. Soc*. **98:** 102-109

Fernandez-Leborans G. (2001) A review of the species of protozoan epibionts on crustaceans. III. Chonotrich ciliates. *Crustaceana* **74:** 581-607

Fernandez-Leborans G., Castro de Zaldumbide M. (1986) The morphology of *Anophrys arenicola* sp. nov. (Ciliophora, Scuticociliatida). *J. Nat. Hist.* **20:** 713-721

Fernandez-Leborans G., Gómez del Arco P. (1996) A new species of the genus *Corynophrya* (Protozoa, Ciliophora): an epibiont of decapod crustaceans. *Microbios* **86:** 27-37

Fernandez-Leborans G., Tato-Porto M. L. (2000a) A review of the species of protozoan epibionts on crustaceans. I. Peritrich ciliates. *Crustaceana* **73:** 643-683

Fernandez-Leborans G., Tato-Porto M. L. (2000b) A review of the species of protozoan epibionts on crustaceans. I. Suctorian ciliates. *Crustaceana* **73:** 1205-1237

Fernandez-Leborans G., Tato-Porto, M. L., Sorbe J. C. (1996) The morphology and life cycle of *Ophryodendron mysidacii* sp. nov. a marine suctorian epibiont on a mysid crustacean. *J. Zool*. **238:** 97-112

Fernandez-Leborans G., Herrero Cordoba M. J., Gomez del Arco P. (1997) Distribution of ciliate epibionts on the portunid crab *Liocarcinus depurator* (Decapoda: Brachyura). *Invertebrate Biol*. **116:** 171-177

Guilcher Y. (1950) Sur quelques Acinétiens nouveaux ectoparasites de Copépodes Harpacticides. *Arch. Zool. exp. et gén*. **87:** 24-30

Hudson D. A., Lester R. J. G. (1994) A parasitological survey of the mud crab *Scylla serrata* (Forskål) from southern Moreton Bay, Queensland, Australia. *Aquaculture* **120:** 183-199

Jankowski A. V. (1973) Taxonomic sketch class Suctoria Claparède and Lachmann, 1858. *Akad. Nauk SSSR Zool. Inst.* 30-31

Montagnes D. J. S., Lynn D. H., Roff J. C., Taylor W. D. (1988) The annual cycle of heterotrophic planktonic ciliates in the waters surrounding the Isles of Shoals, Gulf of Maine: an assessment of their trophic role. *Marine Biology* **99:** 21-30

Morado J. F., Small E. B. (1995) Ciliate parasites and related diseases of Crustacea: a review. *Rev. Fish. Sci.* **3:** 275-354

Sprague V., Couch J. (1971) An annotated list of protozoan parasites, hyperparasites and commensals of decapod Crustacea. *J. Protozool*. **18:** 526-537

Takayama H. (1981) Preparation of red tide plankton for scanning electron microscopy. *Bull. Hiroshima fish. exp. Stat.* **11:** 101-112

Zhadan D. G., Mikrjukov K. A. (1996) *Podocyathus paguri* sp. n. (Suctoria, Ephelotidae), an ectocommensal of the White Sea hermit-crab. *Zool. Zh.* **75:** 309-312 (in Russian)

Received on 27th September, 2001; accepted on 12th December, 2001

Acta Protozool. (2002) 41: 85 - 89

ACTA
PROTOZOOLOGICA

Short communication

Impact of Melatonin on the Cell Division, Phagocytosis and Chemotaxis of *Tetrahymena pyriformis*

László KŐHIDAI[1], Olli VAKKURI[3], Márk KERESZTESI[1], Éva PÁLLINGER[2], Juhani LEPPÄLUOTO[3], György CSABA[1]

[1]Department of Genetics, Cell and Immunobiology, Semmelweis University, Budapest, Hungary, [2]Molecular Immunological Research Group of the Hungarian Academy of Sciences, Budapest, and [3]Department of Physiology, University of Oulu, Finland

Summary. Melatonin is produced, stored and secreted by *Tetrahymena*. In the present experiments the effects of exogeneously given melatonin to *Tetrahymena pyriformis* was studied. Melatonin, between 10^{-6} and 10^{-10} M concentrations, significantly stimulated the *E. coli* phagocytosis of *Tetrahymena*. Melatonin also suppressed the multiplication of *Tetrahymena* cultures. Melatonin had chemotactic effect depending on illumination: it was chemoattractant in light and chemorepellent in darkness at the concentration of 10^{-11} M. Functional and evolutionary conclusions are discussed.

Key words: cell division, chemotaxis, evolution, melatonin, phagocytosis, *Tetrahymena*.

INTRODUCTION

The unicellular *Tetrahymena* express hormone receptors (Csaba 1980, 1984, 2000; Kovács and Csaba 1990a, Christopher and Sundermann 1992,1995) and produces, stores and secretes vertebrate hormone-like molecules (LeRoith *et al.* 1980, 1983). If vertebrate hormones are given to *Tetrahymena* its receptors can bind it and - possessing signal transduction system (Kuno *et al*. 1979, Kovács and Csaba 1990b) - the cell can react to them. This reaction is specific in many cases, namely insulin influences glucose metabolism, thyroxin effects cell division, histamine stimulates phagocytosis etc (Csaba 1994).

In previous experiments (Kőhidai *et al.,* in press) melatonin - a hormone, ubiquitous in the living world (Hardeland 1999) - was found in *Tetrahymena*, the production of which was influenced by light conditions, as in vertebrates. Considering this observation, the effect of exogeneously administered melatonin on the basic physiological indices of *Tetrahymena* was investigated in an attempt to identify a possible functional role of this agent.

Address for correspondence: György Csaba, Department of Genetics, Cell and Immunobiology, Semmelweis University, H-1445 Budapest, POB 370 Hungary; Fax: (36-1) 210-2950; E-mail: csagyor@dgci.sote.hu

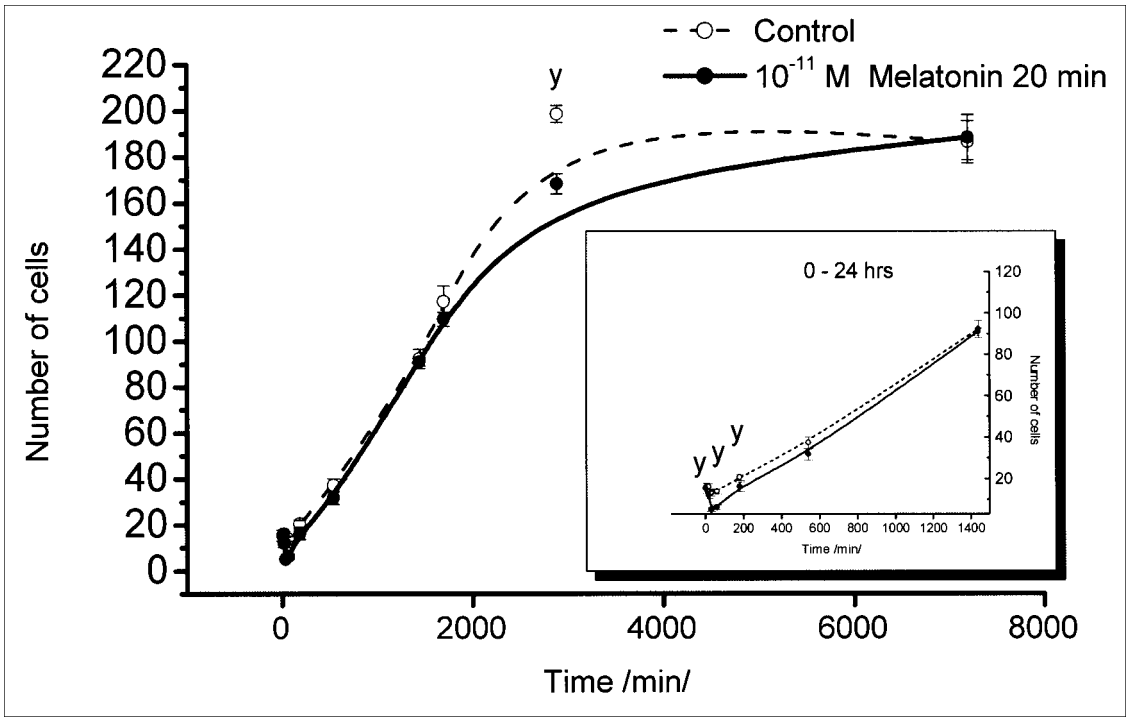

Fig. 1. Effect of exogenous melatonin on the growth of *Tetrahymena* cultures. Treatment with 10^{-11} M melatonin results a suppressed multiplication of cells in early phase (0-200 min. in the insert); and in the late phase (2-3 days) of growing. (y - $p<0.01$)

MATERIALS AND METHODS

Tetrahymena pyriformis GL cells were maintained in axenic cultures containing 1% tryptone and 0.1% yeast extract (Difco, Michigan, USA). The starting density of cultures was $5x10^2$ cell/ml.

Cell division. Low-density cultures of *Tetrahymena* (10^1 cell/ml) were treated with 10^{-11} M melatonin for 20 min. Our pilot experiments had shown that the applied concentration of exogenous melatonin is neutral on phagocytosis, and equal with the concentration of endogenous melatonin of *Tetrahymena* released to the medium. The density of control and melatonin -treated samples was counted in Neubauer haemocytometer after 0, 15, 30, 60, 180, 540, 1440, 1700, 2880 and 7200 min. Each data set of the experiment represented the average of counts of 10 individual parallels.

Phagocytotic activity. Phagocytotic activity of cells treated with 10^{-10}, 10^{-8} and 10^{-6} M melatonin was evaluated with FITC-labelled *E. coli* particles (Phagotest; Orpegen Pharma) (Bassone 1984). Bacteria (20 µl), *Tetrahymena* cells (100 µl) with different concentrations of melatonin were incubated for 10 min. Then the samples were fixed with 4% formaldehyde in PBS. The extracellular fluorescent activity was neutralized with quenching solution. The samples were washed with PBS trice. The number of fluorescent particles taken up by cells was measured with fluorescent-activated cell sorter (FACS-Calibur, Becton-Dickinson). The number of evaluated cells was 10000/sample.

Chemotaxis assay. Two-chamber capillary chemotaxis assay of Leick and Helle (1983) was modified as previously published (Kőhidai and Csaba 1998, Kőhidai 1999). In this assay we used an 8-channel micropipette, where the tips of pipette filled with test substance served as inner chambers, while 96-well microtiter plates, filled with *Tetrahymena* cultures (cell density 10^4 cell/ml), served as outer chambers. In the assay the concentration course of chemotactic responsiveness (10^{-12} -10^{-6} M) was tested in light- and darkness-stressed cultures. The incubation time was 20 min. Based on pilot experiments with several other ligands this is the optimal incubation time when the concentration gradient required for chemotaxis is still present in the chamber. The shorter times provided an insufficient number of cells in the sample, while at times longer than 20 min it was not possible to distinguish chemotactic-responder cells from chemokinetic-responder cells. The samples were fixed in 4% formaldehyde containing PBS. The number of cells was counted in a Neubauer cytometer by light microscopy.

Light and darkness effect. Chemotaxis was observed in cultures kept in light or darkness. For light stress, an intensity of 7500 lux was applied, while cultures kept in darkness were wrapped in special aluminium foil.

Statistical analysis. Data of experiments were analysed with ANOVA test. Standard deviations (S.D.) and levels of significance are shown in the figures (x - $p<0.05$; y - $p<0.01$; z - $p<0.001$).

RESULTS AND DISCUSSION

In an earlier experiment the presence, storage and secretion of melatonin in *Tetrahymena* were demonstrated. The aim of the present experiments was to study

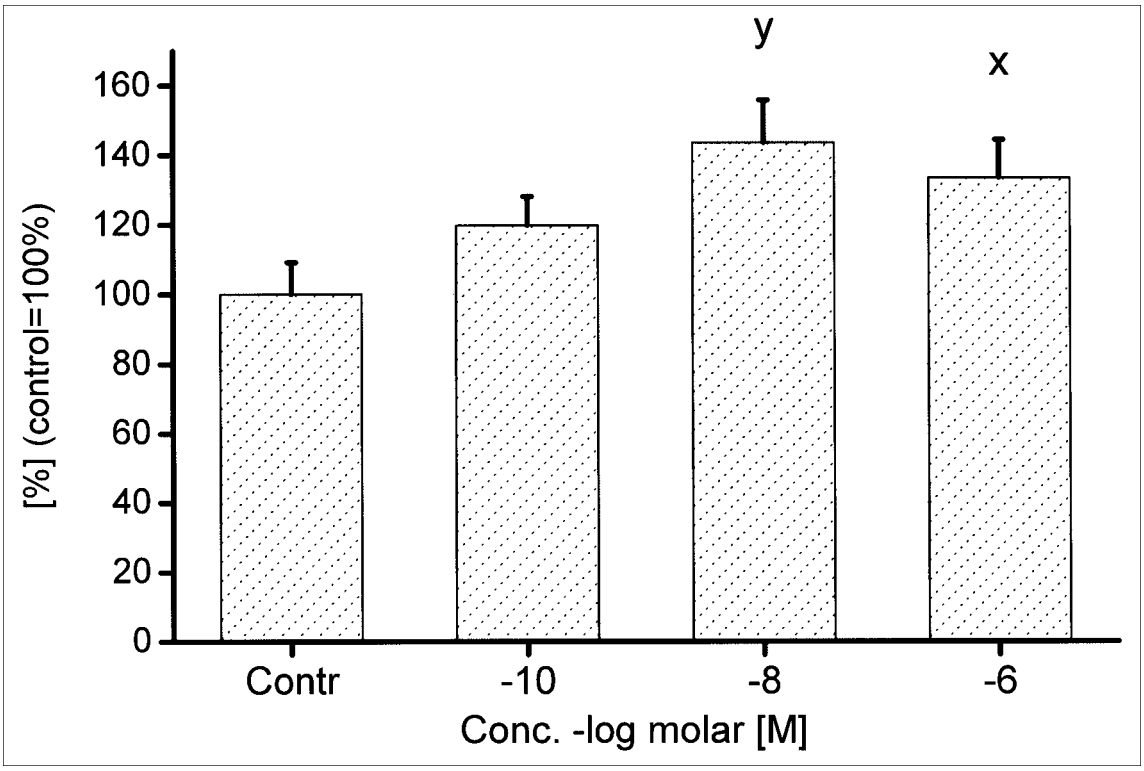

Fig. 2. Flow-cytometric evaluation of the uptake of FITC labelled *E. coli* particles by *Tetrahymena* cells. The phagocytic activity of cells is induced with 10^{-10}, 10^{-8} and 10^{-6} M melatonin. (x - $p<0.05$; y - $p<0.01$)

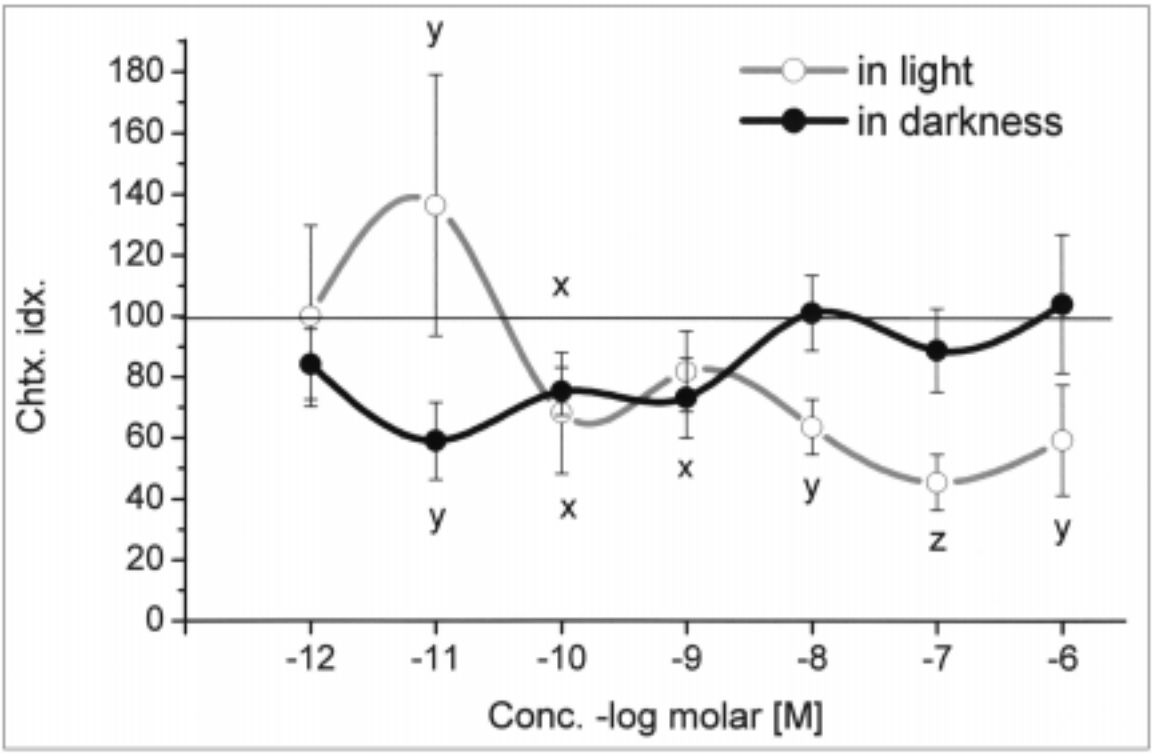

Fig. 3. Chemotactic effects of exogenous melatonin in light- and darkness-stressed *Tetrahymena* cultures. In light 10^{-11} M melatonin acts as a chemoattractant, while the higher concentrations 10^{-10}-10^{-6} M possess chemorepellent effect (open circules). In darkness-stressed cultures melatonin acts as strong chemorepellent even in low concentrations 10^{-11}-10^{-9} M (filled circules). (x - $p<0.05$; y - $p<0.01$; z - $p<0.001$)

the possible effects of melatonin at this low level of phylogeny.

Exogeneously administered melatonin at the concentration of 10^{-11} M suppressed the growth (cell division) of *Tetrahymena* (Fig. 1). The inhibition was significant during the first 3 h ($p<0.01$) also later during the second and third day ($p<0.01$). The phagocytic activity of *Tetrahymena* was increased by 10^{-6} and 10^{-8} M melatonin (133.41% ±10.86 $p<0.05$; 143.35% ±12.3 $p<0.01$ respectively) as shown in Fig. 2. Melatonin had a strong chemoattractant effect at very low concentration (10^{-11} M) in light ($p<0.01$), while at higher concentrations it had the opposite effect (Fig. 3). In darkness melatonin at the concentration of 10^{-11} M showed the most intensive chemorepellent effect which was not seen at 10^{-8} M, or at higher melatonin concentrations.

Melatonin prevents oxidative damage at cellular, tissue, organ and organismic levels (Tan *et al*. 2000). This antioxidant effect has been demonstrated in plants (Tan *et al.* 2000), a dinoflagellate (Antolin *et al.* 1997) and *Trypanosoma* (Macias *et al.* 1999). This allows to suppose that it has the same function in *Tetrahymena*. However, based on our present observations, melatonin in *Tetrahymena* could have also other functions.

Phagocytic activity for a unicellular organism is very important, and in our experiments it was elevated using a low (10^{-10} M) concentration of melatonin, with a peak at 10^{-8} M. The lower concentrations were easily reached in the 96 h cultures of our previous experiments, by secreted melatonin (Kõhidai *et al.,* in press). The cell number was suppressed as a consequence of melatonin (10^{-11} M). On the basis of the present experiments the total amount of exogenous plus endogeneous melatonin in the cultures was unknown, however the data suggest an autocrine regulation by melatonin in both physiological processes. In addition, the chemotactic effect, which is important at this level of phylogeny (Kõhidai and Csaba 1998, Kõhidai 1999), secreted melatonin also could have a regulatory role in a colony of unicells. Considering the presence of melatonin in bacteria (Manchester *et al.* 1995), which during phagocytosis is the main food for *Tetrahymena* under natural conditions, the strong chemoattractant effect in light is also understandable.

In previous experiments serotonin, a precursor molecule of melatonin, was found to have a significant phagocytosis promoting effect in *Tetrahymena* (Csaba and Lantos 1973, Csaba 1993). Melatonin had a similar action in the present experiments. Melatonin metabolites are free radical scavengers, like melatonin itself (Tan *et al.* 2000). These data suggest that this group of indoleamines may have an important role in *Tetrahymena*, which are shared by a broad spectrum of similar molecules.

Acknowledgements. This work was supported by the National Research Fund (OTKA-T-022754 and T- 037303), Hungary.

REFERENCES

Antolin I., Obst B., Burkhardt S., Hardeland R. (1997) Antioxidative protection in a high-melatonin organism: the dinoflagellate *Gonyaulax polyedra* is rescued from lethal oxydative stress by strongly elevated, but physiologically possible concentrations of melatonin. *J. Pineal Res*. **23:** 182-190

Bassone C.-F. (1984) Flow-cytometric studies on phagocyte function in bacterial infections. *Acta Path. Microbiol. Immunol. Scand.* **92:** 167-171

Christopher G. K., Sundermann C. A. (1992) Conventional and confocal microscopic studies of insulin receptor induction in *Tetrahymena pyriformis. Exp. Cell Res.* **201:** 477-484

Christopher G. K., Sundermann C. A. (1995) Isolation and partial characterization of the insulin binding sites of *Tetrahymena pyriformis. Biochem. Biophys. Res. Com*. **212:** 515-523

Csaba G. (1980) Phylogeny and ontogeny of hormone receptors: the selection theory of receptor formation and hormonal imprinting. *Biol. Rev.* **55:** 47-63

Csaba G. (1984) The unicellular *Tetrahymena* as a model cell for receptor research. *Int. Rev. Cytol.* **95:** 327-377

Csaba G. (1993) Presence in and effects of pineal indoleamines at very low level of phylogeny. *Experientia* **49:** 627-634

Csaba G. (1994) Phylogeny and ontogeny of chemical signaling: origin and development of hormone receptors. *Int. Rev. Cytol.* **155:** 1-48

Csaba G. (2000) Hormonal imprinting: its role during the evolution and development of hormone receptors. *Cell Biol.Int.* **24:** 407-414

Csaba G., Lantos T. (1973) Effect of hormones on Protozoa. Studies on the phagocytotic effect of histamine 5-hydroxitryptamine and indeleacetic acid in *Tetrahymena pyriformis. Cytobiologie* **7:** 361-365

Hardeland R. (1999) Melatonin and 5-methoxytryptamine in non metazoans. *Reprod. Nutr. Dev.* **39:** 399-408

Kőhidai L. (1999) Chemotaxis: the proper physiological response to evaluate phylogeny of signal molecules. *Acta Biol. Hung*. **50:** 375-394

Kőhidai L., Csaba G. (1998) Chemotaxis and chemotactic selection induced with cytokines (IL-8, RANTES and TNFa) in the unicellular *Tetrahymena pyriformis. Cytokine* **10:** 481-486

Kőhidai L., Vakkuri O., Keresztesi M., Pállinger É., Leppäluoto J., Csaba G. (2002) Melatonin in the unicellular *Tetrahymena*: effects of different lighting conditions. *Cell Biochem. Funct.* (in press)

Kovács, P., Csaba G.(1990a) Evidence of the receptor nature of the binding sites induced in *Tetrahymena* by insulin treatment. A quantitative cytofluorimetric technique for the study of binding kinetics. *Cell Biochem. Funct*. **8:** 49-56

Kovács, P., Csaba G. (1990b) Involvement of phosphoinositol (PI) system in the mechanism of hormonal imprinting. *Biochem. Biophys. Res. Com.* **170:** 119-126

Kuno T., Yoshida N., Tanaka C. (1979) Immunocytochemical localization of cyclic AMP and cyclic GMP in synchronously dividing *Tetrahymena. Acta Histochem.* **12:** 563

Leick V., Helle J. (1983) A quantitative assay for ciliate chemotaxis. *Anal. Biochem.* **135:** 466-469

LeRoith D., Schiloach J., Roth J., Lesniak M.A. (1980) Evolutionary origins of vertebrate hormones: substances similar to mammalian insulin are native to unicellular eukaryotes. *Proc. Natl. Acad. Sci. USA* **77:** 6184-6186

LeRoith D, Schiloach J., Berelowitz M., Frohmann L. A., Liotta A. S., Krieger B.T., Roth J. (1983) Are messenger molecules in microbes the ancestors of the vertebrate hormones and tissue factors? *Fed. Proc.* **42:** 2602-2607

Macias M., Rodriguez-Cabesas M. N., Reiter R. J., Osuna A., Acuna-Castroviejo D. (1999) Presence and effects of melatonin in *Trypanosoma cruzi. J. Pineal Res.* **27:** 86-94

Manchester L. C., Poeggeler B., Alvares F. L., Ogden G. B., Reiter R. J. (1995) Melatonin immunoreactivity in the photosynthetic prokaryote *Rhodospirillum rubrum*: implications for an ancient antioxydant system. *Cell Molec. Biol. Res.* **41:** 391-395

Tan D. X., Manchester L. C., Reiter R. J., Qui W. B. Karbownik M., Calvo J. R. (2000) Significance of melatonin in antioxidative defense system: reaction and products. *Biol. Signal. Recept.* **9:** 137-159

Received on 20th September, 2001; accepted on 7th December, 2001

INSTRUCTIONS FOR AUTHORS

Acta Protozoologica is a quarterly journal that publishes current and comprehensive, experimental, and theoretical contributions across the breadth of protistology, and cell biology of lower Eukaryote including: behaviour, biochemistry and molecular biology, development, ecology, genetics, parasitology, physiology, photobiology, systematics and phylogeny, and ultrastructure. It publishes original research reports, critical reviews of current research written by invited experts in the field, short communications, book reviews, and letters to the Editor. Faunistic notices of local character, minor descriptions, or descriptions of taxa not based on new, (original) data, and purely clinical reports, fall outside the remit of *Acta Protozoologica.*

Contributions should be written in grammatically correct English. Either British or American spelling is permitted, but one must be used consistently within a manuscript. Authors are advised to follow styles outlined in The CBE Manual for Authors, Editors, and Publishers (6th Ed., Cambridge University Press). Poorly written manuscripts will be returned to authors without further consideration.

Research, performed by "authors whose papers have been accepted to be published in *Acta Protozoologica* using mammals, shall have been conducted in accordance with accepted ethical practice, and shall have been approved by the pertinent institutional and/or governmental oversight group(s)"; this is Journal policy, authors must certify in writing that their research conforms to this policy.

Nomenclature of genera and species names must agree with the International Code of Zoological Nomenclature (ICZN), International Trust for Zoological Nomenclature, London, 1999; or the International Code of Botanical Nomenclature, adopted by XIV International Botanical Congress, Berlin, 1987. Biochemical nomenclature should agree with "Biochemical Nomenclature and Related Documents" (A Compendium, 2nd edition, 1992), International Union of Biochemistry and Molecular Biology, published by Portland Press, London and Chapel Hill, UK.

Except for cases where tradition dictates, SI units are to be used. New nucleic acid or amino acid sequences will be published only if they are also deposited with an appropriate data bank (e.g. EMBL, GeneBank, DDBJ).

All manuscripts that conform to the Instructions for Authors will be fully peer-reviewed by members of Editorial Board and expert reviewers. The Author will be requested to return a revised version of the reviewed manuscript within four (4) months of receiving the reviews. If a revised manuscript is received later, it will be considered to be a new submission. There are no page charges, but Authors must cover the reproduction cost of colour illustrations.

The Author(s) of a manuscript, accepted for publication, must transfer copyrights to the publisher. Copyrights include mechanical, electronic, and visual reproduction and distribution. Use of previously published figures, tables, or brief quotations requires the appropriate copyright holder's permission, at the time of manuscript submission; acknowledgement of the contribution must also be included in the manuscript. Submission of a manuscript to *Acta Protozoologica* implies that the contents are original, have not been published previously, and are not under consideration or accepted for publication elsewhere.

SUBMISSION

Authors should submit manuscript to: Dr Jerzy Sikora, Nencki Institute of Experimental Biology, ul. Pasteura 3, 02-093 Warszawa, Poland, Fax: (4822) 8225342; E-mail: jurek@nencki.gov.pl or j.sikora@nencki.gov.pl.

At the time of submission, authors are encouraged to provide names, E-mails, and postal addresses of four persons who might act as reviewers. Extensive information on *Acta Protozoologica* is available at the website: **http://www.nencki.gov.pl/ap.htm**; however, please do not hesitate to contact the Editor.

Hard copy submission: Please submit three (3) high quality sets of text and illustrations (figures, line drawing, and photograph). When photographs are submitted, arranged these in the form of plate. A copy of the text on a disk or CD should also be enclosed, in PC formats, preferably Word for Windows version 6.0 or higher (IBM, IBM compatible, or MacIntosh). If they do not adhere to the standards of the journal the manuscript will be returned to the corresponding author without further consideration.

E-mail submission: Electronic submission of manuscripts by e-mail is acceptable in PDF format only. Illustrations must be prepared according to journal requirement and saved in PDF format. The accepted manuscript should be submitted as a hard copy with illustrations (two copies, one with lettering + one copy without lettering) in accordance with the standards of the journal.

ORGANIZATION OF MANUSCRIPTS

Text: Manuscripts must be typewritten, double-spaced, with numbered pages (12 pt, Times Roman). The manuscript should be organized into the following sections: Title, Summary, Key words, Abbreviations, Introduction, Materials and Methods, Results, Discussion, Acknowledgements, References, Tables, and Figure legends. Figure legends must contain explanations of all symbols and abbreviations used. The Title Page should include the title of the manuscript, first name(s) in full and surname(s) of author(s), the institutional address(es) where the work was carried out, and page heading of up to 40 characters (including spaces). The postal address for correspondence, Fax and E-mail should also be given. Footnotes should be avoided.

Citations in the text should be ordered by name and date but not by number, e.g. (Foissner and Korganova 2000). In the case of more than two authors, the name of the first author and *et al.* should be used, e.g. (Botes *et al.* 2001). Different articles by the same author(s) published in the same year must be marked by the letters a, b, c, etc. (Kpatcha *et al.* 1996a, b). Multiple citations presented in the text must be arranged by date, e.g. (Small 1967, Didier and Detcheva 1974, Jones 1974). If one author is cited more than once, semicolons should separate the other citations, e.g. (Lousier and Parkinson 1984; Foissner 1987, 1991, 1994; Darbyshire *et al.* 1989).

Please observe the following instructions when preparing the electronic copy: (1) label the disk with your name; (2) ensure that the written text is identical to the electronic copy; (3) arrange the text as a single file; do not split it into smaller files; (4) arrange illustrations as separate files; do not use Word files; *.TIF, *.PSD, or *.CDR graphic formats are accepted; (5) when necessary, use only italic, bold, subscript, and superscript formats; do not use other electronic formatting facilities such as multiple font styles, ruler changes, or graphics inserted into the text; (6) do not right-justify the text or use of the hyphen function at the end of lines; (7) avoid the use of footnotes; (8) distinguish the numbers 0 and 1 from the letters O and l; (9) avoid repetition of illustrations and data in the text and tables.

References: References must be listed alphabetically. Examples for bibliographic arrangement:

Journals: Flint J. A., Dobson P. J., Robinson B. S. (2003) Genetic analysis of forty isolates of *Acanthamoeba* group III by multilocus isoenzyme electrophoresis. *Acta Protozool.* **42:** 317-324

Books: Swofford D. L. (1998) PAUP* Phylogenetic Analysis Using Parsimony (*and Other Methods). Ver. 4.0b3. Sinauer Associates, Sunderland, MA

Articles from books: Neto E. D., Steindel M., Passos L. K. F. (1993) The use of RAPD's for the study of the genetic diversity of *Schistosoma mansoni* and *Trypanosoma cruzi*. In: DNA Fingerprinting: State of Science, (Eds. S. D. J. Pena, R. Chakraborty, J. T. Epplen, A. J. Jeffreys). Birkhäuser-Verlag, Basel, 339-345

Illustrations and tables: After acceptance of the paper, drawings and photographs (two copies one with lettering + one copy without) must be submitted. Each table and figure must be on a separate page. Figure legends must be placed, in order, at the end of the manuscript, before the figures. Figure legends must contain explanations of all symbols and abbreviations used. All line drawings and photographs must be labelled, with the first Author's name written on the back. The figures should be numbered in the text using Arabic numerals (e.g. Fig. 1).

Illustrations must fit within either a single column width (86 mm) or the full-page width (177 mm); the maximum length of figures is 231 mm, including the legend. Figures grouped as plates must be mounted on a firm board, trimmed at right angles, accurately mounted, and have edges touching. The engraver will then cut a fine line of separation between figures.

Line drawings should be suitable for reproduction, with well-defined lines and a white background. Avoid fine stippling or shading. Prints are accepted only in *.TIF, *.PSD, and *.CDR graphic formats (Grayscale and Colour - 600 dpi, Art line - 1200 dpi) on CD. Do not use Microsoft Word for figure formatting.

Photographs should be sharp, glossy finish, bromide prints. Magnification should be indicated by a scale bar where appropriate. Pictures of gels should have a lane width of no more than 5 mm, and should preferably fit into a single column.

PROOF SHEETS AND OFFPRINTS

After a manuscript has been accepted, Authors will receive proofs for correction and will be asked to return these to the Editor within 48-hours. Authors will be expected to check the proofs and are fully responsible for any undetected errors. Only spelling errors and small mistakes will be corrected. Twenty-five reprints (25) will be furnished free of charge. Additional reprints can be requested when returning the proofs, but there will be a charge for these; orders after this point will not be accepted.

Indexed in: Current Contents, Biosis, Elsevier Biobase, Chemical Abstracts Service, Protozoological Abstracts, Science Citation Index, Librex-Agen, Polish Scientific Journals Contents - Agric. & Biol. Sci. Data Base at: **http://psjc.icm.edu.pl**, Microbes.info "Spotlight" at **http://www.microbes.info**, and electronic version at Nencki Institute of Experimental Biology website in *.PDF format at http://www.nencki.gov.pl/ap.htm now free of charge.

ACTA PROTOZOOLOGICA

ORIGINAL ARTICLES

SHORT COMMUNICATION

2002 FEBRUARY

VOLUME 41 NUMBER 1